

**CZECH TECHNICAL UNIVERSITY IN PRAGUE**  
**Faculty of Electrical Engineering**

**HABILITATION THESIS**

2012

Zdeněk Bečvář

Czech Technical University in Prague  
Faculty of Electrical Engineering  
Department of Telecommunication Engineering

# **Mobility Management for Small Cells in LTE-A Networks**

**HABILITATION THESIS**

**Ing. Zdeněk Bečvář, Ph.D.**

Prague, (September 2012)

Telecommunication Engineering

## **ACKNOWLEDGEMENT**

I would like thank to all my colleagues and co-workers for their cooperation in research work. Especially, I thank to dr Pavel Mach for support in writing project applications, and for cooperation in scientific work and publications.

This habilitation thesis has been performed mostly in the framework of the FP7 project FREEDOM (No. ICT-248891), which is funded by the European Commission. I would like to acknowledge all colleagues from FREEDOM consortium for fruitful and enriching cooperation.

**ABSTRACT**

Fourth generation mobile networks implement so-called small cells to cover gaps in signal such as inside buildings to improve users' experienced quality of services. The small cells can be connected to the core network via either conventional operator's backhaul or a user's internet connection, such as ADSL. The former one are represented by microcells and picocells while the later one are known as femtocells. If a user is moving along the area with dense deployment of the small cells, a user equipment can be forced to perform frequent handovers. This leads to redundant signaling overhead and to a degradation of quality of service for users due to short interruption in communication during handover. This thesis tackles problems related to mobility management in fourth generation mobile networks with small cells. First, two innovative solutions for elimination of redundant hard handovers in small cells are described. As the simulation results show, both proposals on hard handover are able to improve network performance comparing to existing and competitive proposals. Nevertheless, to overcome the problem of the handover interruption, the fast cell selection must be implemented. Therefore, an improvement of a fast cell selection is proposed to overcome the drop in quality of service for the scenario with femtocells with limited capacity of backhaul. The proposed algorithm for the fast cell selection eliminates handover interruption and it also improves user's throughput and reduces signaling overhead comparing to the competitive proposals. Last, a management procedure for temporary access of visiting UEs to femtocells with closed access is proposed. Two options of management communication are designed: in-band and out-of-band. The out-of-band communication technology leads to higher energy consumption at all involved user equipments. However, it does not introduce additional overhead on communication channels as does the in-band approach.

---

**TABLE OF CONTENT**

ACKNOWLEDGEMENT.....	I
ABSTRACT .....	II
LIST OF TABLES.....	V
LIST OF FIGURES .....	VI
LIST OF ABBREVIATIONS .....	VIII
1 INTRODUCTION .....	1
2 RELATED WORKS.....	4
2.1 HARD HANDOVER .....	4
2.2 FAST CELL SELECTION.....	6
2.3 TEMPORARY ACCESS TO CLOSED FAP .....	9
3 MOTIVATION AND OBJECTIVES.....	10
4 SCENARIOS AND EVALUATION METHODOLOGY .....	14
5 HARD HANDOVER FOR SMALL CELLS.....	17
5.1 ADAPTIVE TECHNIQUES FOR ELIMINATION OF REDUNDANT HANDOVERS .....	18
5.1.1 PRINCIPLE OF THE PROPOSED ADAPTATION TECHNIQUES .....	18
5.1.2 PERFORMANCE EVALUATION OF ADAPTIVE TECHNIQUES .....	22
5.1.3 RESULTS OF SIMULATIONS .....	23
5.1.4 COMPARISON OF PERFORMANCE OF ADAPTIVE TECHNIQUES .....	31
5.2 HANDOVER DECISION BY ESTIMATION OF THROUGHPUT GAIN .....	32
5.2.1 NOTATION AND ASSUMPTIONS FOR ETG.....	32
5.2.2 PRINCIPLE OF ETG.....	33
5.2.3 ANALYTICAL EVALUATION OF ETG PERFORMANCE.....	38
5.2.4 EVALUATION OF ETG PERFORMANCE BY SIMULATIONS.....	44
5.2.5 DISCUSSION OF BACKHAUL OVERHEAD DUE TO ETG HANDOVER.....	46
5.3 CONCLUSION.....	47
6 FAST CELL SELECTION .....	48
6.1 FCS IN OFDMA NETWORKS WITH SMALL CELLS.....	48
6.1.1 SYSTEM MODEL FOR FCS PERFORMANCE EVALUATION .....	51
6.1.2 SIMULATION RESULTS .....	55
6.1.3 DISCUSSION OF RESULTS AND SUGGESTIONS FOR MOBILITY SUPPORT .....	59
6.2 ACTIVE SET MANAGEMENT .....	60
6.2.1 PROPOSED ALGORITHM FOR ACTIVE SET MANAGEMENT.....	61
6.2.2 SYSTEM MODEL FOR EVALUATION.....	66
6.2.3 SIMULATION RESULTS .....	67

---

6.2.4	CONTROL INFORMATION FOR THE PROPOSED ACTIVE SET MANAGEMENT .....	74
6.3	CONCLUSIONS .....	76
7	TEMPORARY ACCESS TO CLOSED FAP .....	78
7.1	CONTROL PROCEDURE ENABLING ACCESS OF V-UES .....	79
7.1.1	GENERAL FRAMEWORK .....	79
7.1.2	IN-BAND APPROACH .....	81
7.1.3	OUT-OF-BAND APPROACH .....	83
7.2	MANAGEMENT MESSAGES FOR VISITOR ACCESS .....	84
7.3	IMPACT OF THE TEMPORARY V-UE ACCESS ON THE V-UE'S PERFORMANCE .....	86
7.4	CONCLUSIONS .....	88
8	CONCLUSIONS AND FUTURE WORK.....	89
	SUMMARY OF RESEARCH CONTRIBUTIONS.....	91
	REFERENCES .....	93
	APPENDIX .....	97

---

**LIST OF TABLES**

<i>Table 1. Selection of MCS according to CINR [45].....</i>	<i>16</i>
<i>Table 2. Simulation setting.....</i>	<i>23</i>
<i>Table 3. Summarization of performance of adaptive techniques.....</i>	<i>31</i>
<i>Table 4. Notation of parameters used for description of ETG.....</i>	<i>32</i>
<i>Table 5. Parameters for ETG evaluation.....</i>	<i>39</i>
<i>Table 6. Comparison of ETG performance with competitive algorithms.....</i>	<i>42</i>
<i>Table 7. Simulation parameters for evaluation of ETG.....</i>	<i>45</i>
<i>Table 8. Simulation results for corporate scenario.....</i>	<i>46</i>
<i>Table 9. Procedures for FCS support in OFDMA-based networks with small cells.....</i>	<i>51</i>
<i>Table 10. Simulation Parameters.....</i>	<i>53</i>
<i>Table 11. Average throughput per user for <math>\Delta_{HM} = 3dB</math>, <math>T_{add} = 3dB</math>, and <math>T_{del} = 3dB</math>; 8 Mbps backhaul capacity.....</i>	<i>59</i>
<i>Table 12. Average throughput per user for <math>\Delta_{HM} = 3dB</math>, <math>T_{add} = 3dB</math>, and <math>T_{del} = 3dB</math>; 100 Mbps backhaul capacity.....</i>	<i>59</i>
<i>Table 13. Notation of parameters used for description of the proposed algorithm.....</i>	<i>61</i>
<i>Table 14. Parameters and models used for evaluation of active set management algorithms.....</i>	<i>66</i>
<i>Table 15. Structure of V-UE Request message.....</i>	<i>84</i>
<i>Table 16. Structure of V-UE Response message.....</i>	<i>85</i>
<i>Table 17. Structure of V-UE Info message.....</i>	<i>85</i>
<i>Table 18. Structure of V-UE Confirm message.....</i>	<i>86</i>

---

**LIST OF FIGURES**

Figure 1. Problem related to the dense femtocell deployment.....	10
Figure 2. Frequency reuse constrain in case of FCS with FAPs.....	11
Figure 3. Route of data to UE in case of FCS with FAPs.....	12
Figure 4. LTE-A TDD frame structure used in the simulations.....	15
Figure 5. Principle of adaptive hysteresis margin.....	19
Figure 6. Cell radius over $RSSI_{min}$ according to ITU-R P.1238 path loss model.....	20
Figure 7. Average amount of handovers over $\Delta_{HM,max}$ for determination of optimum $RSSI_{min}$ .....	24
Figure 8. Average DL throughput over $\Delta_{HM,max}$ for determination of optimum $RSSI_{min}$ .....	24
Figure 9. Impact of different methods for determination of $\Delta_{HM}$ on average amount of handovers.....	24
Figure 10. Impact of different methods for determination of $\Delta_{HM}$ on DL throughput.....	24
Figure 11. Impact of conventional and adaptive HM on amount of handovers for different densities of FAPs ( $CINR_{win}=50$ ).....	25
Figure 12. Impact of conventional and adaptive HM on DL throughput for different densities of FAPs ( $CINR_{win}=50$ ).....	25
Figure 13. Average amount of handovers over the Street Width for CINR based adaptive HM.....	26
Figure 14. Average DL throughput of UEs over the Street Width for CINR based adaptive HM.....	26
Figure 15. Impact of different $\Delta_{HM,min}$ values on the amount of performed handovers.....	27
Figure 16. Impact of different $\Delta_{HM,min}$ values on the downlink throughput.....	27
Figure 17. Impact of different EXP values on the amount of performed handovers.....	28
Figure 18. Impact of different EXP values on the downlink throughput.....	28
Figure 19. Impact of adaptive WS on the amount of initiated handovers.....	29
Figure 20. Impact of adaptive WS on average DL throughput.....	29
Figure 21. Impact of adaptive HDT on the amount of initiated handovers.....	31
Figure 22. Impact of adaptive HDT on the DL throughput of UEs.....	31
Figure 23. Gain obtained by handover to a FAP.....	34
Figure 24. Deployment for analytical evaluation.....	39
Figure 25. Impact of $m_{Thr}$ on amount of performed handover.....	40
Figure 26. Impact of $m_{Thr}$ on relative throughput of outdoor user.....	40
Figure 27. Optimum $m_{Thr}$ over traffic offered by outdoor user.....	41
Figure 28. Impact of error in estimation of $k_c$ on the amount of performed handovers.....	44
Figure 29. Impact of error in estimation of $k_c$ on throughput of users.....	44
Figure 30. Example of simulation deployment for evaluation of ETG.....	44
Figure 31: Possible introduction of Fast Cell Selection into LTE-A architecture.....	50
Figure 32. Simulation deployment and model of a house.....	52
Figure 33. Interval between mobility events for hard handover and FCS.....	55
Figure 34. Average interruption experienced by UEs due to mobility.....	56
Figure 35. Served throughput of indoor UEs for open and hybrid accesses.....	58
Figure 36. Served throughput of outdoor UEs for open and hybrid accesses.....	58

---



---

Figure 37. Served throughput of cell-edge UEs for open and hybrid accesses.....	58
Figure 38. Proposed algorithm for active set management.....	62
Figure 39. Impact of $\alpha$ on active set size.....	67
Figure 40. Impact of $\alpha$ on frequency of active set updates.....	67
Figure 41. Impact of $\alpha$ on users throughput.....	68
Figure 42. Impact of $\alpha$ on ratio of users whose requirements on capacity are not fulfilled.....	68
Figure 43. Average throughput of UEs during simulation over amount of offered traffic by the UEs; throughput of: (a) only indoor users; (b) only outdoor users; (c) all users.....	70
Figure 44. Average amount of changes in active set of individual users per a simulation step; changes in active set of: (a) only indoor users; (b) only outdoor users; (c) all users.....	71
Figure 45. Average amount cells included in active set for: (a) only indoor users; (b) only outdoor users; (c) all users.....	72
Figure 46. Average ratio of time spent in the state when UEs requested capacity is not fully provided for: (a) only indoor users; (b) only outdoor users; (c) all users.....	73
Figure 47. Reference scenario for management of visiting users.....	78
Figure 48. General outline of the procedure for V-UE entering the CSG FAP.....	80
Figure 49. Flow of control messages for V-UE access using IB approach.....	82
Figure 50. Flow of control messages for V-UE access using OOB approach.....	84
Figure 51. SINR experienced by V-UE if temporary access is not enabled (dashed blue line) and if the V- UE is enabled to access this FAP (solid red line).....	87
Figure 52. SINR experienced by V-UE over distance between MBS and FAP if temporary access is not enabled (dashed blue line) and if the V-UE is enabled to access this FAP (solid red line).....	88
Figure 53. Notation for determination of $t_c$ limits.....	97
Figure 54. Deviation of $t_{c,min}$ and $t_{c,max}$ over relative distance of users' path from the FAP's position. ....	98

---

**LIST OF ABBREVIATIONS**

4G	Fourth Generation of mobile networks
ADSL	Asynchronous Digital Subscriber Line
AS	Active Set
CDMA	Code Division Multiple Access
CINR	Carrier to Interference plus Noise Ratio
CLC	Closed subscriber group List Control
CSG	Closed Subscriber Group
DL	Downlink
ETG	Estimation of Throughput Gain
FAP	Femto Access Point
FCS	Fast Cell Selection
HDT	Handover Delay Timer
HM	Hysteresis Margin
IB	In-band
IINR	Interference to other Interferences plus Noise Ratio
IMSI	International Mobile Subscriber Identity
LTE(-A)	Long Term Evolution (-Advanced)
MBS	Macrocell Base Station
MCS	Modulation and Coding Scheme
MIMO	Multiple-Input Multiple-Output
OFDMA	Orthogonal Frequency Division Multiple Access
OOB	Out-of-band
PCI	Physical Cell Identification
PRWMM	Probabilistic Random Walk/Waypoint Mobility Model
QoS	Quality of Service
RB	Resource Block
RE	Resource Element
RSSI	Received Signal Strength Indication
S-GW	Serving Gateway
SNR	Signal to Noise Ratio
SINR	Signal to Interference plus Noise Ratio
TDD	Time Division Duplex
TTI	Transmission Time Interval
TTT	Time-To-Trigger
UE	User Equipment
UL	Uplink
USIM	Universal Subscriber Identity Modul
V-UE	Visiting UE
WLAN	Wireless Local Area Network
WS	Window Size

# 1 INTRODUCTION

The fourth generation (4G) mobile networks are assumed to be deployed at frequencies in order of GHz (e.g., 2 or 2.6 GHz). Transmission at such frequencies leads to higher attenuation of signal propagated from a transceiver to a receiver comparing to former bands at roughly 0.9 GHz utilized for GSM. To cover potential gaps in coverage due to heavy attenuation of a signal at higher frequencies, small cells can be deployed. In general, two types of small cells are distinguished: femtocells and pico/microcells. In both cases, radius of cells is low, i.e., in order of tens of meters.

The femtocell, denoted as Femto Access Point (FAP), is assumed to be placed in user's premises (houses, flats) or enterprises. The FAPs are owned by users and also controlled by users. Their connection to a core network is enabled via a backhaul of limited capacity and variable quality. Typically, Asynchronous Digital Subscriber Line (ADSL) is used as the backhaul connection. Generally, three types of user's accesses can be provided by the FAPs: open, closed, and hybrid [1]. In the case of the open access, all users in the coverage of a FAP can connect to it. A benefit of the open access consists in an opportunity to offload a Macrocell Base Station (MBS) by serving some users in areas with heavy traffic load or users far from the MBS [2]. On the contrary, the FAP with closed access admits only users included in so called Closed Subscriber Group (CSG) list. The CSG list contains identification of all user equipments (UEs) that can access the FAP. Users not listed in CSG are not allowed to attach to the closed FAP. Interference in the case of the closed access should be carefully managed in areas with dense deployment of the FAPs in order to avoid an impairment of the system performance. A combination of both open and closed accesses is known as hybrid access. If the hybrid access is considered, a part of capacity is dedicated for the CSG users and the rest of the bandwidth can be shared by other users. As presented in [3], the open access provides higher throughput experienced by users when compared to the

closed one. This fact is emphasized especially for low density of the macrocell users [4].

The pico/microcells can be also deployed in users' premises; however, these cells are supposed rather for deployment in enterprises or public areas [5]. Contrary to femtocells, the pico/microcells are under full control of the operator. Moreover, the pico/microcells should be interconnected with operator's backhaul by a high quality link with sufficient capacity to serve all traffic transmitted over the air.

Dense deployment of small cells introduces new challenges related especially to interference mitigation for the closed access and users' mobility management for the open or hybrid accesses [6]. This habilitation thesis is focused on mobility management. A mobile user is forced to perform handover from a serving cell to a target cell to keep the quality of service (QoS). If the user is moving close to the area with dense deployment of small cells, large number of handovers can be performed within a short time interval. Then, a drop in QoS is introduced due to the short interruption as a consequence of hard handover. This is notable especially for real-time services. The amount of handovers can be adjusted by techniques used for elimination of redundant handovers, such as a hysteresis or a time-to-trigger [7], [8]. Unfortunately, those techniques considerably decrease user's throughput in networks with small cells [9]. Moreover, an interruption is still observed if a conventional hard handover is performed as the user is disconnected from a serving cell before a new connection to a target cell is established [10]. Fast Cell Selection (FCS) can be exploited instead of the hard handover to suppress the problem of the handover interruption and QoS decrease in the networks with dense deployment of the small cells. However, an implementation of FCS to real networks is more demanding and more complex comparing to hard handover.

This thesis provides two solutions for hard handover that targets on reduction of amount of handovers to minimize negative impact of handover interruption. At the same time, both approaches keeping the same or even improved throughput of the users in the networks with small cells. Furthermore, FCS is evaluated for both femto and pico/micro cells to show its efficiency in heterogeneous networks with small cells. Also an algorithm for management of an active set considering amount of consumed radio resources is proposed to overcome inefficiency of FCS in networks with small cells. Last, we propose management procedure for admission of a visiting UE to the CSG

cells. In this thesis, we focus mostly on femtocells as those are more challenging due to lower quality of the backhaul than pico/microcells. However, all the proposed solutions for hard handover and FCS are applicable to pico/micro cells as well.

The rest of the thesis is organized as follows. The next chapter describes and analyzes related works in the area of the mobility management in 4G wireless networks. Chapter III defines motivation and objectives of this thesis. Methodology and scenarios used for the performance evaluations are addressed in Chapter IV. Then, Chapter V provides description and assessment of two proposals on the management of hard handover. Chapter VI is focused on advanced mobility support by means of FCS. Chapter VII defines the management procedure for support of a temporary access of so-called visiting users to the CSG FAPs. The last chapter summarize major conclusions and defines potential directions for the future research.

## 2 RELATED WORKS

This chapter gives an overview of the state of the art of the work related to the mobility management in the mobile wireless networks. The research contributions presented later in this habilitation thesis with respect to the presented related works is also presented in this chapter.

### 2.1 HARD HANDOVER

A conventional hard handover is based on comparison of signal levels of serving and target cells. Handover is executed if the signal level of the target cell exceeds the one of the serving cell. Several techniques such as Hysteresis Margin (HM) [11], [12], Time-To-Trigger (TTT) or windowing (also known as signal averaging) [11] are defined to eliminate redundant handovers in conventional networks without small cells. In the case of using any conventional technique for elimination of redundant handovers a drop in throughput is introduced. This is due to a short time when the UE communicates with the serving station even if a potential target station provides channel of a higher quality. A drop in throughput is even more significant if the conventional techniques (e.g., HM, TTT, or windowing) are utilized for elimination of redundant handovers in scenario with the small cells [9]. A modification of the conventional HM is defined in [13]. The authors evaluate so-called adaptive HM in scenario with deployed MBSs but without FAPs. The paper assumes exact knowledge of the distance among an UE and its serving MBS and exact and invariant radius of the MBSs. The radius of all cells is assumed to be the same. Nevertheless, the radius is slightly varying in time in the real networks. Moreover, the radius of individual cells is largely different if the small cells overlapping with macrocells are deployed. Beside, the exact position of the FAPs is not defined by operators as it is in charge of the user. Thus, the cell radius of the FAPs cannot be precisely estimated. Therefore technique proposed in [13] cannot be applied into the networks with small cells and especially with the FAPs.

The handover mechanism for FAPs considering asymmetry of a transmitting power of the FAP and the MBS is introduced in [14] and further extended in [15]. This mechanism compares the level of the average signal received from the potential target FAP with the absolute threshold value of -72 dB. Besides, the signal of the MBS is compared with a combination of the signals from the MBS and the FAP. After the comparison of the individual results, either the MBS or the FAP is selected as the serving station. This proposal increases the probability of handover to the FAP if this FAP provides signal above the threshold and if the FAP is deployed far from the MBS. Otherwise, if the threshold is not met, the handover is performed as in the conventional way. Unfortunately, the paper provides no solution for the scenario with overlapping femtocells. As the authors indicate, the proposed algorithm eliminates redundant handovers if the FAP is close to the MBS. However, overall amount of handovers is even increased comparing to the conventional approach. The authors also do not consider limited capacity of the FAP backhaul in evaluations.

The combination of additional parameters, such as user's speed and QoS requirements, for improvement of the handover decision is presented in [16]. Although the number of the unnecessary handovers is reduced, the throughput is also negatively influenced. Another speed-aware algorithm is proposed in [17]. The authors exploit a fuzzy-logic system for the handover decision. The similar idea is further elaborated and extended in [18] where a new fuzzy-logic based handover algorithm with awareness of the speed is introduced. However, both papers are focused only on the conventional networks with macrocells while specifics of the small cells are not taken into account.

Another approach eliminating redundant handovers is to adapt the transmission power of the FAPs. The proposals dealing with power control adjustment to reduce the number of redundant handovers in femtocells are presented, e.g., in [19], [20], [21]. All these proposals eliminate majority of the redundant handovers. Nevertheless, the advantage of the throughput gain due to the utilization of the open or hybrid accesses (illustrated in [1]) is also distinctively suppressed by the reduction of the FAP's transmitting power. Therefore, these solutions are more suitable for the closed access.

The authors of [22] discuss vertical handover between IEEE 802.16e and Wireless Local Area Network (WLAN) to maximize user's satisfaction. Taking lower cost of the connection via WLAN into account, the authors suggest keeping the user connected to WLAN if it provides sufficient capacity to the user. However, the handover decision

based only on the current bit rate achieved by the UE leads to the redundant handovers if WLAN's load fluctuates frequently. Moreover, the authors assume invariable throughput for users no matter what is its relative position with respect to the MBSs and the WLAN access points. It means a variability of the throughput in dependence on the distance between the user and its serving and interfering nodes is not considered.

Furthermore, prediction-based algorithms can be exploited for handover to improve its efficiency (see, e.g., [23], [24], [25]). The prediction-based approaches reach high efficiency in determination of the target MBS. However, by deployment of small cells, the prediction accuracy is strongly affected since small cells' radius is very low and since the small cells overlapping with MBSs. Moreover, even if the prediction reaches high efficiency in term of high ratio of correctly predicted target cells; the handover to the estimated target cell can be inefficient if this cell is a small cell. This is due to a short time spent by the UE under the small cell's coverage or due to limited capacity of the femtocells backhaul.

The first contribution of this thesis exploits an idea of the adaptive HM and adapts it to be easily implemented to 4G networks and also to modify the procedure of HM adaptation to be applicable in 4G networks with femtocells. We propose to utilize conventionally reported metrics such as RSSI (Received Signal Strength Indicator) or CINR (Carrier to Interference plus Noise Ratio) for dynamic adaptation of an actual value of HM. The second contribution related to hard handover is the algorithm for the handover decision based on a profitability of handover to the FAP. Handover is performed only if an estimated throughput offered to a UE by the FAP exceeds the throughput offered by the MBS. Both radio as well as backhaul parameters of the FAPs and the MBSs are taken into account in the proposed handover decision. Consequently, the proposed procedure rejects only those handovers to the FAPs that do not introduce any considerable improvement in users' throughput. In other words, the purpose of the proposed handover decision is to reduce amount of initiated handovers to the FAPs with low profit (or even with loss) for either network (operator) or users.

## **2.2 FAST CELL SELECTION**

Even if all the proposed modifications related to hard handover are somehow able to improve the network performance, an interruption due to the hard handover cannot be eliminated. Moreover, a degradation of a channel quality for cell-edge users is observed



due to heavy interference if the small cells and the macrocells share the same frequency bands.

To minimize the problem of the handover interruption, FCS can be implemented. The FCS has been introduced in 3GPP Release 99 as the SSDT (Site Selection Diversity Transmission) feature (see [26], [27]). In 3GPP Release 99, FCS strongly relies on the use of CDMA while only the MBSs are considered. Therefore, modifications required for utilization of FCS in OFDMA networks with small cells should be defined.

In the case of FCS, the AS is defined for each UE. The AS is comprised of several neighboring cells of the UE. Neighbor cells are added/removed to/from the AS depending on the signal level measured by the UE [26]. In [28], the authors compare fractional frequency reuse in a single cell transmission scenario with FCS enhanced by adaptive Multiple-Input Multiple-Output (MIMO) mode selection in combination with interference avoidance technique. The investigation is done for the active set encompassing two and three MBSs. The active set is updated according to the signal level received from the neighboring MBSs. Consideration of a relation among the signal levels of neighboring cells is the conventional approach for FCS.

In [29], [30], the authors propose new metric, denoted as IINR (Interference to other Interferences plus Noise Ratio), for the active set management. In comparison to the conventional SINR, the IINR does not take the signal level of the serving cell into account. The measurement of IINR requires no transmission on the Resource Elements (REs) that are occupied by reference signals of the neighboring MBSs. The IINR introduces a gain in spectral efficiency for the cell-edge users and simultaneously it reduces amount of candidate cells reported by the UE. This way, the load in uplink is reduced while the downlink is unaffected.

The authors of [31] propose a frequency muting for FCS. The muting is applied to the second strongest cell according to the UE's measurement. As the results show, this approach can introduce roughly 10% gain in throughput of the cell-edge users comparing to the single cell transmission. Further gain of additional 10% can be introduced by a joint processing. However, this is obtained at the cost of much higher complexity. Further extension of the muting idea is presented in [32]. The authors propose the adaptive muting based on a capacity calculation and a power allocation based on a muting mode selection. The muting is applied to all Resource Blocks (RBs)

to avoid power wasting. Hence, the transmitting power at some RBs is lowered while the power at some RBs is boosted. Nevertheless, the overall transmission power is kept as in the conventional case. The muting mode is considered only if the UE's throughput is at least double comparing to the non-muting mode. The results show improvement in throughput by roughly 5.5% comparing to the single cell transmission.

Analyzing an impact on throughput if a new cell is included in an active set is presented also in [33]. The authors compare the performance in the case when the candidate cell would be included with the case when it is not. If the gain by the inclusion of the cell exceeds the predefined threshold, the update of the active set is performed.

The FCS introduces a gain in throughput especially at the cell edges where the interference is not marginal as shown, for example, in [33], [34], [35]. All above-mentioned papers investigate FCS in the scenario with macrocells only. However, deployment of the small cells introduces several problems related to the limited backhaul and small cell radius that could negatively influence the performance of FCS in the networks with small cells. Therefore, we first evaluate performance of FCS and compare it with the conventional hard handover in the networks with small cells. Performance is assessed in terms of the management overhead and the handover interruption.

Moreover, we also propose the algorithm for more efficient management of the active set respecting specifics of the small cells. Comparing to the listed related work on active set management, our proposal differs in several aspects. First, we consider deployment of the FAPs and its related backhaul problems. Large amount of radio resources of an MBS could be wasted if the MBS would be included in active set together with a FAP with weak signal. Therefore, comparing to [31], [32], our proposal is based on evaluation of the impact of the active set enhancement on the amount of consumed radio resources of the MBS. Further, a limitation of the FAP backhaul capacity and delay are considered in our proposal. As the FAPs are supposed to be connected mostly via ADSL connection, the backhaul capacity is significantly lower than the capacity of the MBS backhaul. Thus, each inclusion of a FAP into the active set should take the backhaul limitation into account. In addition, FAP backhaul delay is a new parameter considered when updating active set in our proposal since this delay is typically higher than the delay of MBS backhaul.

---

## 2.3 TEMPORARY ACCESS TO CLOSED FAP

In LTE-A networks, the list of CSG users is defined by either a FAP subscriber or an operator and update of this list requires manual modification of the records in CLC entity (CSG List Control) [36], [10], [37]. In combination with up to four or eight UEs allowed to be simultaneously included in CSG list per FAP [6], it is not possible to update the CSG list frequently. This can be a significant limiting aspect in dense deployment of FAPs due to inflexible management of the CSG list. A frequent update can be required, for example, if visitors or guests who attend a subscriber of a FAP would like to access the FAP. If the subscriber is not willing to include this visitor to the CSG permanently (for example, due to the limited number of CSG members or due to the limited throughput of the FAP), the subscriber must manually include and remove the visitor to and from the CSG list. The manual update of a CSG list is inconvenient and uncomfortable for the most of the users. A solution for enabling more comfortable access of the Visiting UE (V-UE) to a CSG FAP is presented in [38]. The authors propose new message flow to handle the management of the CSG list for the V-UEs. The solution is based on a configuration of records stored in an operator's CLC server. Nevertheless, the authors define only a general framework of the procedure with focus only on the core network management signaling and do not discuss details on initiation of the access of the V-UE to the CSG FAP and the management procedures at radio interface.

Our contribution consists in the design of the control procedure for enabling non-CSG users to temporarily access a CSG FAP. We propose control messages and their flow at all involved interfaces for access of the V-UE to the CSG FAP. Two various approaches, in-band and out-of-band, are proposed and discussed.

### 3 MOTIVATION AND OBJECTIVES

According to originating standards for 4G mobile networks, the small cells are expected to be deployed in future mobile and wireless networks to improve coverage in specific areas with low signal quality. By placing additional stations to the network, new cell boundaries are introduced. Since heavy deployment of the small cells with low radius is expected in 4G networks, the procedures for the user's mobility becomes initiated more frequently (see Figure 1). Therefore, more often scanning of higher amount of entities in UE's neighborhood must be performed. Moreover, each handover generates some management overhead and introduces interruption in user's communication. All these aspects lead to a drop of user's throughput and QoS. This is getting more apparent with dense deployment of small cells. Hence, large and efficient deployment of the small cells requires optimizing the principles of user's mobility support to ensure continuous high level of service quality.

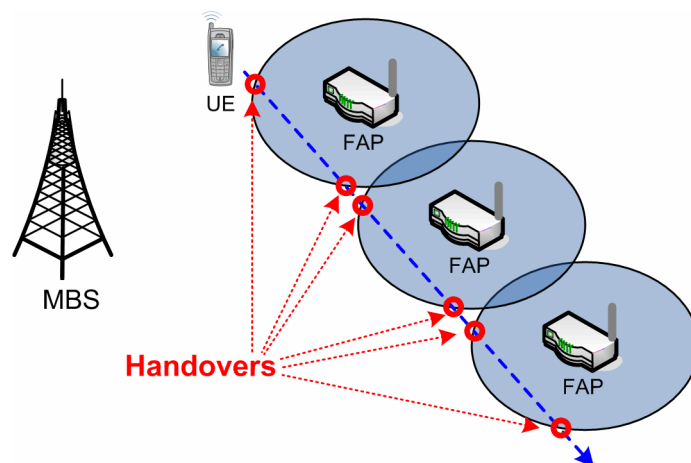


**Figure 1. Problem related to the dense femtocell deployment.**

Before mentioned weaknesses could be minimized or even fully eliminated by implementing FCS. However, deployment of FAPs introduces several problems in the

active set management that must be solved for efficient selection of the cells to be included in the active set for FCS in 4G networks with the FAPs. First, in the conventional FCS with frequency muting, if a UE consumes significant part of the resources at the FAP (e.g., due to low signal level), the same resources (at the same frequencies and in the same time intervals) cannot be used by the MBS included in the same active set. Thus, it could limit the radio capacity of the MBS.

This situation is shown in Figure 2. The active set of the UE1 contains two FAPs as well as one MBS. If the FAP1 transmits data to the UE1 at frequencies corresponding to RB #0 to RB #6, those frequencies can be occupied by neither the FAP 1 nor the MBS. On one hand, the interferences  $I_{MBS-UE1}$  and  $I_{FAP2-UE1}$  are eliminated and less RBs can be consumed by the FAP1 to serve the UE1. On the other hand, RBs at the frequencies corresponding to those used by the FAP1 for delivery of data to the UE1 are wasted. In the case of dense deployment of the FAPs, this can lead to the situation when the most of the MBS's resources are disabled from utilization due to its occupation by the FAPs involved in the active sets of the UEs along with the MBS.

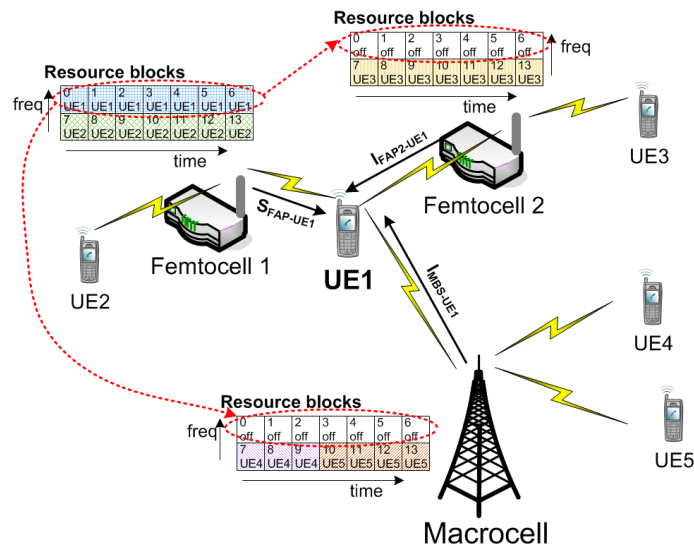


**Figure 2. Frequency reuse constrain in case of FCS with FAPs.**

Second, if FCS is enabled, user's data intended for each UE must be routed to all cells in its active set (see Figure 3). Due to the limitation of FAP backhaul, inclusion of FAPs in active sets should consider also the backhaul capacity of individual cell especially if the FAP is inactive in transmission to the UE. This situation is depicted in Figure 3. Data destined for the UE1 must be routed to both FAPs in the active set of the

UE1. Hence, the backhauls of both FAPs are loaded with all data (in our case, with seven packets). However, only a part of these packets is transmitted. For example, the packets #2 and #6 are not transmitted by the FAP1 in Figure 3. These packets are discarded. On the side of FAP2, only two packets out of seven are transmitted to the UE1. Other five packets are discarded and those only increases load of the FAP2 backhaul. This problem does not occur in scenario with the MBSs only as the MBS backhaul is of a very high capacity. Nevertheless, the backhaul of FAPs is typically of a lower quality.

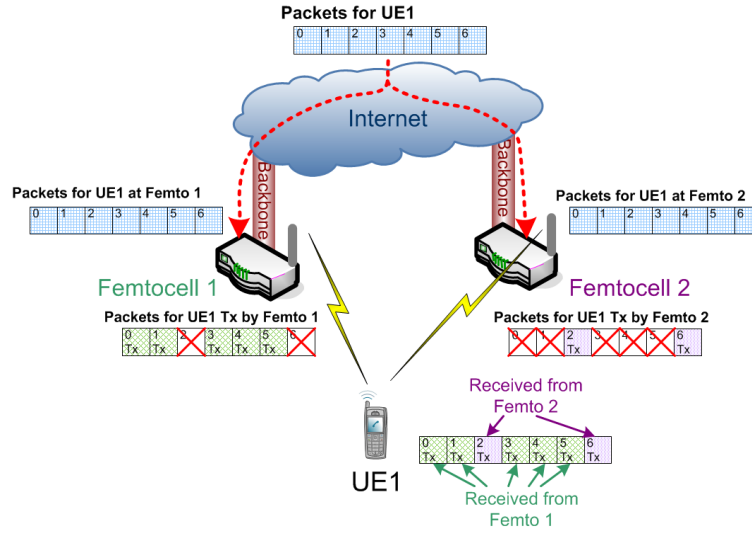


**Figure 3. Route of data to UE in case of FCS with FAPs.**

Third, the FAP backhaul is also of a variable quality. If two FAPs are in an active set of a UE, we can assume that those belong to the same operator (otherwise, the FCS would not be possible as user is usually subscribed only at one operator). If an MBS and one or several FAPs are included, we have to ensure that data will be ready at the same time at all FAPs and MBSs included in the active set. In real networks, it means to increase packet delay to the maximum delivery delay observed among all cells in the active set as expresses the next formula:

$$D = \max\{D_{1,A^i}, D_{2,A^i}, \dots, D_{j,A^i}\} \quad (1)$$

where  $D_{j,A^i}$  represents delay of  $j$ -th cell included in the active set of  $i$ -th UE.

The general objective of this habilitation thesis is to minimize negative impact of the management procedures for mobility support on the network performance and QoS experienced by users.

Therefore, the first objective is to define algorithms for hard handover decision to minimize amount of initiated handovers. This way, the QoS of users and overall networks performance are improved.

The second objective is to investigate possibility of FCS implementation in the networks with small cells and further, provide enhanced algorithm for the active set management considering specifics of small cells.

Last goal is to develop mechanism for easy management of CSG list to enable faster deployment of CSG femtocells. This part is composed of the proposal of new management messages and their flow for enabling temporary access of visiting users.

## 4 SCENARIOS AND EVALUATION METHODOLOGY

The performance evaluation focuses investigation of an impact of the proposed procedures on the network metric such as network throughput, distribution function of signal level experienced by users, and amount of initiated mobility events.

All evaluations are done via simulations in MATLAB since it is common and universal simulation tool used for mobile networks. Moreover, MATLAB enables simple implementation of wide range of procedures and algorithms. All models for simulations and for analytical analysis are in line with models conventionally used for evaluation of 4G mobile networks. These models are summarized by IMT-Advanced [39].

For simulation of outdoor user's movement, we consider conventionally used models such as Direct Movement model, also known as multiple moving mobility model [40]; Probabilistic Random Walk Mobility Model (PRWMM) [41]; Manhattan Mobility Model [42]. For indoor user's the mobility model is based on [19].

Street layout and deployment of all network entities follow the general requirements on simulations as defined in [39] and it is aligned also with the latest recommendations related to the small cells specifics defined by Small Cell Forum [43]. We consider both rural scenario with less density of users as well as corporate scenario with high density of users [44].

In all investigated areas of UE's mobility in networks with small cells, only the slow moving users can perform handover to a small cell. Handover of vehicular users is usually useless, since high-speed users spend only very short time in the small cell due to its low radius [16].

In all evaluations, we assume the same 20 MHz wide channel is shared by the MBSs and the small cells. This channel is at 2.0 GHz for LTE-A. Transmission power of the MBSs and the small cells is set to 46 dBm and 15 dBm respectively.



Unified TDD frame structure of LTE-A release 10 is used in all simulations. The frame is divided into 10 subframes and 20 slots (see Figure 4). The frame duration is 10 ms and uplink–downlink (UL–DL) configuration “1” is chosen. This configuration splits the frame into four downlink subframes, four uplink subframes, and two special subframes (SSs). The SS configuration “0” is utilized for all simulations in this document. Seven symbols (i.e., Normal cyclic prefix) per subcarrier and 12 subcarriers per one RB are considered. The spacing of subcarriers is  $\Delta f = 15 \text{ kHz}$ . The amount of bits carried in one RE depends on available Modulation and Coding Scheme (MCS), which is derived according to [45]. Each slot consists of RBs, which are further composed of REs. The number of RE per RB ( $N_{RE}^{RB}$ ) is defined by the next equation:

$$N_{RE}^{RB} = N_{SC}^{RB} \times N_{ymb} \quad (2)$$

where  $N_{SC}^{RB}$  is a number of subcarriers per RB; and  $N_{ymb}$  is a number of symbols per the subcarrier.

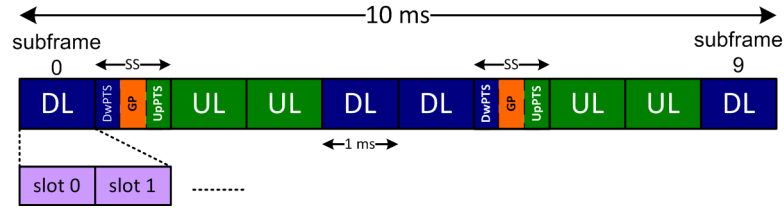


**Figure 4. LTE-A TDD frame structure used in the simulations.**

Seven symbols per subcarrier and typically 12 subcarriers per one RB are used for a normal cyclic prefix. The spacing of the subcarriers is  $\Delta f = 15 \text{ kHz}$ . The amount of the bits carried in one RE depends on available Modulation and Coding Scheme (MCS). The assignment of the MCS is based on the signal quality according to Table 1 (the values are taken from [45]).

Downlink throughput of a user is furthermore calculated according to the subsequent formula:

$$Thr_{DL} = \Gamma \times n_{RB} \times N_{SC}^{RB} \times N_{ymb} = \Gamma \times n_{RB} \times N_{RE}^{RB} \quad (3)$$

where  $n_{RB}$  is the number of occupied RBs (depending on a channel bandwidth as indicated in [46]), and  $\Gamma$  is the transmission efficiency expressed as the amount of bits carried per symbol.

**Table 1. Selection of MCS according to CINR [45]**

CINR [dB]	MCS	Transmission efficiency $\Gamma$ [bits/symbol]
$\text{CINR}_{\min} < \text{CINR} \leq 1.5$	1/3 QPSK	0.66
$1.5 < \text{CINR} \leq 3.8$	1/2 QPSK	1
$3.8 < \text{CINR} \leq 5.2$	2/3 QPSK	1.33
$5.2 < \text{CINR} \leq 5.9$	3/4 QPSK	1.5
$5.9 < \text{CINR} \leq 7.0$	4/5 QPSK	1.6
$7.0 < \text{CINR} \leq 10.0$	1/2 16QAM	2
$10.0 < \text{CINR} \leq 11.4$	2/3 16QAM	2.66
$11.4 < \text{CINR} \leq 12.3$	3/4 16QAM	3
$12.3 < \text{CINR} \leq 15.6$	4/5 16QAM	3.2
$15.6 < \text{CINR} \leq 17.0$	2/3 64QAM	4
$17.0 < \text{CINR} \leq 18.0$	3/4 64QAM	4.5
$18.0 < \text{CINR}$	4/5 64QAM	4.8

Algorithm specific evaluation metrics and simulation parameters are further defined in description of individual proposals.

## 5 HARD HANDOVER FOR SMALL CELLS

Handover can be initiated due to several reasons, for example, to ensure QoS to users, to improve coverage or to balance load in networks.

To avoid redundant handovers that increase neither network's nor users' performance, several techniques modifying condition for the handover decision are defined by standards or in literature. Mostly used techniques are: HM, windowing (also denoted signal averaging), and TTT or its enhancement known as Handover Delay Timer (HDT) [47].

While HM is implemented, the handover decision and initiation is based on a comparison of one or several signal parameters (e.g., CINR or RSSI) of a serving cell and a target cell. The handover is initiated if the signal parameter of the target cell exceeds the signal parameter of the serving cell at least by a hysteresis ( $\Delta_{HM}$ ):

$$s_t^{Tar} > s_t^{Ser} + \Delta_{HM} \quad (4)$$

where  $s_t^{Tar}$  and  $s_t^{Ser}$  represents the signal quality parameter of the serving and target cells respectively in the time instant  $t$ .

In the case of the windowing, the handover decision is done if the average value of the observed signal parameter (e.g., CINR, RSSI, etc.) from the serving cell drops under the average level of the same parameter at the target cell (see formula (5)). The average value is calculated over a number of samples denoted as Window Size (WS).

$$\frac{\sum_{i=1}^{WS} s_i^{Tar}}{WS} > \frac{\sum_{i=1}^{WS} s_i^{Ser}}{WS} \quad (5)$$

where  $s_i^{Tar}$  and  $s_i^{Ser}$  represent  $i$ -th sample of the level of the observed signal parameters at the target and serving cells respectively.

Implementation of the HDT is based on the insertion of a short delay between the time when the handover conditions are met and the time when the handover initiation is executed. This delay is labeled HDT. The handover conditions have to be fulfilled over the whole duration of HDT to initiate handover. Generally, handover is performed if:

$$s_t^{Ser} < s_t^{Tar} | t \in (t_{HO}, t_{HO} + HDT) \quad (6)$$

where  $HDT$  represents the duration of the handover delay timer; and  $t_{HO}$  is the time instant when the handover conditions are fulfilled.

These techniques perform well in the common networks without FAPs. However, their efficiency drops with implementation of the FAPs [9]. To overcome this problem, two ways of the handover decision improvement are proposed and investigated in the following subsections: i) adaptive techniques and ii) throughput gain prediction.

## 5.1 ADAPTIVE TECHNIQUES FOR ELIMINATION OF REDUNDANT HANDOVERS

First, the proposals on the adaptation of hysteresis, HDT, and WS are described. Then, all three adaptive techniques are evaluated by means of simulations in MATLAB and their performance is confronted with the conventional (non-adaptive) approaches.

### 5.1.1 PRINCIPLE OF THE PROPOSED ADAPTATION TECHNIQUES

In the conventional HM, the level of the hysteresis is constant. The adaptive HM is based on the modification of an actual  $\Delta_{HM}$  value according to the position of the user in the cell. The  $\Delta_{HM}$  is decreasing with UE moving closer to the cell boarder. It is presented in the next equation (defined in [13]):

$$\Delta_{HM} = \max \left\{ \Delta_{HM,max} \times \left( 1 - \frac{d}{R} \right)^4 ; 0 \right\} \quad (7)$$

where  $\Delta_{HM,max}$  is the maximum value of HM that can be setup (in the middle of the cell);  $d$  is the distance between the serving MBS and the UE; and  $R$  is the radius of the serving MBS cell.

The parameters  $d$  and  $R$  can be easily obtained or determined neither by the network nor by the UE (see Figure 5). Especially when the FAPs are deployed in the networks, its exact position is user dependent and it is not known to the operator.

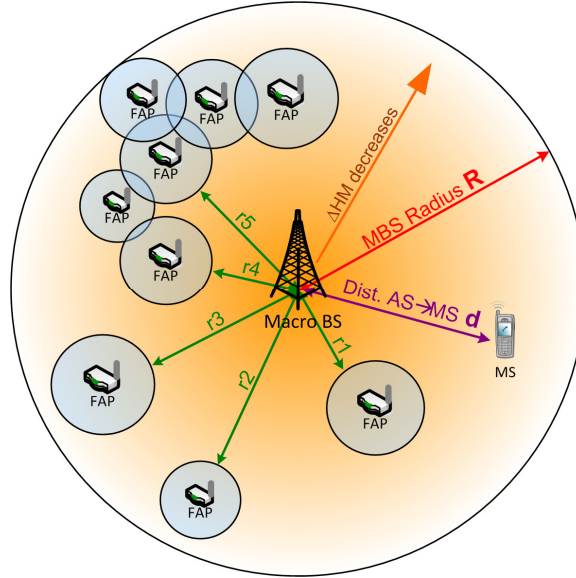


**Figure 5. Principle of adaptive hysteresis margin.**

Therefore, we propose to replace the parameters  $d$  and  $R$  by another metric that can be utilized more easily and efficiently.

The most of the path loss models describe the relation between the distance  $d$  of a UE from a cell and a path loss ( $PL$ ) in the following way:

$$PL(d) \sim X(f) + N \log_{10}(d) \quad (8)$$

where  $X(f)$  represents the dependence of the path loss model on the frequency and other terms usually used in the models; and  $N$  is the coefficient related to the type of the environment. Functions  $X(f)$  and  $N$  are dependent on the individual path loss model.

The level of the received signal strength at a specific distance ( $RSSI(d)$ ) depends on the path loss and the transmission power of the MBS ( $TP_{st}$ ) as defined in the next formula:

$$RSSI(d) = TP_{st} - PL(d) \quad (9)$$

Furthermore, the distance  $d$  can be expressed as an exponential function based on (8) and (9) as follows:

$$\begin{aligned}
 RSSI &= TP_{st} - (X(f) + N \log_{10}(d)) \\
 \log_{10}(d) &= \frac{1}{N} (TP_{st} - X(f) - RSSI) \\
 d &= 10^{\frac{1}{N} (TP_{st} - X(f) - RSSI)}
 \end{aligned} \tag{10}$$

Considering (10), formula (7) can be modified in the following manner:

$$\begin{aligned}
 \Delta_{HM} &= \max \left\{ \Delta_{HM,max} \times \left( 1 - \frac{10^{\frac{1}{N} \times (TP_{st} - X(f) - RSSI)}}{10^{\frac{1}{N} \times (TP_{st} - X(f) - RSSI_{min})}} \right)^{EXP} ; \Delta_{HM,min} \right\} \\
 &= \max \left\{ \Delta_{HM,max} \times \left( 1 - 10^{\frac{1}{N} \times (RSSI - RSSI_{min})} \right)^{EXP} ; \Delta_{HM,min} \right\}
 \end{aligned} \tag{11}$$

where  $EXP$  represents the exponent (in the former adaptive HM defined by (7) equal to 4); and  $\Delta_{HM,min}$  is the minimum HM that can be set up (in (7) equal to 0). The parameters  $EXP$  and  $\Delta_{HM,min}$  can influence the performance of the HM adaptation. The investigation of the optimal setting of both parameters is tackled later in this document.

The cell radius is typically defined as the distance where a minimal allowed level of RSSI, denoted as  $RSSI_{min}$ , is reached. The typical value of RSSI at the cell's edge equals to  $-90$  dBm [48]. However, in the case of the FAP, the cell radius is in order of tens of meters if the ITU-R P.1238 path loss model [49] is considered (see Figure 6). Note that the wall loss of 10 dB is included at house boundaries in Figure 6. The impact of the FAPs radius defined by different  $RSSI_{min}$  on the redundant handovers elimination is analyzed later in this chapter.

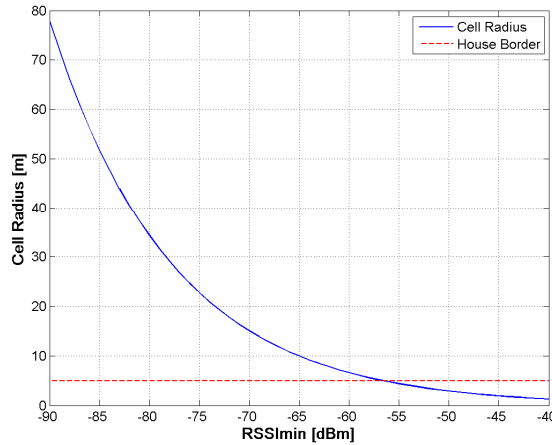


Figure 6. Cell radius over  $RSSI_{min}$  according to ITU-R P.1238 path loss model.

In fact, the border of the cells are neither regular circles nor hexagons since the system is not distance or signal level limited but it is interference limited. Therefore, the shape of the cells is strongly influenced also by the interference. Hence, we further investigate impact of implementation of CINR instead of RSSI for calculation of the actual level of  $\Delta_{HM}$ . Generally, a signal level influenced by the interference and noise ( $IN$ ) can be described according to the next equation:

$$CINR = TP_{st} - PL - IN = RSSI - IN \quad (12)$$

The CINR level is in different range of values than RSSI. Thereupon, it has to be related to the difference between maximum and minimum CINRs in the observed area. Thus, the actual  $\Delta_{HM}$  according to CINR is derived as follows:

$$\Delta_{HM} = \max \left\{ \Delta_{HM,max} \times \left( 1 - 10^{\frac{CINR_{act} - CINR_{min}}{CINR_{min} - CINR_{max}}} \right)^{EXP} ; \Delta_{HM,min} \right\} \quad (13)$$

where  $CINR_{act}$  is the actual CINR measured by the UE;  $CINR_{min}$  and  $CINR_{max}$  are minimum and maximum values in the investigated area respectively.

The actual CINR of a UE can be easily measured during UE's operation. It is usually performed with purpose of the handover decision and initiation. However, also the minimum and maximum CINR values have to be known for the utilization of the adaptive HM.  $CINR_{min}$  corresponds to the cell radius and to the CINR level at which the UE is able to receive data. Therefore, it is set up as a fix value for each FAP and MBS.  $CINR_{max}$  can be determined by two ways: i) measurement of CINR by a FAP at the point of its location; or ii) monitoring and reporting of CINR by all UEs connected to the given FAP and then selecting the highest CINR from all known values as the  $CINR_{max}$ . The first way implies to equip all FAPs with ability to measure CINR. Hence, it is not furthermore considered in the evaluations. The second approach utilizes the knowledge of previous CINR values in the area reported by the UEs. Since the channel is time variant, the time interval for selection of the  $CINR_{max}$  should be determined. The parameter  $CINR_{win}$  represents a number of the latest samples utilized for  $CINR_{max}$  derivation. The optimum value of  $CINR_{win}$  is analyzed later in this chapter.

Analogical modification as for adaptive HM can be done for adaptation of WS and HDT. Even if neither WS nor HDT are directly related to the signal level, both

influence the time spent by the UEs under the coverage of individual cells. Therefore, both influence the time of the handover decision. Due to the UEs movement, the time of the handover decision is related to the level of the signals received from all neighboring cells. The derivation of the actual values for both adaptive techniques is defined by the following equations:

$$WS = \max \left\{ WS_{max} \times \left( 1 - 10^{\frac{CINR_{act} - CINR_{min}}{CINR_{min} - CINR_{max}}} \right)^4 ; WS_{min} \right\} \quad (14)$$

$$HDT = \max \left\{ HDT_{max} \times \left( 1 - 10^{\frac{CINR_{act} - CINR_{min}}{CINR_{min} - CINR_{max}}} \right)^4 ; HDT_{min} \right\} \quad (15)$$

where  $WS_{max/min}$  and  $HDT_{max/min}$  are maximum/minimum levels of WS and HDT respectively.

### 5.1.2 PERFORMANCE EVALUATION OF ADAPTIVE TECHNIQUES

Evaluations of the modified adaptive technique are performed in the deployment of FAPs and MBSs along a direct street with a width of 8 m and a length of 500 m as defined in [44]. The vertical and horizontal distances between neighboring FAPs is 20 and 23 m respectively. Two MBSs are deployed 500 m from the middle of the street. The direct movement mobility model with the speed of 1 m/s is considered for the determination of the users' position. During the simulation, the users are equally distributed over the street width with spacing of 0.2 m. Major simulation parameters are summarized in Table 2.

Two metrics for the performance evaluation are monitored: i) amount of performed handovers, and ii) throughput in downlink. The amount of handovers is obtained as a number of all initiated handovers. It means, if all conditions for the handover initiation are fulfilled, handover is counted no matter if it is finished or not.

The throughput via wireless interface is supposed to be with no limitation caused by the FAP backhaul connection since the FAPs are supposed to be connected to the backhaul through a high speed optical fiber. Full buffer traffic model is assumed in the simulations to determine maximum throughput of the UEs.



**Table 2. Simulation setting**

Parameter	Value
Carrier frequency	2.0 GHz
Channel bandwidth	20 MHz
Noise spectral density	-174 dBm /Hz
Transmitting power of MBS/FAP	46 / 15 dBm
Number of MBSs / FAPs	1 / 50
Speed of outdoor UEs	1 m/s
CINR <sub>min</sub>	-3 dB
Number of simulation drops	25

### 5.1.3 RESULTS OF SIMULATIONS

Results of the performance of three adaptation techniques are presented in following subsections. All proposed algorithms are also confronted with the conventional techniques without adaptation.

#### 5.1.3.1 ADAPTIVE HYSTERESIS MARGIN

Determination of the optimal  $RSSI_{min}$  for the evaluation of the actual  $\Delta_{HM}$  is shown in Figure 7 and Figure 8. As the best performing  $RSSI_{min}$  value should be the one enabling maximum reduction of the amount of handovers simultaneously with minimum impact on the throughput. Based on both figures, the derived optimum  $RSSI_{min}$  is equal to  $-80$  dBm. The figures also show that the selection of inappropriate  $RSSI_{min}$  eliminates the positive effect of the adaptive HM on the amount of handovers (see e.g., the light blue curve with triangle marker for  $RSSI_{min} = -75$  dBm in Figure 7). Note that the  $x$  axis in all following figures in this section represents the actual value of  $\Delta_{HM}$  (or WS or HDT) for the conventional HM (or windowing or HDT). In the case of HM, WS or HDT with adaptation, the  $x$  axis expresses  $\Delta_{HM,max}$ ,  $WS_{max}$  or  $HDT_{max}$  (see equations (7) and (8)).

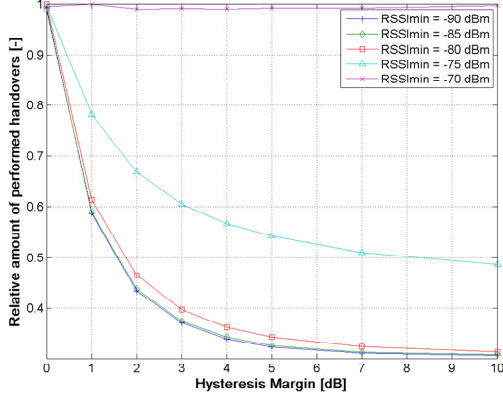


**Figure 7. Average amount of handovers over  $\Delta_{HM,max}$  for determination of optimum  $RSSI_{min}$ .**

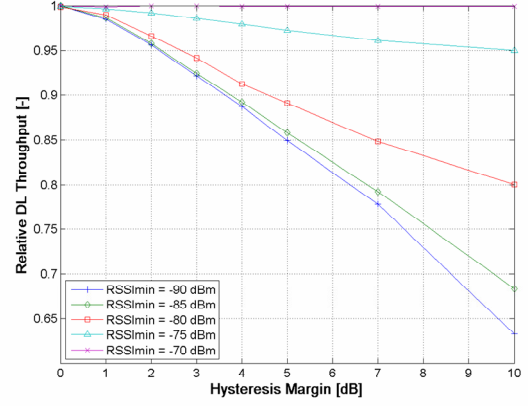


**Figure 8. Average DL throughput over  $\Delta_{HM,max}$  for determination of optimum  $RSSI_{min}$ .**

As stated before, the significant weakness of the RSSI based definition of the cell edge is that the system is largely influenced by the interference. The comparison of different approaches of actual  $\Delta_{HM}$  derivation is presented in Figure 9 and Figure 10. Both figures are analogical to Figure 7 and Figure 8. The optimum interval  $CINR_{win}$  as well as the comparison with RSSI based method and the conventional fixed (non-adaptive) HM can be observed from Figure 9 and Figure 10.

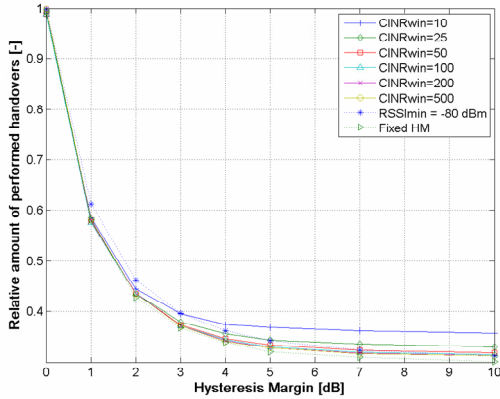


**Figure 9. Impact of different methods for determination of  $\Delta_{HM}$  on average amount of handovers.**

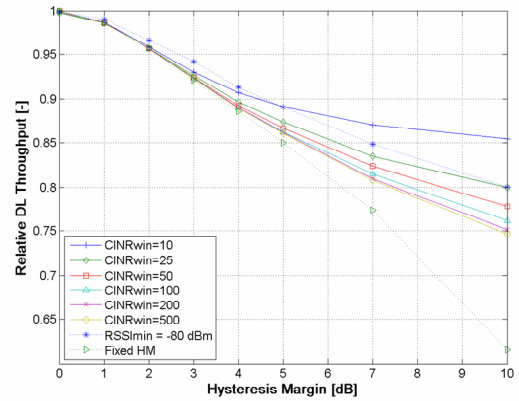
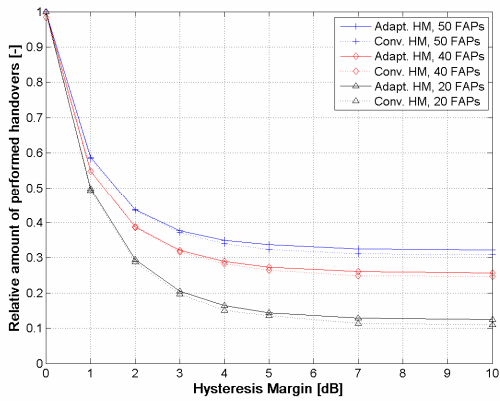


**Figure 10. Impact of different methods for determination of  $\Delta_{HM}$  on DL throughput.**

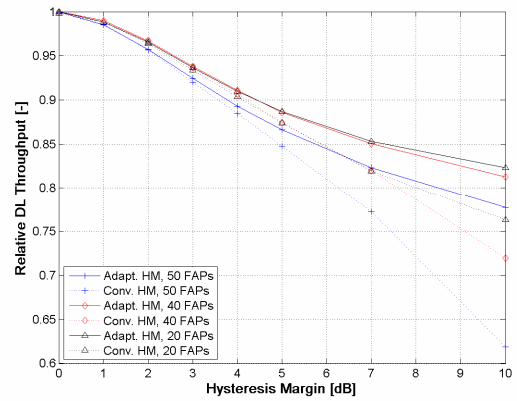
The utilization of CINR can achieve the same efficiency as the determination of  $RSSI_{min}$  while the CINR based approach is not so sensitive to the  $CINR_{win}$  since the impact of  $CINR_{win}$  on the number of handovers is negligible. Only a very low  $CINR_{win}$  leads to a decrease in the handover elimination efficiency. From the throughput point of view, the lower  $CINR_{win}$  is preferred. Nevertheless, its impact is minor. Comparing to the conventional fixed HM, the proposed solution reaches the same reduction of the

number of handovers with lower negative impact on the throughput. According to previous figures, roughly 25-50 samples can be determined as the optimum length of  $CINR_{win}$ .

So far, high density of FAPs (50 FAPs along a street with length of 500 m) was investigated. Figure 13 and Figure 14 show the impact of the adaptive HM on the throughput and the amount of initiated handovers for lower densities of FAP densities (40 FAPs and 20 FAPs along a street with length of 500 m). Lower density of the FAPs increases efficiency of both conventional as well as the proposed algorithms. In terms of the amount of initiated handovers, the results obtained by both ways are nearly the same with only marginally higher efficiency of the conventional approach (less than 2% for low density and high hysteresis). On the other hand, the increase in throughput is significant even for low density of FAPs and high hysteresis (up to roughly 6%). The efficiency of the proposed adaptive HM with relation to the conventional one increases with the density of FAPs. This is important conclusion for the future when a dense deployment of the FAPs is expected.



**Figure 11. Impact of conventional and adaptive HM on amount of handovers for different densities of FAPs ( $CINR_{win}=50$ ).**



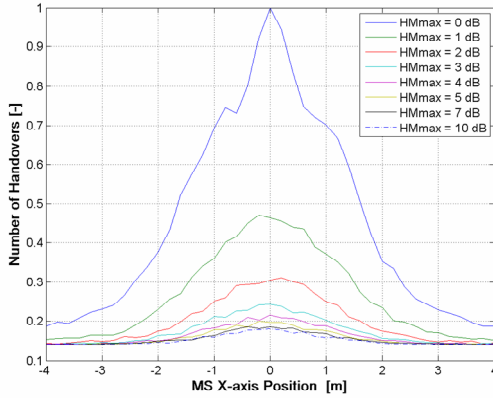
**Figure 12. Impact of conventional and adaptive HM on DL throughput for different densities of FAPs ( $CINR_{win}=50$ ).**

Figure 13 presents the distribution of an average amount of handovers over the street width for different levels of  $\Delta_{HM, min}$ . The number of handovers is average out over all simulation drops and over the whole street length. The figure contains results for CINR based adaptive HM for  $CINR_{min} = -3$  dB and  $CINR_{win} = 50$ . As can be observed, the amount of handovers significantly rises with the UE getting closer to the middle of the street since the difference among all CINRs from cells on both sides is very low. On

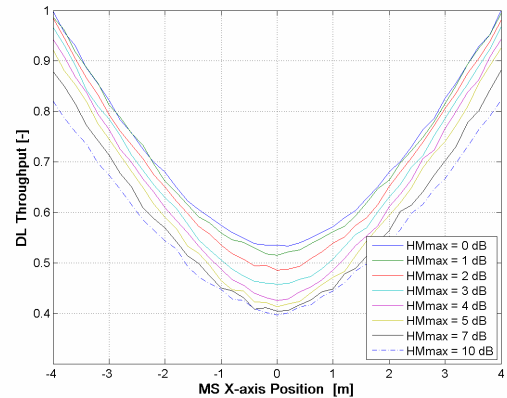
the other hand, the signal received from the FAPs at the same side as the sidewalk along which the UE is moving is distinctively higher than the signal from other cells. Therefore, the UE usually performs the handover only among adjacent FAPs. The elimination of the most handovers at the sidewalks is achieved even if the  $\Delta_{HM} = 2 \text{ dB}$  while the suggested value in the middle of the street is at least 4 dB (but rather 5 or 7 dB).

Figure 14 illustrates the dependence of the average DL throughput over the street width. The drop in the throughput when the UE is moving closer to the middle is obvious. The decrease in the throughput results from lower CINR received if the FAPs on both sides are roughly in the same distance.

Considering the results presented in Figure 13 and Figure 14, the optimum value on the sidewalks is  $\Delta_{HM} = 2 \text{ dB}$  as it eliminates almost all redundant handovers whilst throughput is not influenced. On the contrary, the optimum value in the middle of the street should be defined based on the priority either of the elimination of handovers or of the throughput. As an optimum  $\Delta_{HM}$  value should be selected roughly 5 or 7 dB. For this value, the number of the handovers reaches its minimum; however, the throughput is still decreasing uniformly. The tradeoff between elimination of the redundant handovers and throughput should be considered in the middle of the street.



**Figure 13. Average amount of handovers over the Street Width for CINR based adaptive HM.**

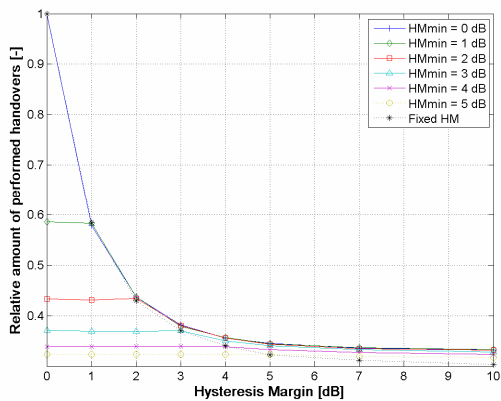


**Figure 14. Average DL throughput of UEs over the Street Width for CINR based adaptive HM.**

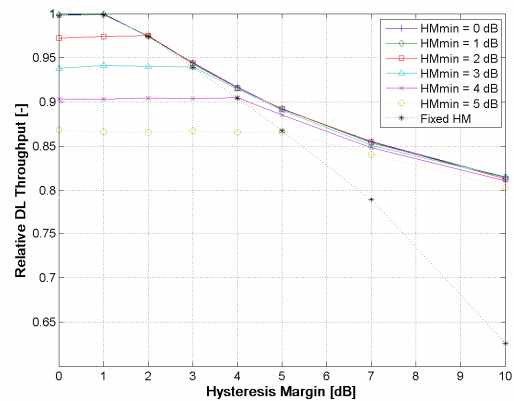
As the requirements on the  $\Delta_{HM,max}$  depends on the position within the street, the determination of the general optimum value of  $\Delta_{HM,max}$  in (11) should be done with respect to the usual distribution of the users along the street. In the most cases, only the pedestrians are assumed to exploit open/hybrid access since vehicular users spend very

short time in the FAP's cell due to higher speed. Hence, the major part of users should be placed on the sidewalks. Consequently, the value of 2 – 3 dB for  $\Delta_{HM,max}$  can be selected as the optimum value. Nevertheless, the same scenario can express also the boulevard where users are moving along the whole street width. In this case,  $\Delta_{HM,max}$  in range of 5 – 7 dB is more efficient since low values do not eliminate handovers efficiently enough.

The evaluation of the optimal values of the parameters  $\Delta_{HM,min}$  and  $EXP$  are performed in the same scenario as all previous simulations. The ratio of the eliminated handovers and the relative throughput for the determination of the optimal  $\Delta_{HM,min}$  are presented in Figure 15 and Figure 16 respectively. The throughput as well as the ratio of eliminated handovers are constant until  $\Delta_{HM}$  reaches the  $\Delta_{HM,min}$ . The selection of  $\Delta_{HM}$  over 1dB leads to the significant elimination of handovers; however the throughput is also decreased at least by 2.5% per 1dB. While  $\Delta_{HM,min} = 1dB$ , only less than 60% of handovers are performed (i.e., over 40% of handovers are eliminated) and simultaneously, absolutely no negative impact on the throughput is noticed. Thus,  $\Delta_{HM,min} = 1dB$  should be determined as the optimum value since all other values automatically results into some drop in throughput whereas maximum throughput can be still achieved for 1dB. Higher efficiency in the elimination of the redundant handovers while  $\Delta_{HM,min} = 1dB$  can be reached by selection of proper  $\Delta_{HM,max}$ .



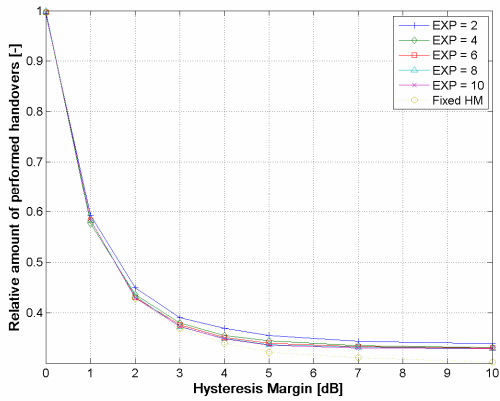
**Figure 15. Impact of different  $\Delta_{HM,min}$  values on the amount of performed handovers.**



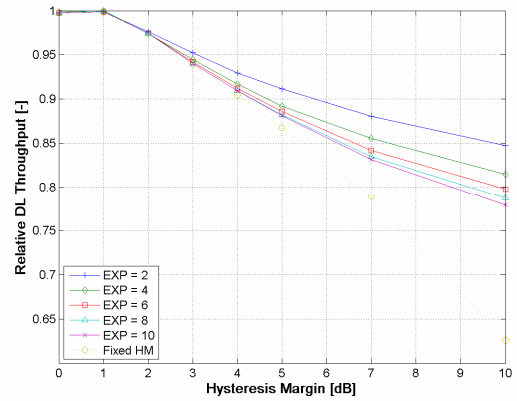
**Figure 16. Impact of different  $\Delta_{HM,min}$  values on the downlink throughput.**

Figure 21 and Figure 22 show the results of the amount of performed handovers and the downlink throughput for the derivation of the optimum  $EXP$  value respectively. As can be observed from Figure 21, efficiency of the elimination of the redundant

handovers is influenced only very slightly by varying  $EXP$  and it is increasing with  $EXP$ . No improvement is achieved for  $EXP$  higher than 4. The efficiency in the elimination of the redundant handovers is very close to the performance of the conventional fixed HM for all investigated values of  $EXP$ . The impact of  $EXP$  on the UE's throughput is also only minor especially for  $EXP \geq 6$ . Therefore, the  $EXP$  from range (2, 4) should be determined as the optimum value. Nevertheless, the  $EXP$  influences the performance of adaptive HM only insignificantly and there is a trade-off between the amount of performed handovers and throughput.



**Figure 17. Impact of different  $EXP$  values on the amount of performed handovers.**



**Figure 18. Impact of different  $EXP$  values on the downlink throughput.**

### 5.1.3.2 ADAPTIVE WINDOW SIZE

As it is depicted in Figure 19, the adaptive WS leads to the significant elimination of the performed handovers for low number of averaged samples (roughly up to 7 samples). Then the efficiency of the adaptive technique drops down and the handovers are performed more often. The decreasing efficiency for higher WS is due to the low radius of the FAPs. Thus, the signal received from the FAP rises and drops rapidly if the UE is moving. Therefore, the high WS leads to consideration of the samples obtained long time ago with respect to the small FAP radius and users' speed. These samples misrepresent the actual WS and thus the handover is initiated in improper places.

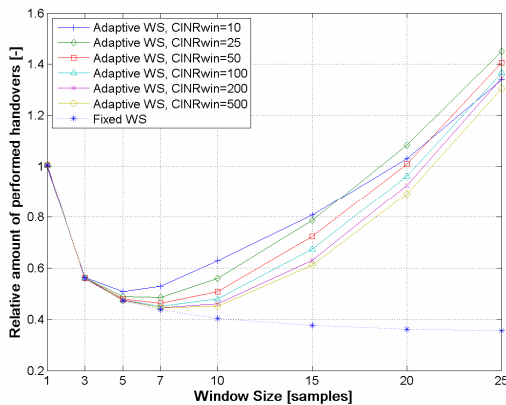
The impact of  $CINR_{win}$  is only minor for a short window. The optimum  $WS_{max}$  for the adaptive WS is roughly 7 samples since the ratio of performed handovers is the lowest. Further, the efficiency of handover elimination is rising with  $CINR_{win}$ . However,

the results for  $CINR_{win}$  equal to 50 and 500 samples are very close to each other at  $WS = 7$  samples.

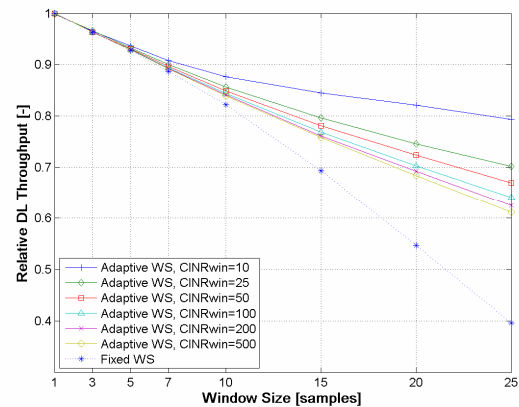
The ratio of the eliminated handovers behaves different for the conventional windowing with fixed amount of the averaged samples. In this case, the amount of the initiated handovers is continuously decreasing with growing WS. The efficiency improvement by approximately 6% is achieved if WS is increased from 7 to 25 samples. Comparing the conventional and the proposed adaptive windowing, Figure 19 does not proof any benefit in the elimination of handovers by implementation of the adaptive WS.

Figure 20 presents the impact of WS on the downlink throughput. This figure shows no considerable difference between the adaptive and the fixed WS size if WS value is up to 5 samples. Then, the proposed adaptive WS with shorter  $CINR_{win}$  is preferable since it leads to a gain in throughput.

By combining the results presented in Figure 19 and Figure 20, it can be observed that the optimum length of  $CINR_{win}$  is roughly 50 samples. Both figures further show some throughput gain of the adaptive WS. However this gain is at the cost of lower efficiency in handover elimination. Thus the adaptation of WS is not profitable comparing to the conventional fixed WS as it only increases complexity of the system and it does not introduce any considerable improvement in the performance.



**Figure 19. Impact of adaptive WS on the amount of initiated handovers.**



**Figure 20. Impact of adaptive WS on average DL throughput.**

### 5.1.3.3 ADAPTIVE HANDOVER DELAY TIMER

The impact of HDT adaptation on the amount of handovers and the downlink throughput is depicted in Figure 21 and Figure 22 respectively. The range of the HDT values up to 30 s ( $x$  axis in Figure 21 and Figure 22) can be considered since only pedestrians are assumed to perform handover to a FAP. The vehicular users do not spend enough time in the femtocell to complete whole handover.

Figure 21 shows that the most of handovers is eliminated by HDT equal to 2 s. Additional prolongation of HDT up to 6 s leads to moderate decrease of the handover amount. The HDT over 6 s does not eliminate any further noticeable portion of handovers.  $CINR_{win}$  influences the results only insignificantly if more than 10 samples are used.

The conventional as well as adaptive HDTs eliminate handovers with the similar efficiency except the  $HDT = 2$  s. For this value, the conventional HDT outperforms the adaptive one roughly by 5 %. Nevertheless, the efficiency of the handover elimination of both adaptive and fixed HDT can be considered as nearly the same for all other values of HDT.

As can be observed from Figure 22, increasing length of  $CINR_{win}$  decreases users' throughput. Hence the shorter length of  $CINR_{win}$  is suggested to eliminate throughput drop. Comparing the fixed and adaptive HDTs, significantly more negative impact on the throughput is caused by the technique with no adaptation. The adaptive HDT enables to reach significant gain in the throughput comparing to the conventional one. The gain noticeably rises with HDT duration.

Considering the results presented in Figure 21 and Figure 22, the optimum  $CINR_{win}$  is roughly 25 samples and the most efficient length of HDT is between 4 and 6 s. The adaptive as well as fixed HDTs achieve the similar level of the handover elimination. Nevertheless, the proposed adaptation of HDT enables throughput gain between 8 % and 13% for the optimum HDT and  $CINR_{win}$ .



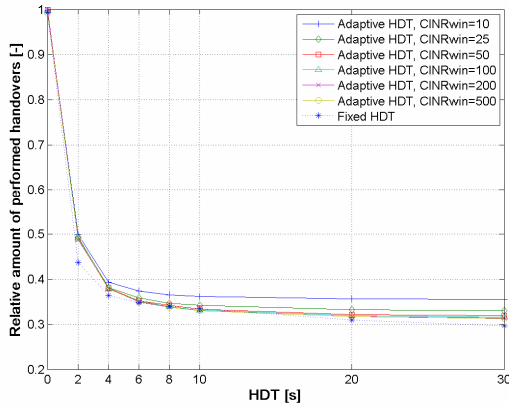


**Figure 21. Impact of adaptive HDT on the amount of initiated handovers.**

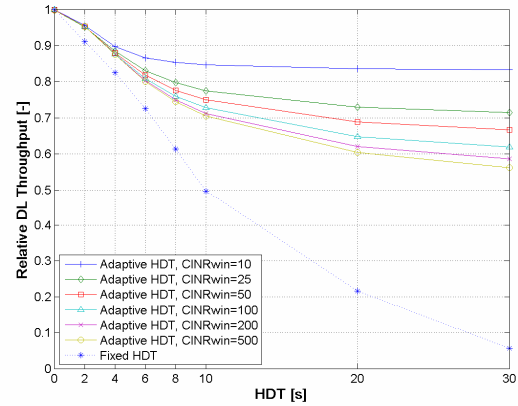


**Figure 22. Impact of adaptive HDT on the DL throughput of UEs.**

### 5.1.4 COMPARISON OF PERFORMANCE OF ADAPTIVE TECHNIQUES

Table 3 summarizes the performance of all three adaptive techniques with relation to the conventional non-adaptive ones. It is clear that the most profitable is the adaptation of HDT since it increases the throughput up to 13% while the same efficiency in the elimination of the redundant handovers as in the case of the conventional techniques is retained. Also the adaptive HM is profitable; however the throughput gain is not so significant. In the case of the adaptive HM, the gain in throughput increases with FAPs density. Contrary to the both previous techniques, the adaptive WS does not improve network performance since it increases throughput at the cost of decrease in the elimination of redundant handovers. Therefore, the same results can be achieved by modification of the parameter WS without adaptation. Optimum values of  $EXP$  belongs to the interval (2, 4). For  $HM_{min}$ , a value of 1 dB is the most efficient one. As only signal level parameters are considered for the adaptive techniques, the same procedures can be applied also to pico/micro cells.

**Table 3. Summarization of performance of adaptive techniques**

	Optimal value	Optimal $CINR_{win}$	Elimination of redundant HOs wrt non-adaptive	Throughput gain wrt non-adaptive
<b>Adaptive HM</b>	2 – 7 dB	25 – 50	Negligible decrease	0 – 3 % for low FAP density 0 – 6 % for high FAP density
<b>Adaptive WS</b>	~ 7 samples	~ 50	Decrease	Increase
<b>Adaptive HDT</b>	4 – 6 s	~ 25	Same	8 – 13 %

## 5.2 HANDOVER DECISION BY ESTIMATION OF THROUGHPUT GAIN

Algorithm using adaptation proposed in the previous section is very simple and requires neither any significant modification of the current standards nor any advance computation. In this section, we provide more complex solution for handover decision that is based on estimation of throughput gain acquired by performing handover to a FAP. This approach is further denoted as ETG (Estimation of Throughput Gain). The application of the novel technique involves several assumptions and requirements summarized in the next subsection.

### 5.2.1 NOTATION AND ASSUMPTIONS FOR ETG

To easy following the explanation of the ETG procedure, summarization of the parameters used in the description of ETG is presented in Table 4.

**Table 4. Notation of parameters used for description of ETG**

Symbol	Definition
$t_c, k_c$	Time in Cell. Mean time spent by users in the cell expressed as a time interval and number of signal level samples respectively. $t_c = (k_c - 1) \times t_s$ , where $t_s$ is the channel quality measurement and reporting period.
$k_{HO,in}, k_{HO,out}$	Index of signal samples respective to the time instant of the handover decision ( $k_{HO,in}$ ) and of hand-out from the serving FAP ( $k_{HO,out}$ ).
$s_{b,avg}, s_{f,avg}$	Estimated mean values of the signals received from the MBS and the FAP in the time interval $k \in \langle k_{HO}, k_2 \rangle$ .
$C_{FAP}$	Maximum capacity of the FAP available for outdoor user's limited by the backhaul.
$d_{UE,t_c}$	Data prepared for transmission by the UE during $t_c$ .
$g_{HO}$	Real gain in the signal level due to performing handover to the FAP.
$g_{HO,est}$	Estimated gain in the signal level due to performing handover to the FAP.
$T_{BS,est}, T_{FAP,est}$	Estimated transmission rate of the UE if it stays connected to the MBS and if it performs handover to the FAP respectively.
$G_{HO,est}$	Throughput gain without consideration of $C_{FAP}$ and $d_{UE,t_c}$ .
$TG_{HO,est}$	Throughput gain taking $C_{FAP}$ and $d_{UE,t_c}$ into account.
$\gamma_{Thr}$	Relative threshold for ETG handover initiation.
$bps_s$	Current bit rate experienced by the UE at the serving station.
$m_{Thr}$	Multiplier of $bps_s$ to determine $\gamma_{Thr}$ ; $\gamma_{Thr} = m_{Thr} \times bps_s$ .
$n_{conn}^{\min}$	Minimum amount of connections to a FAP that has to be performed before considering ETG in handover decision.

For implementation of our proposal, we assume the FAP's transmitting power set to a maximum value to maximize profit of the open access. The FAP's power control procedure change transmitting power only for purposes of balancing the interference level in the network. It means, the power control is initiated only in the case of a rapid change in interference, e.g., due to neighboring FAP's turn on/off.

### 5.2.2 PRINCIPLE OF ETG

The principle of the proposed ETG handover can be explained as follows. Let  $s_b(k)$  and  $s_f(k)$  represent the signal levels of the MBS and the FAP respectively. Both signals are obtained by periodic measurements and reporting of the signals transmitted by the MBS and the FAP. The signal level received by a UE is influenced by transmitting power of the MBS (denoted as  $P_{b,Tx}$ ) / the FAP (denoted as  $P_{f,Tx}$ ), by path losses ( $PL_b$ ,  $PL_f$ ), and by shadowing, fast fading, or measurement errors expressed by parameter  $u_b(k)$  /  $u_f(k)$  for the MBS / the FAP. Thus, the signal levels can be defined as:

$$\begin{aligned} s_b(k) &= P_{b,Tx} - PL_b(k) - u_b(k) \\ s_f(k) &= P_{f,Tx} - PL_f(k) - u_f(k) \end{aligned} \tag{16}$$

To eliminate random effects influencing signal level at the UE, the signal averaging is assumed. Rectangular window  $w(k) = 1$  for  $k \in (i, i - n_w)$  is considered for the sake of simplicity. Parameter  $n_w$  represents the length of the window. The signal levels used by the UE for the handover decision are obtained according to the next formulas:

$$\begin{aligned} \overline{s_b}(k) &= s_b(k) * w(k) \\ \overline{s_f}(k) &= s_f(k) * w(k) \end{aligned} \tag{17}$$

Conventional handover decision is based on comparison of the signal levels received from a potential target station ( $\overline{s_t}(k)$ ) with the signal level received from the serving station ( $\overline{s_s}(k)$ ), i.e., handover is performed if:

$$\overline{s_t}(k) > \overline{s_s}(k) + \Delta_{HM} \tag{18}$$

where  $\Delta_{HM}$  represents hysteresis margin. Signal levels  $\overline{s}_s(k)$  and  $\overline{s}_t(k)$  correspond either to  $\overline{s}_b(k)$  or to  $\overline{s}_f(k)$  depending on a type of handover as follows:

- $\overline{s}_s(k) = \overline{s}_b(k)$  and  $\overline{s}_t(k) = \overline{s}_f(k)$  for hand-in (handover from MBS to FAP);
- $\overline{s}_s(k) = \overline{s}_f(k)$  and  $\overline{s}_t(k) = \overline{s}_b(k)$  for hand-out (from FAP to MBS);
- $\overline{s}_s(k) = \overline{s}_f(k)$  and  $\overline{s}_t(k) = \overline{s}_f(k)$  for inter-FAP handover (between FAPs).

In the proposed ETG handover procedure, general condition for the handover initiation is defined as:

$$g_{HO} > g_{Thr} \quad (19)$$

where  $g_{Thr}$  is a predefined threshold for the handover initiation and  $g_{HO}$  is a gain in signal level. The overall profit in the signal level achieved by handover to the FAP ( $g_{HO}$ ) is proportional to the area limited by  $\overline{s}_b(t)$  and  $\overline{s}_f(t)$  from the time instant  $t_{HO,in}$  till  $t_{HO,out}$ , as depicted in Figure 23.

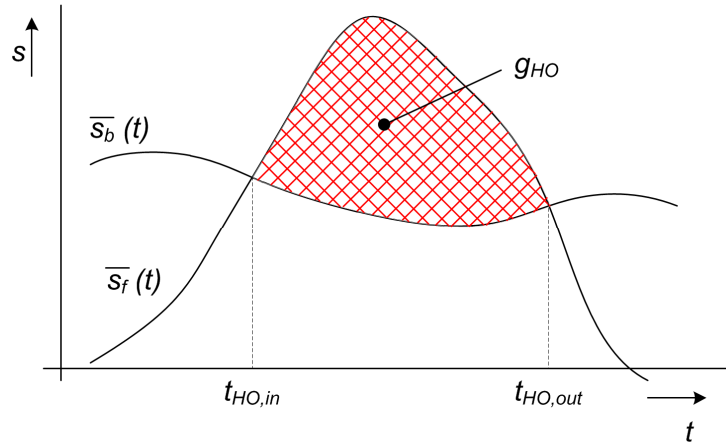


**Figure 23. Gain obtained by handover to a FAP.**

The gain  $g_{HO}$  is defined by subsequent equation:

$$g_{HO} = \int_{t_{HO,in}}^{t_{HO,out}} (\overline{s}_f(t) - \overline{s}_b(t)) dt \quad (20)$$

If discrete signal samples obtained by a periodic measurement are considered, the user's gain is expressed as:

$$g_{HO} = \sum_{i=k_{HO,in}}^{k_{HO,out}} (\overline{s_f(i)} - \overline{s_b(i)}) \quad (21)$$

where  $k_{HO,in}$  and  $k_{HO,out}$  correspond to the indexes of the signal samples obtained at  $t_{HO,in}$  and  $t_{HO,out}$  respectively.

Parameters  $\overline{s_b(k)}$ ,  $\overline{s_f(k)}$ ,  $k_{HO,in}$ , and  $k_{HO,out}$  must be found to determine  $g_{HO}$ . Parameters  $k_{HO,in}$  and  $k_{HO,out}$  represent the instants of the UE's entering and leaving the FAP respectively. In fact, exact knowledge of  $k_{HO,in}$  and  $k_{HO,out}$  is not necessary. Only the difference,  $k_c = k_{HO,out} - k_{HO,in}$ , is sufficient to be determined. In praxis, the parameter  $k_c$  represents a mean time spent by users in the cell of the FAP and it is expressed by amount of sampling periods.

An inaccuracy of  $k_c$  determination can be caused by different movement of users in the cell and by the variable speed of users. Considering low coverage radius of FAPs, the estimation of the throughput gain should be distinctively more precise comparing to the MBS since the difference between minimum and maximum time spent in the cell varies only slightly comparing to MBSs as derived in [50] (see Appendix).

Once  $k_c$  is derived, an estimation of the MBS's and the FAP's signal levels progress must be done. The estimation means a determination of  $\overline{s_b(k)}$  and  $\overline{s_f(k)}$  in interval  $k \in (k_{HO,in}, k_{HO,out})$ . The precise estimation of  $\overline{s_b(k)}$  and  $\overline{s_f(k)}$  over the whole interval  $k \in (k_{HO,in}, k_{HO,out})$  is very complicated since both signal levels are influenced by many random factors. For the sake of simplification and less computational complexity we propose to estimate the mean signal level received by the UE in the interval  $k \in (k_{HO,in}, k_{HO,out})$  from the MBS and the FAP. The mean levels of the signals are denoted as  $\overline{s_{b,avg}}$  and  $\overline{s_{f,avg}}$ . An inaccuracy of the signal level estimation can be compensated by selection of a proper threshold  $g_{Thr}$  for performing handover to the FAP and by its re-adjustment as explained later in this section.

Value of  $\overline{s_{b,avg}}$  is obtained by an extrapolation of  $\overline{s_b(k)}$  in the following way:

$$\begin{aligned} \overline{s_{b,avg}} &= s_b(k_{HO}) + \Delta_{s_b} \\ \Delta_{s_b} &= \frac{k_c}{2 \times i_{max}} \sum_{i=i_{min}}^{k_{HO, in}} \left[ (s_b(i+1) - s_b(i)) \times \left( \frac{i}{i_{max} - 1} \right) \right] \end{aligned} \quad (22)$$

where  $i_{max}$  is the number of the samples considered for the extrapolation; and  $i_{min} = k_{HO, in} - (i_{max} - 1)$ . For the evaluation of  $g_{HO, est}$ , it is necessary also to know  $\overline{s_{f, avg}}$ , which is calculated in the same way as  $\overline{s_{b, avg}}$ . If both estimated signal levels and  $k_c$  are known, the estimated gain  $g_{HO, est}$  is derived as:

$$g_{HO, est} = f_T \left( t_c \times (\overline{s_{f, avg}} - \overline{s_{b, avg}}) \right) \quad (23)$$

where  $f_T$  represents a transformation function for selection of appropriate MCS according to the received signal levels (see, e.g., [45]). The MCS is commonly determined based on interference. However, the interference is much more variable than the signal strength. Therefore, we do not consider interference in our proposal and an estimation of the interference is left for future research that can potentially further improve the performance of ETG at the cost of an increase in computational complexity.

So far, a limitation of FAP backhaul capacity was not considered for the estimation of the gain in signal level ( $g_{HO, est}$ ). Moreover, the handover should be performed only if the UE has data to be send during the connection to the FAP. To incorporate both limiting factors to ETG,  $g_{HO, est}$  must be translated to a gain in user's throughput ( $G_{HO, est}$ ) according to the next formula:

$$G_{HO, est} = (k_c \times (T_{FAP, est} - T_{BS, est})) \quad (24)$$

where  $T_{FAP, est}$  and  $T_{BS, est}$  are defined in Table 4.

The final estimated throughput gain with respect to the backhaul limitation and user's data is expressed by the following equation:

$$TG_{HO, est} = \min(C_{FAP}, d_{UE, t_c} G_{HO, est}) \quad (25)$$

Parameters  $C_{FAP}$  and  $d_{UE, t_c}$  are also explained in Table 4. Note that for pico/micro cells, the  $C_{FAP}$  is assumed to be above  $G_{HO, est}$  as the backhaul is dimensioned by operators to be able serve all radio transmissions.

Information on the available capacity of the backhaul of the FAP should be exchanged between the FAPs and the MBS. This information is delayed due to the transmission via FAP backhaul, which is of a lower quality than the backhaul of the MBSs. This delay is supposed to be roughly tens of milliseconds, which corresponds to the typical end-to-end packet delay for ADSL link [51], [52]. Taking into account the fact that only pedestrians are admitted to the FAPs, the delay of tens milliseconds leads to only negligible shift in users' position (tens of centimeters). Hence, the channel conditions can be considered as stationary during this very short period. Thus, the delay only postpones the decision on handover for tens of milliseconds and the estimation of the throughput gain is affected only insignificantly.

For the handover decision, throughput gain must be confronted with a relative ETG handover threshold ( $\gamma_{Thr}$ ). The threshold  $\gamma_{Thr}$  is related to the actual bit rate of the UE ( $bps_S$ ) and it is expressed as the multiple ( $m_{Thr}$ ) of the current bit rate experienced by the UE at the serving MBS. This can be defined by the following equation:

$$TG_{HO,est} > \gamma_{Thr} = bps_S \times m_{Thr} \quad (26)$$

The  $\gamma_{Thr}$  is used for the elimination of handovers to the FAPs, which offer only moderately higher throughput than current serving station. In this case, handover is not profitable due to a short break in user's connection and additional signaling overhead introduced by the handover initiation.

The level of an over/under-estimation of  $TG_{HO,est}$  in real networks is proportionally the same for all FAPs and MBSs as it is calculated in the same way for all of these entities. Thus the over/under-estimation of  $TG_{HO,est}$  can be reduced by re-adjustment of  $\gamma_{Thr}$  if more/less handovers to the FAPs are desirable, e.g., for the purpose of an MBS's offloading.

The evaluation of ETG handover conditions can be performed either once when the conventional handover conditions, expressed in (18), are met for the first time or continuously during the whole operation of the UE. In our proposal, the evaluation of ETG conditions is performed continuously. This way, an impact of rapid channel variations and an inaccuracy in signal levels estimation are reduced since these phenomena just postpone the handover for a certain time. In order to avoid negative affection of the accuracy of  $TG_{HO,est}$  by the postponing handover due to both factors, a

temporary  $k_{c,t}$  is used for derivation of  $TG_{HO,est}$ . The  $k_{c,t}$  is derived from  $k_c$  by subtraction of the time interval elapsed since the conventional handover conditions are fulfilled.

In real networks, the determination of  $k_c$  is done by an observation of the time spend by all UEs connected to individual serving cells in the past. Therefore, the minimum amount of finished connections ( $n_{conn}^{min}$ ) to the FAP is defined for each FAP. This parameter serves as a trigger for utilization of ETG handover. It expresses the minimum amount of inputs for derivation of  $k_c$  that must be collected before the  $k_c$  is considered as “accurate enough” to be exploited for ETG. Hence, ETG handover is considered only if the amount of finished connections is equal to or greater than  $n_{conn}^{min}$ .

In the case of the UE entering the area where more FAPs meet the conditions for handover initiation, i.e., more FAPs fulfill (26), the FAP with maximum  $TG_{HO,est}$  is selected as the target one. If no FAP fulfils ETG handover condition defined in (26) even if  $n_{conn}^{min}$  is reached, the MBS is selected as the target station. If the UE enters the location with more possible target stations before accurate  $k_c$  for each FAP in the area is set up (usually at the beginning of simulation or network operation), the selection of the target station is based on the conventional handover algorithm.

Since the FAPs are partially controlled by their users, an event such as occasional FAP’s turn-off should be addressed. In this case, the backhaul is used to inform the MBS and all adjacent FAPs about the change in a neighbor cell list. All adjoining FAPs should reinitialize the evaluation of  $k_c$  and disable ETG handover until  $n_{conn}^{min}$  is reached. Nevertheless, this event is assumed to appear very rarely and can be neglected.

### 5.2.3 ANALYTICAL EVALUATION OF ETG PERFORMANCE

For analytical evaluation, an MBS and a FAP are deployed in the scenario with mutual distance  $d_{MBS-FAP}$  as depicted in Figure 24. The users are moving along a direct street with random distance from the FAP, denoted as  $d_{UE-FAP}$ . The distance  $d_{UE-FAP}$  represents the shortest distance between the UE's movement and the FAP during a simulation drop. The performance is evaluated for  $d_{MBS-FAP}$  varying in range from 100 to 400 m. For each  $d_{MBS-FAP}$ , sixty drops with random speed of users, ranging between 0.97 and 1.74 m/s [53], are performed to average out obtained results. The distance  $d_{UE-FAP}$  is equally distributed for each  $d_{MBS-FAP}$ .



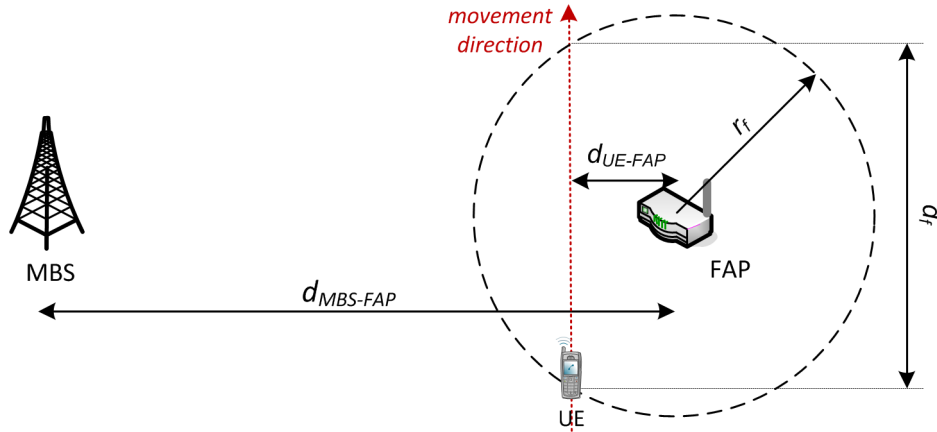


**Figure 24. Deployment for analytical evaluation.**

The outdoor users generate constant bit rate traffic during the simulations. Besides that, fixed indoor users are also considered to generate load of 4 Mbps to the FAP. The hybrid access with fifty percents of overall backhaul capacity assigned to the indoor users is applied. The rest of the capacity is dedicated to the outdoor users. The full backhaul capacity is 8 Mbps. In addition, two scenarios (1 Mbps backhaul with no indoor traffic and 8 Mbps backhaul with no indoor traffic) are evaluated to show the impact of the backhaul on the performance of the proposal. All major parameters used for the evaluation are summarized in Table 5.

**Table 5. Parameters for ETG evaluation**

Parameter	Value
Carrier frequency	2 GHz
Resource blocks per channel	100
Channel bandwidth of MBS and FAP	20 MHz
Noise Power Spectral Density	-174 dBm / Hz
Wall Penetration Loss	10 dB
Physical layer overhead	25 %
Outdoor UE speed	0.97 – 1.71 m/s [53]

First, an impact of  $m_{Thr}$  on the amount of performed handovers and on the throughput of outdoor users are depicted in Figure 25 and Figure 26 respectively. These figures are presented only to investigate an impact of  $m_{Thr}$  on the ETG performance. Therefore, all results in these figures are related to the maximum value obtained for individual level of offered traffic, and there is no relation to other competitive handover techniques.

The amount of initiated handovers decreases with increase in  $m_{Thr}$  until a minimum of the performed handovers is reached. The minimum number of handovers is equal to the number of handovers that have to be performed since the signal from the MBS becomes of a very low quality and it would lead to losing the connection of the UE to the network. In other words, if no handover would be performed in this situation, the UE will not be able to transmit data due to high interference from the neighboring cells. As the results show, the amount of performed handovers depends not only on the ETG threshold value, but also on the traffic offered by the UEs. For higher traffic load, a higher multiplier of the current bit rate of the UE,  $m_{Thr}$ , must be set up to reach maximum efficiency in the elimination of redundant handover. This is since achievable gain in throughput is the multiplication of  $m_{Thr}$  and the current bit rate of the UE, which is related to the offered traffic.

Contrary, an increase in  $m_{Thr}$  leads to only minor drop in the user's throughput. Lowering the throughput is the cost of avoiding the redundant handovers with low gain for users. This is due to a utilization of the channel, which is not of the best quality since the UE stays connected to the MBS although the signal from the FAP is better. Nevertheless, the impact of ETG algorithm on the mean throughput is only marginal (up to approximately 0.17% for  $m_{Thr}=10$  and 4 000 kbps of offered traffic).

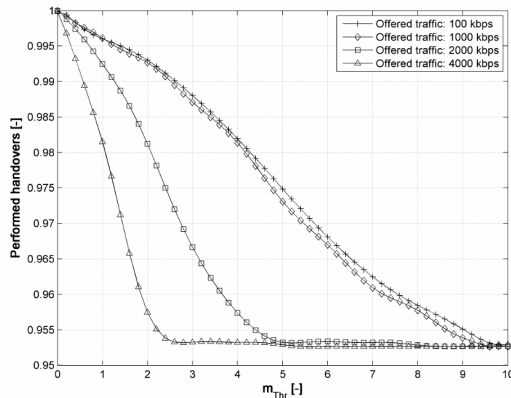


**Figure 25. Impact of  $m_{Thr}$  on amount of performed handover.**

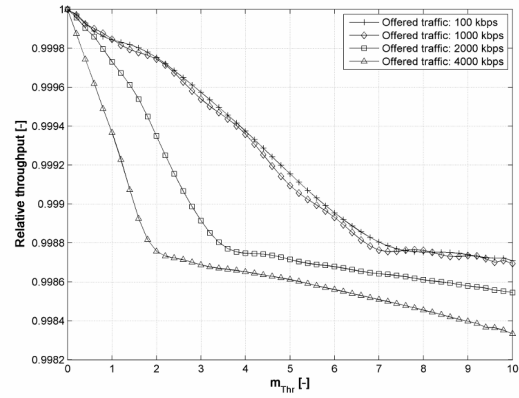


**Figure 26. Impact of  $m_{Thr}$  on relative throughput of outdoor user.**

As the previous results show, the efficiency of ETG depends on the traffic load offered by the UE and on  $m_{Thr}$ . Therefore, an optimal performance of ETG is reached by utilizing appropriate level of  $m_{Thr}$  with relation to the traffic offered by users. The optimum threshold value represents the value of  $m_{Thr}$  at which the most of handovers are eliminated while the throughput is still affected only marginally. In our case, it is the

value when the amount of performed handovers is nearly at its minimum. The optimum  $m_{Thr}$  is depicted in Figure 27. For determination of the optimum  $m_{Thr}$ , the tolerance of 0.5% of performed handovers is considered, i.e., the optimum corresponds to the value when the amount of handovers does not exceed minimum of the performed handovers plus 0.5%. As the results show, the higher  $m_{Thr}$  is profitable for low traffic offered by the UEs. This is because of the fact that higher  $m_{Thr}$  with low offered traffic eliminates all handovers that would lead to only minor gain in throughput. If lower  $m_{Thr}$  would be set up, handovers with only minor gain would be also initiated due to low traffic offered by users. On the other hand, an increase in UE's traffic decreases optimum  $m_{Thr}$  since even low  $m_{Thr}$  leads to the higher threshold if a user offers more traffic.

The optimum  $m_{Thr}$  is also influenced by the backhaul capacity and by the indoor traffic. If more backhaul capacity is available for the outdoor UE, the optimum performance is achieved for higher value of  $m_{Thr}$  as low  $m_{Thr}$  would lead to a lower efficiency in the elimination of the redundant handovers. For the backhaul of very low capacity, the high  $m_{Thr}$  simultaneously with high level of the traffic offered by the outdoor UE is useless since the backhaul is not able to serve all user's data. Contrary, the higher amount of the traffic generated by the indoor UE leads to lowering the optimum  $m_{Thr}$ . This is due to the consumption of a part of the FAP's radio resources by the indoor UE. Consequently, fewer resources are available for the outdoor UE and the gain introduced by handover to this FAP is lower. Therefore, lower value of  $m_{Thr}$  is sufficient to eliminate all redundant handovers.

In praxis, the optimum value of  $m_{Thr}$  can be determined individually for each UE as backhaul load, indoor traffic, and the UE's offered traffic are known to the network.

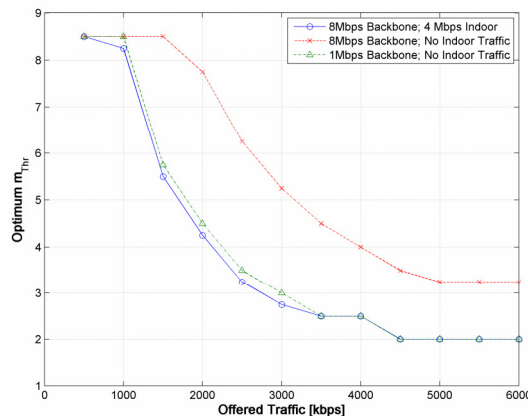


**Figure 27. Optimum  $m_{Thr}$  over traffic offered by outdoor user.**

Comparison of the ETG performance with the conventional hysteresis and with so called Moon's algorithm [15] is presented in Table 6. The table shows the ratio of served outdoor traffic and the ratio of the performed handovers. The ratio of the served traffic represents a proportion between the traffic load offered by the UE and the real traffic transferred by this UE. All results are related to the situation when no techniques for the elimination of the redundant handovers are used (i.e., the conventional handover algorithm with  $\Delta_{HM} = 0dB$ ). For ETG, the results represent the values corresponding to the optimum threshold  $m_{Thr}$ . Note that the impact on the throughput and the amount of performed handovers is roughly the same for all levels of the offered traffic if the optimum  $m_{Thr}$  is set. The values in parentheses show the difference between ETG and other competitive techniques. Comparing ETG with the conventional hysteresis, the hysteresis can eliminate significant amount of the redundant handovers; however, it is associated with noticeable lowering of the user's throughput. ETG is able to eliminate significant part of the redundant handovers as well. Moreover, the user's throughput is nearly unaffected since only those handovers that promise marginal profit for the UEs are eliminated. Therefore, if the same ratio of the redundant handovers is eliminated by ETG as well as by the hysteresis with  $\Delta_{HM} = 5.25 dB$ , the gain of more than 2.5% in the mean user's throughput is introduced by ETG. Another interpretation is that ETG eliminates about 13% more handovers comparing to the hysteresis if both techniques reaches the same throughput ( $\Delta_{HM} = 3.1 dB$ ). It means, additional roughly 47% of handovers are eliminated comparing to the conventional hysteresis.

Table 6 further shows that Moon's algorithm is outperformed by the ETG very significantly. Moon's algorithm causes significant drop in throughput simultaneously with lower efficiency in elimination of redundant handovers.

**Table 6. Comparison of ETG performance with competitive algorithms**

Handover algorithm	Served traffic [%]	Ratio of handovers [%]
ETG	<b>99.87</b>	<b>65.66</b>
Hysteresis; $\Delta_{HM} = 1dB$	99.99 (+0.12)	93.16 (+27.50)
Hysteresis; $\Delta_{HM} = 3dB$	99.97 (+0.10)	79.27 (+13.61)
Hysteresis; $\Delta_{HM} = 3.1dB$	99.85 (-0.02)	<b>78.72 (+13.06)</b>
Hysteresis; $\Delta_{HM} = 3.75dB$	99.05 (-0.82)	74.44 (+8.78)
Hysteresis; $\Delta_{HM} = 5.25dB$	<b>97.36 (-2.51)</b>	65.78 (+0.12)
Moon	<b>95.81 (-4.06)</b>	<b>78.72 (+13.06)</b>

So far, an exact estimation of the  $k_c$  based on the perfect knowledge of the cell radius was assumed. Therefore, an impact of an inaccuracy in the determination of this parameter has to be evaluated to meet realistic conditions in the real networks. An inaccuracy is understood as an error in the determination of  $k_c$ . It can be caused, for example, by movement of the UEs in different distances from the FAP or by variable speed of users. Amount of the performed handovers and the UE's throughput over the deviation of  $k_c$  are illustrated in Figure 28 and Figure 29 respectively. The  $x$ -axis represents maximum error in the estimation of  $k_c$  (denoted as  $\epsilon$ ) related to the exact knowledge of the cell radius. The individual error in  $k_c$  is then defined by uniform distribution in interval  $(-\epsilon, +\epsilon)$ . Both figures show that high estimation error lowers the amount of the performed handovers. This implies that the high  $\epsilon$  leads to the underestimation of the real gain in throughput and thus additional handovers are eliminated. However, this is at the cost of a drop in user's throughput. Comparing to the results of the competitive techniques presented in Table 6, the drop in throughput is still very low. Even if the estimation error is up to  $\pm 100\%$ , the relative throughput (or ratio of served traffic) is decreased by additional roughly  $0.85\%$  comparing to the optimum determination of  $k_c$  (see Figure 29). The similar results for the drop in the ratio of served traffic are obtained by the conventional hysteresis with  $\Delta_{HM} = 3.75dB$  (see the difference between ETG and hysteresis in parenthesis in Table 6. However, roughly  $65\%$  and  $75\%$  of handovers are initiated using our proposed algorithm and the conventional hysteresis respectively. In addition, another  $13\%$  of handovers are not performed due to the error in  $k_c$  and thus, only  $57\%$  is initiated. Therefore, even if error in  $k_c$  estimation is in range of  $\pm 100\%$ , the ETG eliminates additional  $18\%$  of handovers comparing to the conventional hysteresis if both causes the same drop in throughput.

Both Figure 28 and Figure 29 further show that the impact of the estimation error on the throughput as well as on the amount of handovers is nearly independent on the offered traffic loads.

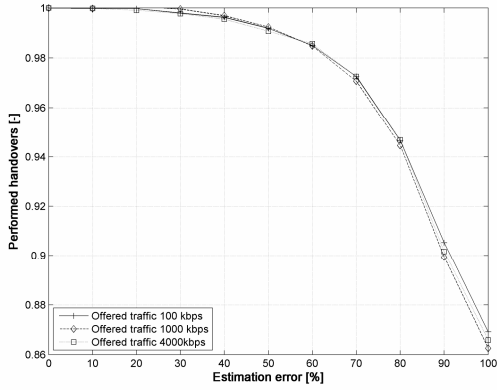


**Figure 28. Impact of error in estimation of  $k_c$  on the amount of performed handovers.**

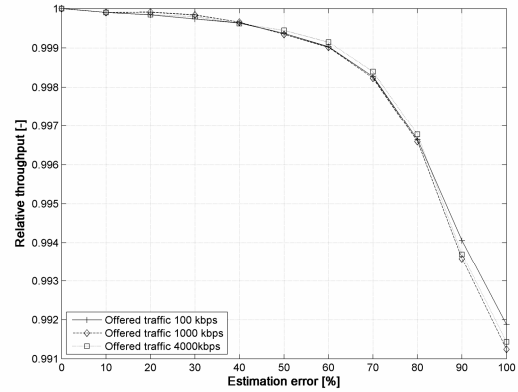


**Figure 29. Impact of error in estimation of  $k_c$  on throughput of users.**

### 5.2.4 EVALUATION OF ETG PERFORMANCE BY SIMULATIONS

Analytical evaluations show higher performance of the ETG comparing to the competitive schemes. However, the performance can be influenced by determination of  $k_c$ . Additionally, more UEs simultaneously connected to a FAP can influence the results. Therefore, we perform simulations for multiplied two stripes scenario with 5x5 blocks of flats (see Figure 30). This multiplication is used to fully exploit UEs mobility in the observed area. The FAPs density is equal to two FAPs per a block of twenty flats, i.e., 10% of flats are equipped with a FAP. Flats equipped with FAPs and the FAPs' position within the flats are generated randomly with uniform distribution.

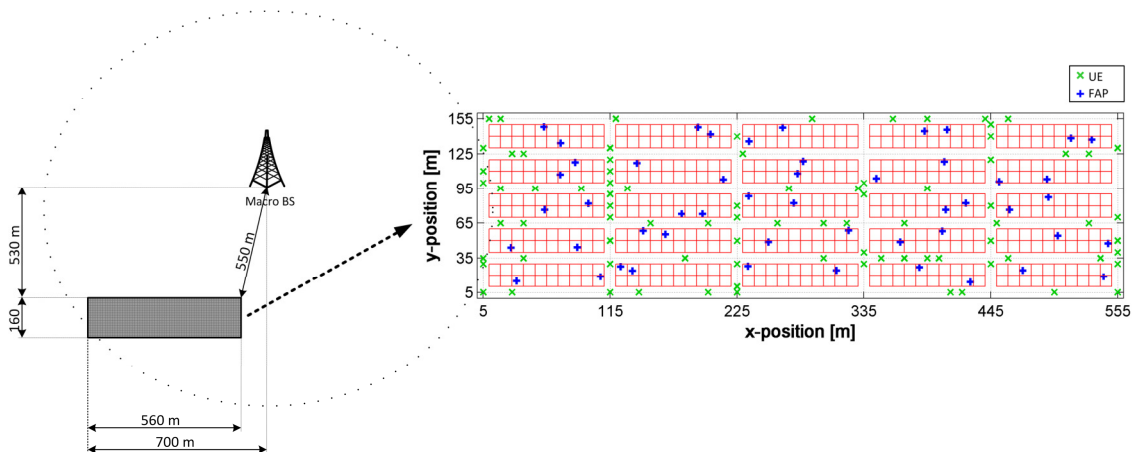


**Figure 30. Example of simulation deployment for evaluation of ETG.**

Each UE generates constant bit rate traffic of randomly selected level. The level of the offered traffic for each UE is generated according to lognormal distribution with mean of 100 kbps over all UEs.

The major simulation parameters are summarized in Table 7.

**Table 7. Simulation parameters for evaluation of ETG**

Parameter	Value
Carrier frequency	2.0 GHz
MBS / FAP transmitting power	46 / 15 dB
Number of MBSs / FAPs	1 / 50
Number of outdoor UEs	50
Speed of outdoor UEs	1 m/s
Wall penetration loss	10 dB
Noise spectral density	-174 dBm / Hz
Speed of outdoor UEs	0.97 – 1.71 m/s [53]
Simulation step	1 s
Simulation real-time	10 800 s

We perform also a simulation of Adaptive HM under the same simulation scenario and deployment to compare both proposed algorithms. The results observed from the simulations are summarized in Table 8. The served traffic as well as the ratio of handovers are related to the situation, when no technique for the elimination of the redundant handovers is used (i.e.,  $\Delta_{HM} = 0$  dB and each UE is connected to the best cell at each time). In other words, 100% of the served traffic or handovers is the value reached by a simulation run with all techniques for the handover elimination disabled. Since each UE in the simulation offers different amount of traffic, we set constant  $m_{Thr}$  over the whole simulation for all UEs. Levels of  $m_{Thr}$  equal to 2 and 3 are selected since those reach similar level of served traffic as the adaptive hysteresis. The constant  $m_{Thr}$  is the simplest way of management but it also slightly decreases efficiency of the ETG. Particular assignment of individual  $m_{Thr}$  for each UE according to its bit rate should slightly reduce overall amount of the performed handovers as presented in 5.2.3. Thus our presented scenario is the worst case scenario from the performance point of view; however, it is also the simplest for implementation.

The results show similar performance of ETG and adaptive hysteresis in term of the served traffic. Both outperform the conventional hysteresis by roughly 1.5% of the served throughput. The adaptive hysteresis reaches the same level of the performed

handovers as the conventional hysteresis. Therefore, it confirms its profit in throughput while nearly no change in the amount of the initiated handovers is reached. This corresponds to the conclusion obtained by the simulations of adaptive hysteresis in section 5.1 for the direct street scenario. Contrary, ETG can introduce a gain in the amount of the eliminated handovers even if a gain in the throughput is still ensured. If the conventional hysteresis with  $\Delta_{HM} = 3dB$  and ETG with  $m_{Thr} = 2$  are compared, ETG increases the amount of the transferred traffic by roughly 1.4% and additional 24.45% of handovers is eliminated (i.e., more than double amount of handovers are eliminated). Comparing the conventional hysteresis with  $\Delta_{HM} = 5dB$  and ETG with  $m_{Thr} = 3$ , the gain in throughput by ETG is nearly 2% and additional 19.64% of handovers is eliminated (roughly 85% increase in the handover elimination efficiency).

**Table 8. Simulation results for corporate scenario**

Handover algorithm	Served traffic [%]	Ratio of handovers [%]
Hysteresis; $\Delta_{HM} = 3dB$	91.93	78.10
Hysteresis; $\Delta_{HM} = 5dB$	85.43	65.36
Adaptive Hysteresis; $\Delta_{HM,max} = 3dB$	93.29	78.12
Adaptive Hysteresis; $\Delta_{HM,max} = 5dB$	86.97	65.66
ETG; $m_{Thr} = 2$	93.28	54.67
ETG; $m_{Thr} = 3$	87.27	45.72

### 5.2.5 DISCUSSION OF BACKHAUL OVERHEAD DUE TO ETG HANDOVER

The cooperation among the FAPs and the MBSs via backhaul must be established to use ETG. The cooperation is used for an exchange of information on the FAP backhaul status to determine maximum available backhaul capacity for the users. Only this information has to be delivered to the MBSs for ETG purposes and it should be available at the MBS in the time instant of the handover decision. Therefore, the reporting of the backhaul status interval should be similar to the reporting period of channel quality. In LTE-A, the channel quality reporting period can range between 2 ms and 160 ms [54]. Considering the worst case, the FAP's load must be reported each 2 ms, i.e., 500 reports per second must be sent to the MBS. The size of the backhaul load report should be in tens of bites as the report contains only the indoor traffic load and the maximum backhaul capacity. Therefore, the maximum overall backhaul overhead of ETG procedure is couple of kbps in the worst case scenario.



Further, an overhead can be generated due to the FAPs' switch-off or switch-on. For this purpose, only a message with FAP's ID is delivered to all neighboring FAPs to inform them about this event. Even if the amount of neighbors would be high (e.g., tens of FAPs), still the overhead in kilobits (tens of FAPs multiplied by tens of bits per message) is generated only very rarely, since frequent turning-on and off the FAP cannot be expected. Both parts of the backhaul overhead can be neglected considering the conventional backhaul capacity in megabits.

### **5.3 CONCLUSION**

Two algorithms for elimination of the redundant handovers are proposed. The first group, adaptive techniques, is based on exploitation of only parameters conventionally observed and monitored by the network. As the results show, the most profitable is the adaptive HDT since it increases the throughput up to 13% while the same efficiency in the elimination of the redundant handovers as in the case of the conventional techniques is achieved. The adaptive HM also outperforms the conventional hysteresis. Nevertheless, a profit of the adaptive HM is lower comparing to the gain introduced by the adaptive HDT. Contrary to the both previous techniques, implementation of the adaptive WS does not improve network performance. On one hand, the adaptive WS increases throughput. On the other hand, the gain in throughput is at the cost of lower efficiency in the elimination of redundant handovers. Therefore, the same results can be achieved by modification of the parameter WS without adaptation.

The second algorithm is based on the estimation of the UE's throughput gain acquired if handover to a FAP is accomplished. This approach is applicable on handover performed to a small cells due to its low radius. The results show high efficiency in the elimination of the redundant handovers while only negligible drop in the users' throughput is observed. As well, the proposed handover decision algorithm implies nearly no additional signaling overhead transmitted by the FAP to the MBS via backhaul. Comparing the proposed algorithm with competitive algorithms, the proposed one provides higher efficiency in reducing the amount of performed handovers while it enables to keep higher throughput of users.

## 6 FAST CELL SELECTION

A solution for ensuring the seamless handover consists in soft handover or FCS. The major difference between both solutions lies in a way of transmission between a UE and neighboring cells included in its active set. In the case of soft handover, all cells in the active set transmit data simultaneously and the receiver combines all data in a macro diversity manner. Contrary, FCS offers means for the UE and/or the networks to decide, which cell in the UE's active set is really going to send data in the next Transmission Time Interval (TTI). To that end, FCS selects and updates the best cell for the transmission at each transmission interval. Thus, the same data are not sent multiple as in the case of soft handover.

Soft handover is known as a CDMA specific technique, which cannot be ported into OFDMA-based systems unless particular algorithms are used at the physical layer in order to achieve cooperation among the MBSs. FCS is actually a technique derived from CDMA soft handover. Consequently, its implementation into OFDMA-based system with small cells requires specific modification at physical layer as well. We focus on FCS since it implicate less complex requirements on UEs than soft handover.

As mentioned before, FCS in networks with small cells introduces new risks related to the small cell radius and to the limited backhaul (in case of the femtocells). Therefore, we first evaluate performance of the networks with small cells to show whether FCS implementation to the networks with the small cells is even feasible and if a gain in the network performance could be expected.

### 6.1 FCS IN OFDMA NETWORKS WITH SMALL CELLS

The first requirement that the OFDMA system has to fulfill for FCS is a time synchronization among cells in the network, as mentioned earlier. Without proper synchronization, only the conventional hard handover is possible, where the UE needs to re-synchronize itself on the target cell after each handover. Synchronizing the system

allows to see FCS as a specific case of joint scheduling, where a set of cells collaborate in such a way that at each TTI, only the best cell in the set can schedule data toward the UE. In the case of TDD, the time synchronization of the small cells could typically be derived from the umbrella MBS. Then each cell in the active set needs to receive the integral data to be scheduled toward the UE. This principle introduces redundancy. However, it allows reaching high rates of the cell switching, without flooding networks with handover events.

Because OFDMA systems such as LTE or LTE-A do not address the notion of soft handover with the active set of cells serving a given UE, a solution is needed to allow several MBSs or small cells to participate in the active set in such systems.

Once a radio bearer is established for a UE with one cell in the data path, then it should be possible to add and remove additional contributing cells. This introduces the notion of a “serving” cell in the active set, which assumes a particular role, as opposed to a simple contributor cells. The standard handover procedures still apply whenever the serving cell in the active set is shifted from a source one to a target one. Figure 31 illustrates required modifications for introducing FCS into LTE-A architecture with small cells.

New procedures should be defined in order to allow including or removing contributing cells to or from the active set. When a contributor cell is added to the active set, then the serving gateway (S-GW) should be notified and it should duplicate packets toward the new cells in the downlink. Similar mechanisms must be proposed for the uplink so that contributing cells may take over a role in both uplink and downlink. In this thesis, we focus on downlink.

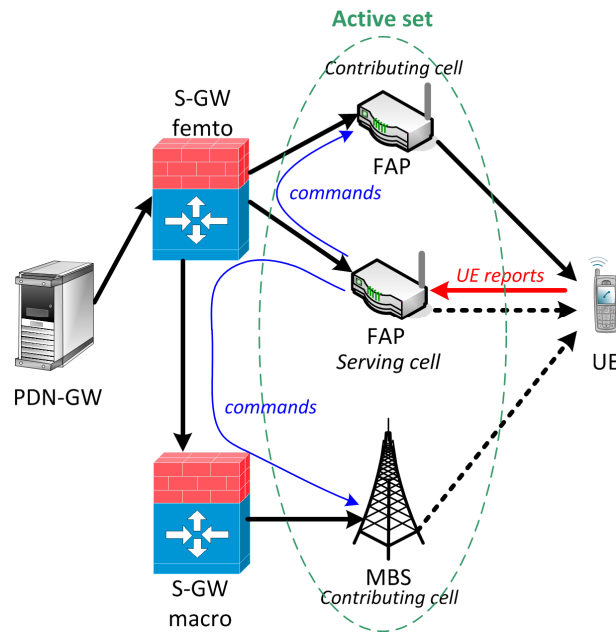


**Figure 31: Possible introduction of Fast Cell Selection into LTE-A architecture.**

The serving small cell or MBS should be in charge of adding and removing additional contributing cells to the active set. Conventionally, this decision is based on measurement reports received from the UE, as it is the case for the hard handover decision itself. A novel algorithm for the active set management is proposed later in this chapter to improve efficiency of FCS.

If the serving cell is shifted from a source one to a target one, then the set of contributing cells should be delivered from the source cell to the target cell as a part of the UE context. Once a successful handover has been achieved for a UE, then the target cell is free to maintain or modify the set of the contributing cells used by the former serving cell.

A solution should also be proposed in order to let the contributing cells know if they are elected to schedule data toward the UE for a given TTI. The solutions defined in the context of 3GPP release 99 are CDMA specific and cannot be applied outside this context. The most natural solution is to let the serving cell communicate this information to the contributing cells on the basis of the UE measurement reports. The serving cell should provide (and update) the list of contributing cells to the UE for this report. Since we mainly assume slow moving UEs, reporting periodicity may be set low enough to maintain low overhead. The nature of the signal level measurement reports should also be a part of the report configuration. In the simplest case, which is also the

most economical one in terms of uplink bandwidth consumption, only the index of the best cell should be sent. If a maximum number of cells in the active set is, for example, 8 cells, only 3 bits are required for addressing those cells.

The serving cell should exploit FCS measurement reports from the UE in order to decide, which cell in the active set will actually be in charge of scheduling data to the UE. Whenever a modification is decided in this respect, the decision should be communicated to the involved contributing cells. This command from the serving cell to the contributing cells should just include the ON/OFF boolean value, together with the reference of the next TTI where this update should be applied.

Table 9 gives a summary of procedures to be added for supporting FCS in current OFDMA-based systems with small cells.

**Table 9. Procedures for FCS support in OFDMA-based networks with small cells**

From	To	Message purpose	Message content
Serving cell	S-GW	Add a contributing cell	Identification of cell to be added
Serving cell	S-GW	Remove a contributing cell	Identification of cell to be removed
Serving cell	UE	Define/update FCS measurement report	Measurement period Measurement content as an index in pre-defined list
UE	Serving cell	FCS measurement report	Measured value
Serving cell	Contributing cell	FCS command	ON/OFF value Identification of next bit of data to be sent (if the contributing cell is turned on)

In the following subsections, the performance of the networks with small cells is evaluated to show whether FCS implementation to the networks with small cells is even feasible and if a gain could be expected.

### 6.1.1 SYSTEM MODEL FOR FCS PERFORMANCE EVALUATION

From the performance evaluation point of view, a difference between the femto and pico/microcells, consists in the capacity of the small cell backhaul. To avoid of mixing all terms, we use the term "small cell" with meaning of the "femtocell" and "pico/microcell" if the backhaul is limited and unlimited respectively. By unlimited backhaul is understood the backhaul able to serve all radio traffic; it means, if the

backhaul capacity exceeds the radio capacity. In our simulations, the "unlimited" backhaul is represented by the backhaul capacity of 100 Mbps.

We assume co-channel deployment of the small cell and MBSs, i.e., all small cells shares the same frequency bandwidth as the MBSs. This deployment is more challenging in term of interference mitigation as all cells interfere to each other. Furthermore, co-channel deployment is more efficient in spectrum usage (higher reuse of frequencies).

For the evaluation, a rural scenario with fifty randomly deployed houses within an MBS is considered according to recommendations defined by the Small Cell Forum [43]. All houses are of a square shape with a size of 10x10 meters as depicted in Figure 32. Each house is equipped with one randomly deployed small cell and one indoor UE. The indoor UE moves in line with the probabilistic waypoint mobility model based on [55]. For this model, several points of stay and a point of decision are defined. In the point of decision, the indoor UE randomly chooses a point of stay with equal probability for all points. The time spent in the point of stay is generated according to the normal distribution taken over from [55]. Beside indoor UEs, also one hundred outdoor UEs are randomly dropped in the simulation area. All outdoor UEs follow PRWMM [41] with a speed of 1 m/s.

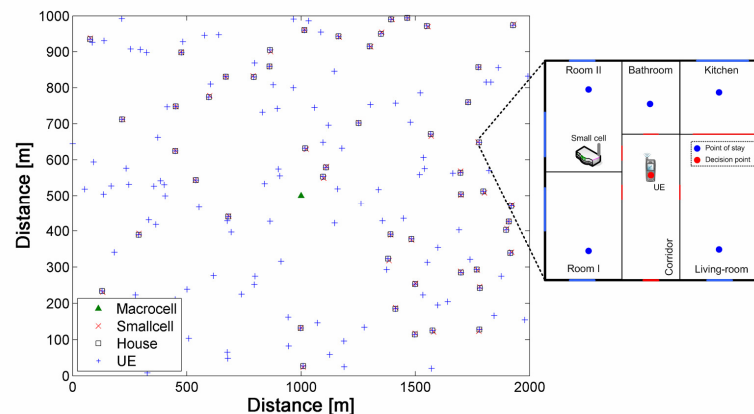


**Figure 32. Simulation deployment and model of a house.**

The channel models are also based on the recommendations of Small Cell Forum presented in [43]. The path loss is modeled according to ITU-R P.1238 and Okumura-Hata for communication with small cells and macrocells respectively. The channel in simulations is influenced also by shadowing with a standard deviation of 8 dB and 4 dB for MBSs and small cells respectively. The transmitting power of the MBS is set to 46

dB while the small cells transmit with 15 dB. Wall losses of 10 dB and 5 dB per outer and inner walls are also considered.

To minimize effects of randomness of all models, ten simulation drops with a duration of 7200 s of real-time per a drop are evaluated and averaged out.

For data transmission, TDD LTE-A physical layer is implemented (see Section 4). Each user (outdoor as well as indoor) offers a constant bit rate traffic during the whole simulation. User's data are served in a manner that the bandwidth is fairly allocated to provide the same throughput for all users. For the open access, indoor as well as outdoor users share the radio resources and the backhaul of the small cells with equal priority. On the other hand, for the hybrid access, a half of the radio and backhaul capacities is reserved for the indoor UEs. All outdoor UEs then share the rest of the available capacity. The major transmission, channel, and simulation parameters are summarized in Table 10.

**Table 10. Simulation Parameters**

Parameter	Value
Frequency band	2 GHz
Channel bandwidth for macro/small cell	20/20 MHz
Transmitting power of macro/small cell	46/15 dBm
Height of macro/small cell/UE	32/1/1.5 m
Std. deviation of shadowing of MBS/FAP	8/4 dB
Loss of outer/inner walls	10/5 dB
Noise density	-174 dBm/Hz
LTE-A physical layer overhead	25%
Speed of outdoor UEs	1 m/s
Number of macro/small cells	1/50
Number of indoor/outdoor UEs	50/100
Number of simulation drops	10
Duration of a simulation drop	7200 s

Several metrics are defined for the performance evaluation: frequency of mobility events, handover interruption ratio, and served throughput for indoor, outdoor, and cell-edge users.

The frequency of mobility events is expressed as the mean interval between two hard handovers or two AS updates. For the hard handover, a mobility event is detected if the handover is performed, i.e., if the next formula is fulfilled:

$$s_t(t) > s_s(t) + \Delta_{HM} \quad (27)$$

where  $s_t$  and  $s_s$  represents the signal level measured by the UE from the target and the serving cells respectively. In the similar way, an event for the FCS is conditioned by fulfilling one of the following equations [26]:

$$\begin{aligned} s_s(t) - s_t(t) &\leq T_{add} & \wedge & & s_s(t-1) - s_t(t-1) &> T_{add} \\ s_s(t) - s_t(t) &\geq T_{del} & \wedge & & s_s(t-1) - s_t(t-1) &> T_{del} \end{aligned} \quad (28)$$

where  $T_{add}$  and  $T_{del}$  represents threshold for adding and removing cells from the AS respectively. In the simulations, we set  $T_{add} = T_{del}$  as it is the most common setting in practice.

The handover interruption ratio is understood as the ratio of the time spent by the UEs in the state of the interruption due to handover to the overall simulation time. This is expressed by the next formula:

$$I_{HO,r} = \frac{I}{t_{sim}} \sum_{h=0}^{n_{HO}} i_h \quad (29)$$

where  $i_h$  stands for the duration of the interruption introduced by the  $h$ -th handover or the  $h$ -th AS update; and  $t_{sim}$  is the overall time of the observation (i.e., the simulation time). It is worth to mention that the interruption in the case of FCS occurs only if one cell is included in the AS of the UE and if the serving cell of the UE is going to be switched. We assume the interruption with duration meeting an IMT-Advanced recommendation for 4G networks. Therefore, we set the interruption to 25 ms.

Served throughput represents the amount of really transferred users' data. It is observed for indoor, outdoor, and cell-edge users. The indoor users are all users located inside the houses (50 indoor UEs in the simulations) while the outdoor are all other users (100 UEs in our simulations). The cell-edge UEs are the users positioned close to the border of two neighboring cells. According to [32], we define the cell-edge UE as the user with the level of the signal from the second strongest cell ( $s_2$ ) within the threshold  $T_{cell\_edge}$  (in the simulations, equals to 1 dB) from the signal level of the strongest cell (i.e., the serving cell,  $s_s$ ) as shown in the subsequent equation:



$$s_s - s_2 < T_{cell\_edge} \quad (30)$$

The amount of the cell-edge users varies in time depending on the users' location. Nevertheless, the trajectories of the UEs are the same for the evaluation of hard handover and FCS. Thus, the amount of the cell-edge UEs is the same for both as well.

### 6.1.2 SIMULATION RESULTS

This section presents the results of hard handover and FCS obtained by the simulations performed in MATLAB.

The impact of  $\Delta_{HM}$  (for hard handover) and  $T_{add}$ ,  $T_{del}$  (for FCS) on the frequency of the mobility events is depicted in Figure 33. The frequency of the events is proportional to the overhead due to the user's mobility (an overhead related to one handover or to one AS update is in order of kb [10]). As the figure shows, FCS introduces more events (shorter mean interval between two events) than hard handover. For hard handover, the amount of the events is notably reduced by higher  $\Delta_{HM}$ . Contrary, the thresholds  $T_{add}$  and  $T_{del}$  for FCS decrease the number of the events negligibly. Nevertheless, the overhead due to the UE's mobility is still insignificant since an update of the AS (i.e., few kilobits) is required less than once per 340 s even for very low thresholds. Note that neither access mode (open/hybrid) nor capacity of the small cell backhaul influence the amount of handovers since it depends only on the relation between the signal levels of the neighboring stations for the conventional handover and FCS.

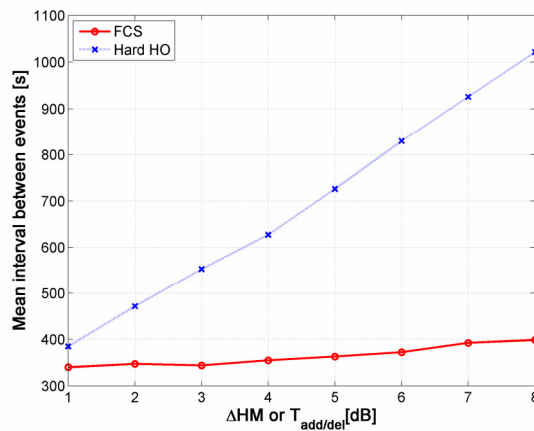
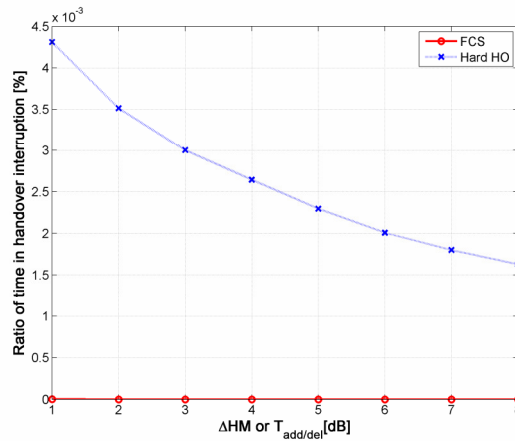


Figure 33. Interval between mobility events for hard handover and FCS.

User QoS is influenced also by the interruption due to handover. The ratio of the time spent by the UEs in the interruption to the overall simulation time is depicted in Figure 34. The overall interruption time in the case of hard handover is decreasing with  $\Delta_{HM}$  as less handovers is performed. However, the hard handover interruption is significantly higher than the one accounting to FCS. FCS is able to fully eliminate the interruption even for very low thresholds. The interruption is critical for real-time services (speech or video calls) as QoS perceived by users is degraded heavily. For non-real-time services, an impact of the interruption is nearly undetectable by the users as it is presented only by negligible lowering of bit rate for a very short time (up to 25 ms for 4G networks [56]).



**Figure 34. Average interruption experienced by UEs due to mobility.**

The amount of the served throughput over the level of the traffic offered by individual types of UEs is depicted in Figure 35 - Figure 37. Each figure consists of two subplots showing average throughput for open (left plots) and hybrid (right plots) accesses. All figures contain results for the backhaul with limited capacity of 8 Mbps (solid lines) and unlimited backhaul with capacity of 100 Mbps (dashed lines).

The figures confirm the fact that an increase in  $\Delta_{HM}$  for hard handover lowers the throughput. This is caused by keeping the UEs connected to the serving cell for a longer time even if a target cell is able to provide a channel with higher quality. For FCS, an impact of the thresholds depends on the type of the access and the backhaul capacity. For the unlimited backhaul, throughput increases with  $T_{add}$  and  $T_{del}$  for the outdoor UEs as more cells are included in the AS and interference experienced by the outdoor UEs is lowered. For the indoor UEs served by the open access cells with the unlimited backhaul, the throughput is limited by the backhaul and the positive impact due to an

increase in  $T_{add}$  and  $T_{del}$  is negligible. If the backhaul is limited, higher  $T_{add}$  and  $T_{del}$  decrease the throughput of the indoor UEs in the case of the open access. It is a cost of sharing the backhaul with more outdoor UEs who experience slight increase in throughput. Nevertheless, this rise in throughput of the outdoor UEs is limited by the backhaul capacity. For the hybrid access with the limited backhaul, an impact incurred by  $T_{add}$  and  $T_{del}$  is negligible due to a fixed allocation of the resources among the indoor and outdoor UEs.

According to Figure 35, FCS is profitable for the indoor UEs if a sufficient backhaul capacity (100Mbps) is provided for both the open and hybrid accesses. If the backhaul is of a limited capacity (8 Mbps), FCS introduces a heavy loss in throughput of the indoor UEs for the open access. This loss is a result of fair sharing the small cell backhaul capacity with outdoor UEs. If the small cell provides higher channel quality than the macrocell, each UE is trying to transmit data via the small cell, but the backhaul is not able to serve the data. The hybrid access with the limited backhaul reaches the same performance for both FCS and hard handover as the fixed ratio of the backhaul capacity is reserved for the indoor UEs.

Performance of the outdoor UEs is influenced in more positive way by FCS (see Figure 36). Again, FCS is profitable for all levels of the offered traffic and both accesses if the small cell backhaul is unlimited. For the limited backhaul, FCS increases throughput for the offered traffic up to 2 and 1.5 Mbps for the open and hybrid accesses respectively. Again, the gain of hard handover for high level of the traffic and the limited backhaul is caused by sharing the resources with more UEs in the case of FCS.

Throughput of the most critical set of users, cell-edge UEs, is depicted in Figure 37. The set of the cell-edge users mostly consists of the outdoor UEs; thus, the behavior of the throughput of the cell-edge UEs follows the results for the outdoor UEs. Therefore, FCS is profitable if a small cell is connected via the unlimited backhaul. If the backhaul capacity is limited, FCS outperforms hard handover only for lower offered traffic like in the case of the outdoor UEs.

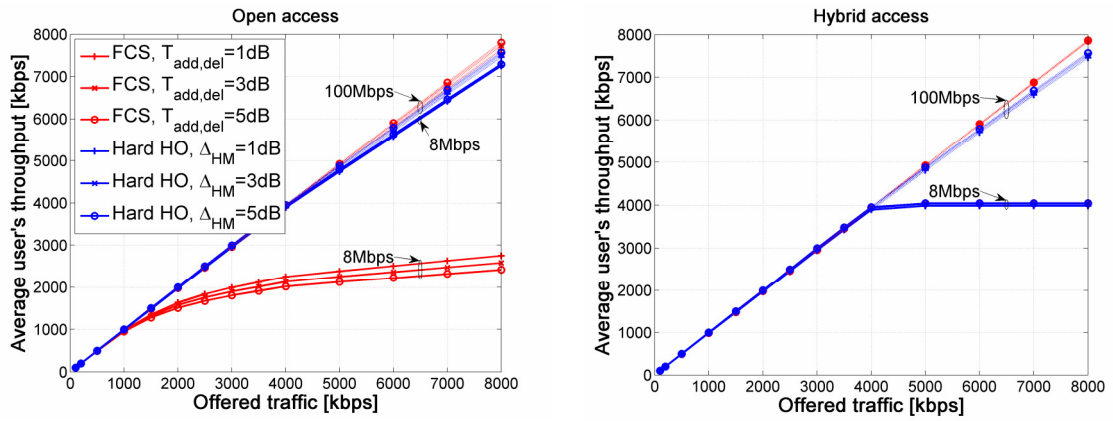


Figure 35. Served throughput of indoor UEs for open and hybrid accesses.

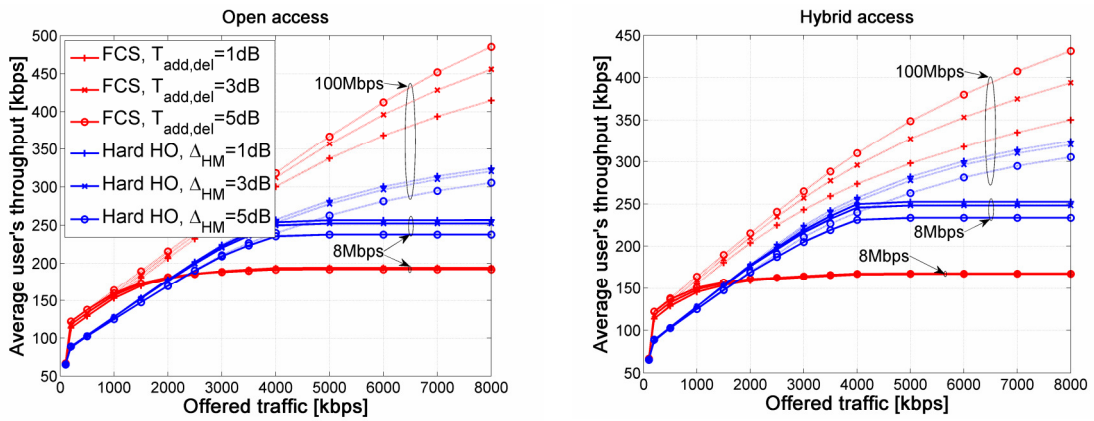


Figure 36. Served throughput of outdoor UEs for open and hybrid accesses.

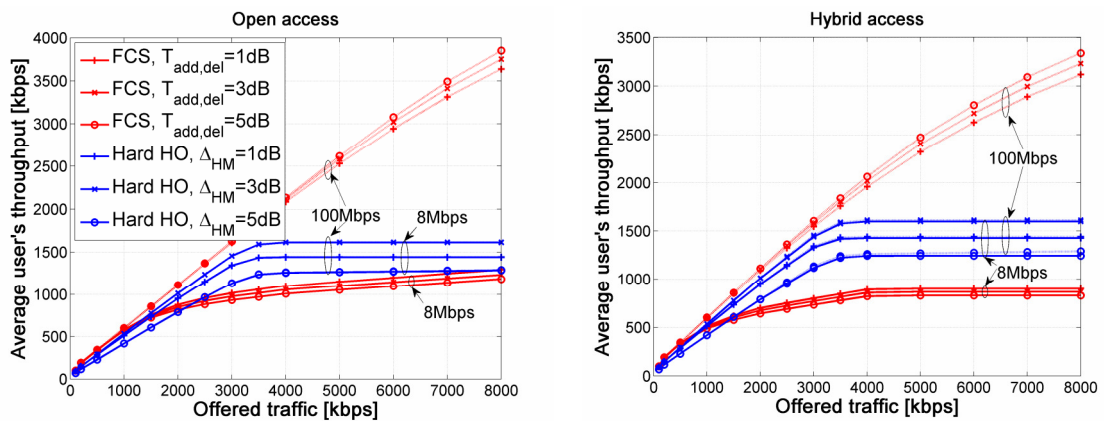


Figure 37. Served throughput of cell-edge UEs for open and hybrid accesses.

Average throughputs observed from the results presented in Figure 35 - Figure 37 are summarized in Table 11 and Table 12 for the limited and unlimited backhails respectively. The numbers in parenthesis represent a gain/drop in throughput introduced by FCS with relation to hard handover. It can be observed that the average throughput is improved by FCS in the case of the unlimited backhaul. If the backhaul capacity is limited, hard handover is more efficient in term of throughput.

**Table 11. Average throughput per user for  $\Delta_{HM} = 3\text{dB}$ ,  $T_{\text{add}} = 3\text{dB}$ , and  $T_{\text{del}} = 3\text{dB}$ ; 8 Mbps backhaul capacity**

	Served throughput [kbps]			
	Indoor UEs	Outdoor UEs	All UEs	Cell-edge UEs
Hard HO Hybrid	2510.5	190.01	2700.5	1103.2
FCS Hybrid	2500.8 (-0.4%)	154.52 (-18.7%)	2655.3 (-1.7%)	661.02 (-40.1%)
Hard HO Open	3097.6	192.44	3290.0	1110.7
FCS Open	1615.4 (-47.8%)	172.98 (-10.1%)	1788.4 (-45.6%)	836.83 (-24.7%)

**Table 12. Average throughput per user for  $\Delta_{HM} = 3\text{dB}$ ,  $T_{\text{add}} = 3\text{dB}$ , and  $T_{\text{del}} = 3\text{dB}$ ; 100 Mbps backhaul capacity**

	Served throughput [kbps]			
	Indoor UEs	Outdoor UEs	All UEs	Cell-edge UEs
Hard HO Hybrid	3144.7	207.28	3351.9	1111.6
FCS Hybrid	3186.6 (+1.3%)	247.81 (+19.6%)	3434.4 (+2.5%)	1557.5 (+40.1%)
Hard HO Open	3144.7	207.28	3351.9	1111.6
FCS Open	3171.6 (+0.9%)	264.16 (+27.4%)	3435.8 (+2.5%)	1677.4 (+50.9%)

### 6.1.3 DISCUSSION OF RESULTS AND SUGGESTIONS FOR MOBILITY SUPPORT

Several general remarks and suggestions can be derived from the performed simulations. First, the performance of hard handover and FCS is influenced by hysteresis and thresholds as follows:

- Hard handover: throughput decreases with rise of  $\Delta_{HM}$  disregarding the backhaul of the small cell.

- FCS: throughput increases with the thresholds for the unlimited backhaul, while it slightly decreases for the limited backhaul.

Following remarks belong to the limitation of the small cells backhaul:

- Unlimited backhaul capacity: FCS always outperforms hard handover.
- Limited backhaul capacity: FCS is profitable only for the outdoor UEs offering lower traffic level (1.5 and 2 Mbps for the hybrid and open accesses respectively).

Last, FCS is profitable for delay sensitive real-time services such as voice calls as it eliminates the problem of handover interruption.

According to the above mentioned, the backhaul influences the performance of FCS and hard handover. In related works focused on macrocells only, FCS outperforms hard handover in all cases (see e.g., [33], [32], [29]). This conclusion is confirmed by our results for the pico/micro cells with unlimited backhaul. However, an efficiency of FCS can be degraded more than efficiency of hard handover if the backhaul capacity is limited. Then, FCS is even outperformed by hard handover for high traffic load. Therefore, we suggest employing FCS only in the case of low traffic offered by the UE. For heavy traffic offered by the UE, the UE should perform hard handover to a target cell if this cell is of the limited backhaul and it is not able to serve the UE according to its requirements. If the target cell is of the unlimited backhaul, this cell is just included to the active set along with the current serving cell to reduce interference. Inclusion of this cell should be performed as soon as possible and the cell should be kept in the active set for a longer time. This can be easily achieved by setting higher  $T_{add}$  and  $T_{del}$  (for example, 5 dB).

## 6.2 ACTIVE SET MANAGEMENT

As the previous section show, FCS can be efficient even in networks with small cells; however, the backhaul capacity needs to be considered in active set management. The proposed solution for a selection of the active set members (i.e., how to determine when a cell should be added/deleted to/from active set) is based on the calculation of amount of consumed radio resources and on backhaul quality consideration. As shown in Section 6.1, pico/micro cells outperforms conventional hard handover even with the

conventional active set management. Therefore, we focus on femtocells only in this section. Note that the same approach can be applied also to the micro/pico cells.

### 6.2.1 PROPOSED ALGORITHM FOR ACTIVE SET MANAGEMENT

The proposed algorithm on the selection of proper members of the active set compares the current amount of the consumed radio resources of an MBS with the radio resources of the MBS consumed if a cell would be added/removed to/from the active set. In addition, the backhaul limitation, in term of the limited capacity and higher delay, is introduced in the proposed active set management procedure.

To easy following the explanation of the proposed algorithm, summarization of parameters used in the description of the active set management is in Table 13.

**Table 13. Notation of parameters used for description of the proposed algorithm**

Symbol	Definition
$N^i$	List of neighboring cells of $i$ -th UE, $N^i = \{N_1^i, N_2^i, \dots, N_{nc^i}^i\}$ .
$A^i$	List of cells included in the active set of $i$ -th UE, $A^i = \{A_1^i, A_2^i, \dots, A_{ac^i}^i\}$ .
$nc^i, ac^i$	Number of cells included in the neighbor cell list and in the active set respectively.
$R_{j \in A^i}^i, R_{j \notin A^i}^i$	Amount of the radio resources consumed by the $i$ -th UE if cell $C_j$ is included in $A^i$ and if it is not included in $A^i$ respectively.
$\alpha$	Gain required for inclusion of a cell into $A^i$ .
$D_j, D_s$	Delay of data delivered though cell $C_j$ , and maximum acceptable delay for the service experienced by the $i$ -th UE.
$b_{j,av}, b^{i,reg}$	Available capacity of the backhaul of $C_j$ and the capacity required by the $i$ -th UE respectively.
$T_{j \in A^i}^i, T_S^i$	Throughput of the $i$ -th UE if $C_j$ would be added to $A^i$ and throughput experienced by the $i$ -th UE from the current serving cell.
$\kappa_j^i$	Gain in amount of the MBS's radio resources released by inclusion of $C_j$ into $A^i$ related to the requested capacity.

Let  $UE = \{UE_1, UE_2, \dots, UE_u\}$  denotes a set of  $u$  users in the networks and  $C = \{C_1, \dots, C_m, C_{m+1}, \dots, C_{m+f}\}$  represents the set of  $k = m + f$  cells in the network, where  $m$  and  $f$  is the amount of the MBSs and the FAPs respectively. Further,  $N^i = \{N_1^i, N_2^i, \dots, N_{nc^i}^i\}$  represents the set of the neighboring cells of  $i$ -th UE. Each  $N^i$

consists of  $nc^i$  neighboring cells. The set  $A^i = \{A_1^i, A_2^i, \dots, A_{ac^i}^i\}$  is composed of cells included in so-called active set of  $i$ -th UE. Note that  $A^i$  is always a subset of  $N^i$ , i.e.,  $A^i \subseteq N^i$ . The amount of cells included in the active set of  $UE_i$  is denoted as  $ac^i$ . The parameter  $ac^i$  is known as active set size.

The principle of the proposed algorithm is depicted in Figure 38. A new cell is included into  $A^i$ , if all defined conditions are met. The cell is removed from the existing  $A^i$  if at least a condition is not fulfilled.

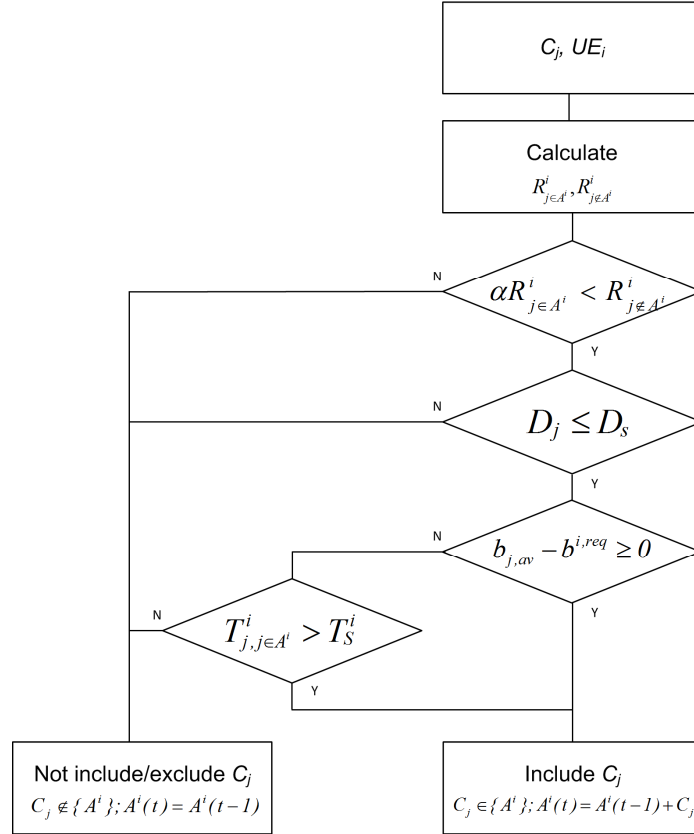


**Figure 38. Proposed algorithm for active set management.**

If  $C_j \in N^i$  and  $C_j \notin A^i$ , then the cell can be included into the  $A^i$  if:

$$\alpha R_{j \in A^i}^i < R_{j \notin A^i}^i \quad (31)$$

where  $R_{j \in A^i}^i$  represents the amount of the MBS's radio resources consumed by the  $UE_i$  if the  $C_j$  would be included in the  $A^i$ ,  $R_{j \notin A^i}^i$  represents the amount of the MBS's radio resources consumed by the  $UE_i$  if the  $C_j$  would not be included in the  $A^i$ , and  $\alpha$



represents a gain required for the inclusion of the  $C_j$  in  $A^i$ . The MBS's resources are considered in this equation rather than the FAP's resources since each FAP is supposed to serve only low amount of users comparing to the MBS. Thus, any change in an active set influences large amount of the macrocell users but only couple femtocell users.

Both  $R_{j \in A^i}^i$  and  $R_{j \notin A^i}^i$  are derived from the reports on signal quality (e.g. SNR) measured by the  $UE_i$  from all cells included in  $N^i$  (see, e.g., [32]). If SNR of all cells included in  $N^i$  is measured, SINR can be determined. Then, SINR is mapped to a modulation and coding scheme (MCS) according to, for example, [45]. Each MCS defines a modulation and a coding rate. Therefore, an amount of bits in a RE, denoted as  $b_{RE}$ , can be derived as a multiplication of the coding rate ( $cr$ ) and amount of bits per symbol of the modulation ( $bps$ ), i.e.,  $b_{RE} = cr \times bps$ . Knowing amount of the radio resources required by the  $UE_i$  and  $b_{RE}$  of appropriate channel between the  $UE_i$  and the  $C_j$ , the amount of the consumed resources is determined as a simple ratio of data intended to be sent by the  $UE_i$  ( $d_{UE}$ ) and  $b_{RE}$ ;  $R^i = d_{UE}/b_{RE}$ . Difference in derivation of both  $R_{j \in A^i}^i$  and  $R_{j \notin A^i}^i$  consists in consideration of the  $C_j$  in the interference evaluation. For  $R_{j \in A^i}^i$ , the signal from the  $C_j$  is not taken into account since no cell included in the  $A^i$  can transmit at the same frequencies as the serving cell. Contrary, the signal from the  $C_j$  is included in the interference for  $R_{j \notin A^i}^i$ .

Once the inclusion of the  $C_j$  in the  $A^i$  is profitable from the amount of consumed radio resources of the MBS point of view, the quality of the backhaul of the  $C_j$  is evaluated. A problem of a packet delay due to transmission via the backhauls with different quality is fixed as follows. To cope with the delay, we suggest an additional condition for inclusion of a cell into the  $A^i$  as defined by the next formula:

$$D_j \leq D_s^i \quad (32)$$

where,  $D_j$  is the delay of data delivered though  $C_j$ , and  $D_s^i$  is the maximum acceptable delay for the service experienced by the  $UE_i$ . Note that this problem is common problem of the handover procedure. Therefore, it should be considered even in the conventional hard handover. However, the backhaul of the MBS typically provides

high quality of the connection with low delay and this condition is fulfilled automatically.

The backhaul of the MBSs is planned to be able to serve all the data transmitted via the radio interface. It means the bottleneck does not appear on the backhaul of the MBSs. In the FAPs, the situation is exactly the opposite. Since the FAPs are supposed to be connected to the networks via a backhaul with limited capacity, previous conditions (31) and (32) are complemented by additional one focused on the backhaul capacity. The next condition is considered only if the  $C_j$  is a FAP. The femtocell  $C_j$  can be potentially included in  $A^i$  only if:

$$b_{j,av} - b^{i,req} \geq 0 \quad (33)$$

where  $b_{j,av}$  and  $b^{i,req}$  is the available backhaul capacity of the  $j$ -th FAP and the backhaul capacity requested by the  $UE_i$  respectively. After fulfilling (33), the  $C_j$  is included in temporary active set  $A_{temp}^i$ . The  $A_{temp}^i$  is composed of all cells that should be included in  $A^i$  as those meet (31), (32), and (33). If only one UE is supposed to newly include the  $C_j$  into  $A^i$ , then the temporary active set can be added to the  $A^i$ , i.e.,  $\{A^i\} = \{A^i\} + \{A_{temp}^i\}$ . If more UEs would like to include the  $C_j$  in their  $A^i$ , then the backhaul limit is reconsidered. The cell  $C_j$  should be added to more active sets only if the FAP will be still able to serve all UEs as expresses the following equation:

$$b_{j,av} - \sum_{i,i|j \in A_{temp}^i} b^{i,req} \geq 0 \quad (34)$$

If (34) if not fulfilled, only  $A^i$  of the selected UEs will be updated. A procedure for the selection of the most appropriate UEs, whose active set will be enhanced by the  $C_j$  should be defined. For this purpose, we define new parameter  $\kappa_j^i$ . This parameter represents a ratio of the gain caused by the inclusion of the  $C_j$  to the requested backhaul capacity. It is defined by the next formula:

$$\kappa_j^i = \frac{R_{j \notin A^i}^i - R_{j \in A^i}^i}{b^{i,req}} \quad (35)$$

The  $C_j$  is included only to the  $A^i$  of the UEs that leads to the highest  $\kappa_j^i$ . For this purpose, the  $\kappa_j^i$  is reordered in descending order as follows:

$$\text{sort}(\kappa_j^i \big|_{j=\text{const}}) = \{\max\{\kappa_j^i\}, \max\{\kappa_j^i - \max\{\kappa_j^i\}\}, \dots\} \quad (36)$$

Then the  $C_j$  is sequentially added to the  $A^i$  for  $i=1, \dots, b_{\max}$ . The  $b_{\max}$  is determined as  $\max(b)$ ;  $b=(1, \dots, u)$  for which the following formula is still valid:

$$b_{j,av} - \sum_{i=1}^b b^{i,req} \geq 0 \quad (37)$$

A specific situation, when (31) and (32) are fulfilled while (33) is not can occur. In this case, a FAP can provide higher throughput even if other UEs with this FAP in the active set could suffer from the inclusion of the FAP into the  $A^i$ . Nevertheless, the drop in throughput of the UEs served by the FAP can be insignificant and the throughput of all of these UEs can be still above the one provided by the MBS. Therefore, the cell  $C_j$  is included into  $A^i$  even if not enough available backhaul is provided by the  $C_j$ . The inclusion is conditioned by fulfilling subsequent equation:

$$T_{j,j \in A^i}^i > T_S^i \quad (38)$$

where  $T_{j,j \in A^i}^i$  is the throughput of  $UE_i$  if the  $C_j$  would be added to  $A^i$  and  $T_S^i$  represents the throughput experienced by the  $UE_i$  from the current serving cell. To add the  $C_j$  to the  $A^i$ , all UEs currently served by the  $C_j$  must still be experiencing higher capacity than the capacity provided by the MBS.

Description above focuses on conditions and algorithm for inclusion of a cell into an active set. The opposite case, that is, removal of a cell from the active set must be defined. In our proposal, the  $C_j$  is deleted from the  $A^i$  if it results in lesser consumption of the MBS's radio resources. In other words, the  $C_j$  is removed if condition (31) is no longer met. Of course, the cell is removed if its backhaul capacity or delay changes and either (32) or (33) becomes not fulfilled.

Selection of a serving cell is based on comparison of the signal levels measured by the UE. If the cell with the strongest signal measured by the  $UE_i$  can fully served this particular  $UE_i$ , then the cell is selected as the serving. However, if even this cell cannot provide enough capacity, the cell providing maximum throughput is selected.

### 6.2.2 SYSTEM MODEL FOR EVALUATION

The transmission power and path loss models follows those used in evaluation of FCS in section 6.1. This section describes especially parameters, in which both simulations differ.

Since the main objective is to assess when active set of the UEs should be updated, the outdoor UEs are supposed to be moving in comparison with the previous evaluations. The individual parameters, and values set for the evaluation of the proposal are presented in Table 14. The outdoor UEs are moving according to PRWMM (see [41]) with a constant speed of 1 m/s. All UEs transmit data according to constant bit rate model with a bit rate in the range from 60 kbps to 4Mbps. Each UE has different requirements on the delay for its services. The required delay is selected among three possible classes: high demands (delay of backhaul  $\leq 50$  ms), medium demands (delay of backhaul  $\leq 75$  ms), low demands (delay of backhaul  $> 75$  ms). The selection of the delay requirements is done randomly. The probability that UE's demands on the delay is high/medium/low is 5%/20%/75%.

**Table 14. Parameters and models used for evaluation of active set management algorithms**

Parameters	Value
Carrier frequency	2.0 GHz
MBS / FAP transmitting power	46 / 15 dB
Number of MBSs / FAPs	1 / 50
Number of indoor/outdoor UEs	50 / 100
Speed of outdoor UEs	1 m/s
Wall penetration loss	10 dB
Noise spectral density	-174 dBm / Hz
Size of simulation area	2000 x 1000m

The FAPs' backhaul is limited to 8 Mbps for downlink and 50 % of its capacity is supposed to be consumed due to ADSL aggregation and signaling overhead. Consequently, the real available capacity of the FAP backhaul dedicated for the UEs in

the simulation is 4 Mbps. The delay of each backhaul is selected according to the measurement in a real network provided by Telkom Indonesia in [52]. To eliminate an effect of random variables, the simulation duration is set to 3600 seconds of real time and we run five simulation drops.

### 6.2.3 SIMULATION RESULTS

The results obtained by the simulations in MATLAB are split into two subsections. The first one presents the results for determination of appropriate  $\alpha$  for the proposed algorithm. The second part of the results shows the comparison of the proposed algorithm with selected competitive proposals.

#### 6.2.3.1 EVALUATION OF THE PROPOSED ALGORITHM

As Figure 39 shows, the average size of the active set per a UE over the whole simulation decreases with the amount of the traffic offered by the UEs. This is due to the limited capacity of the backhaul of the FAPs. Once the backhaul is fully utilized, the FAP is included into other active set(s) only if it improves the throughput of the UE and ensures enough capacity even for all UEs with the FAP in current active set. On the other hand, higher value of  $\alpha$  lowers the size of the active set since lower profit must be achieved at the side of the MBS to include a FAP into the active set (see (32)). Analogically, the frequency of an active set updates (Figure 40) rises with lowering  $\alpha$  or offered traffic. The active set update rate represents the average amount of changes in the active set of a user per a simulation step (a second). Each inclusion or removing of a cell into an active set represents one change.

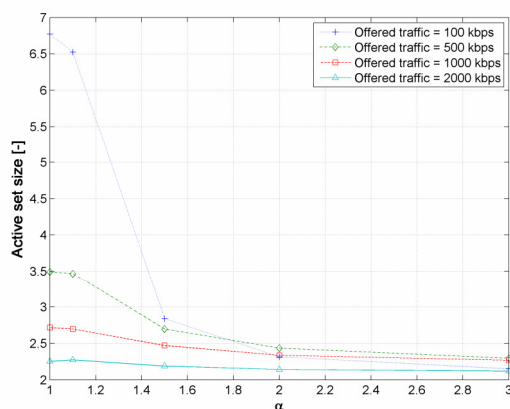


**Figure 39. Impact of  $\alpha$  on active set size.**

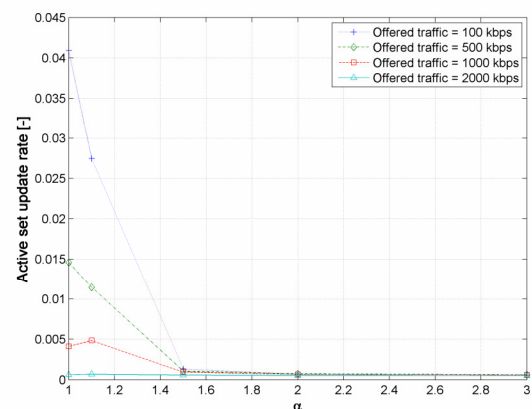


**Figure 40. Impact of  $\alpha$  on frequency of active set updates.**

Besides the active set,  $\alpha$  influences also user's throughput (Figure 41) and so called capacity outage (Figure 42). The throughput is affected by  $\alpha$  only for higher offered traffic loads. All cells, even FAPs, are able to serve high amount of users without reaching a backhaul limit for low offered traffic. Thus, no impact of  $\alpha$  on the throughput is observed. However, if the offered traffic increases, high  $\alpha$  leads to the selection of only considerably profitable cells as candidates to be included in the active sets. If  $\alpha$  is low, each FAP is included in large number of active sets and all users connected to this FAP must share the limited backhaul. Note that we assume proportional fair sharing of the FAP backhaul capacity among all users connected to it.

The capacity outage is understood as a time for which a UE's requirements in term of throughput are not fully served. In other words, the real transferred capacity is lower than the traffic offered by the UE during this time. For a low offered traffic, the capacity outage rises with  $\alpha$ . Contrary, the performance is slightly improved for a higher  $\alpha$  or if a heavy traffic is generated by the UEs. This opposite behavior is a result of a load balancing among individual cells. For a low offered traffic, a higher  $\alpha$  limits exploitation of the available backhaul of the FAP even if the MBS is not able to fulfill all UE's requirements. On the other hand, for a heavy traffic, low  $\alpha$  leads to more FAPs included in the active sets. Thus, more UEs share the FAP backhaul capacity and the backhaul limit leads to a higher number of unsatisfied UEs.

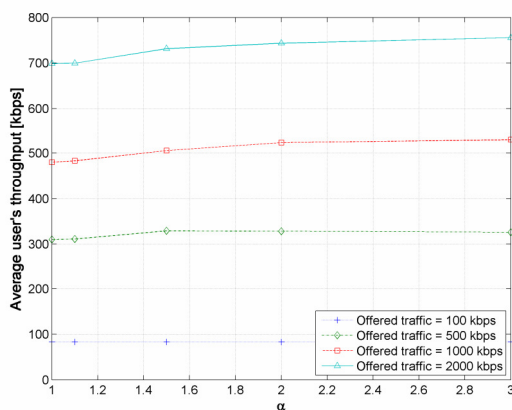


**Figure 41. Impact of  $\alpha$  on users throughput.**

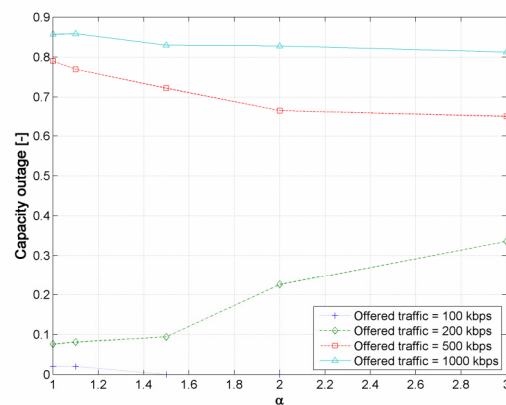


**Figure 42. Impact of  $\alpha$  on ratio of users whose requirements on capacity are not fulfilled.**

Based on the presented results,  $\alpha > 2$  is considered as the appropriate gain since maximum throughput and minimum amount of active set updates are generated. For the

purpose of evaluation of the proposal and competitive schemes,  $\alpha = 2$  and  $\alpha = 3$  are selected.

### 6.2.3.2 COMPARISON OF COMPETITIVE ALGORITHMS

The proposal is compared with two algorithms: conventional FCS active set management [27] and with the proposal on capacity based FCS active set management proposed in [32]. The capacity based FCS is selected for the comparison since this proposal outperforms any other similar proposals as presented in [32].

As shown in Figure 43, the proposed active set management algorithm improves throughput of all UEs (indoor as well as outdoor) comparing to the conventional and the capacity based FCS (Figure 43c). The gain in throughput rises with the amount of offered data by the UEs and it is nearly independent on the level of  $\alpha$ . The throughput gain for the indoor users (Figure 43a) is up to roughly 28%, 17%, and 41% comparing to the capacity based FCS, the conventional FCS with  $\Delta_{HM} = 3\text{dB}$  and the conventional FCS with  $\Delta_{HM} = 5\text{ dB}$  respectively. For outdoor users, a minor gain (up to 4%) comparing to the capacity based FCS is notable up to 2000 kbps (Figure 43b). Then both schemes perform similarly. Comparing the proposal with the conventional FCS, the gain rises up to 20% with the offered traffic up to 2000 kbps. For the offered traffic over 2000 kbps, the gain gets stable and equals approximately to 7%. The rapid drop experienced by the proposal and the capacity based FCS at 2000 kbps is due to the FAP backhaul limitation and it can be explained as follows. For each FAP, a UE is deployed indoor in our simulation deployment. Therefore, this UE is attached to this FAP most of the time. Including the FAP in the active sets of other outdoor UE, the backhaul must be shared by all UEs with this FAP in the active set. Since the available backhaul capacity is 4000 kbps in average in the simulations, an inclusion of the FAP to an active set of any outdoor UE automatically limits the transmission capacity up to 2000 kbps.

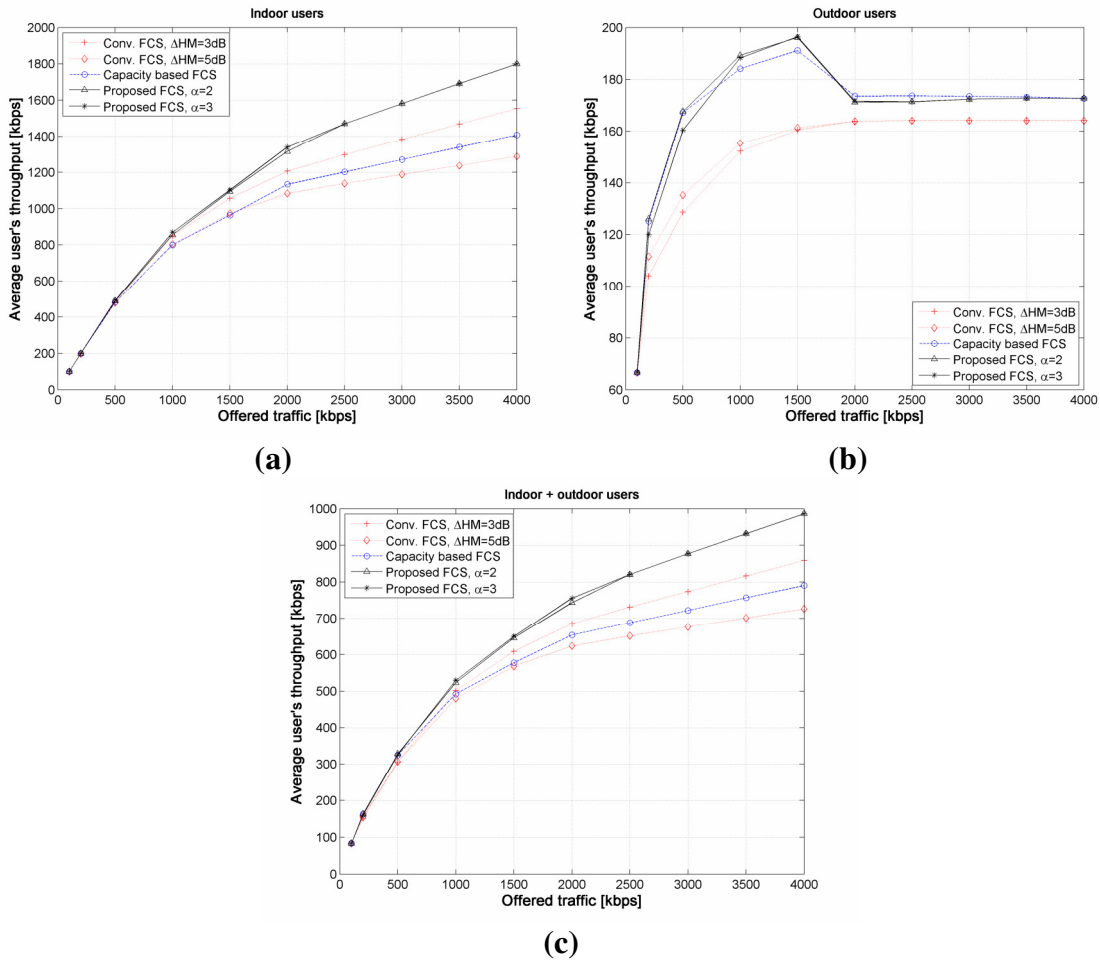


**Figure 43. Average throughput of UEs during simulation over amount of offered traffic by the UEs; throughput of: (a) only indoor users; (b) only outdoor users; (c) all users.**

Frequency of active set updates is presented in Figure 44. Each event in the active set (either inclusion/deletion of a cell to/from active set) is linearly interconnected with certain amount of a management overhead. Therefore, these figures represent also the related amount of control overhead generated due to the active set management. In the case of the indoor users only (Figure 44a), the lowest rate of the active set update is reached by the conventional FCS. However, it is at the cost of significantly decreased throughput as presented in Figure 43a. The capacity based FCS and the proposed scheme performs similarly in term of the active set update rate. The sudden rise in the case of the proposal is again due to the backhaul limit as explained above for the throughput. Regarding outdoor users presented in Figure 44b, the results are exactly opposite. The lowest rate of the active set update is reached by the proposal. The rate of updates decreases with higher values of  $\alpha$  and with an increase in offered throughput for our proposal. Lower frequency of the active set updates for a higher  $\alpha$  or for a



higher offered traffic is due to a lower probability of fulfilling condition (32) or a higher requirements of all connected UEs on the FAP backhaul respectively. Note that frequency of the active set updates of the indoor users is roughly ten times lower comparing to the outdoor users. Thus, the proposed scheme outperforms the conventional FCS and the capacity based FCS roughly by 58% - 65% and by 20% - 43% (depending on the amount of the offered traffic) respectively if overall rate of the active set update (indoor as well as outdoor UEs) is evaluated (Figure 44c). Based on the results, we can stated, that the proposal generates significantly less overhead comparing to the both competitive scheme.

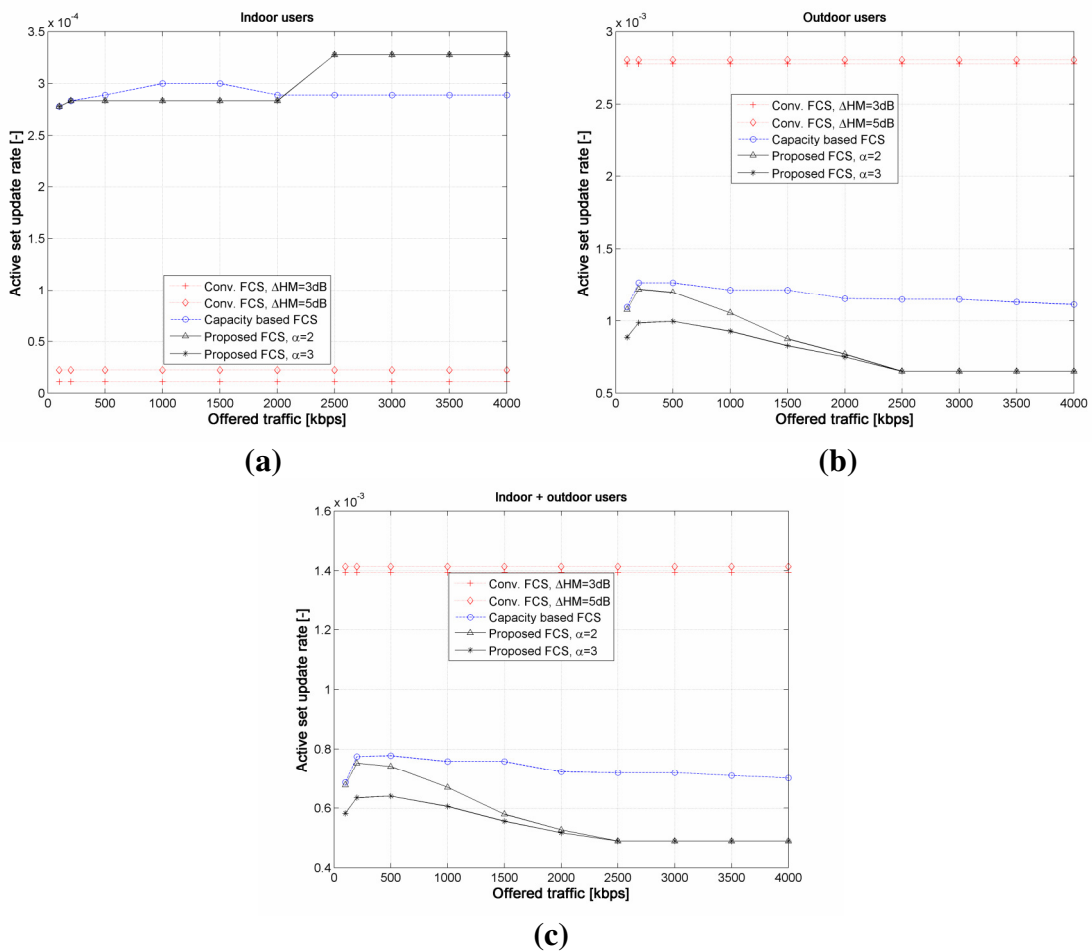


**Figure 44. Average amount of changes in active set of individual users per a simulation step; changes in active set of: (a) only indoor users; (b) only outdoor users; (c) all users.**

In Figure 45, the average size of the active set per UE over the whole simulation is depicted. For the indoor UEs (Figure 45a), only roughly one cell is included in the active set for the conventional FCS. This cell is typically a local FAP deployed in the same house as the UE. Signals of other cells' (either FAPs or MBSs) are usually

attenuated significantly due to intervening walls. Hence, these cells do not provide signal with sufficient quality to be included in the active set. For the capacity based and proposed FCS, roughly two cells are included in the active set on average. This is typically an MBS and the local FAP. Other FAPs provide weak signal (at least two walls are in between the FAP and the UE) to be included in the active set.

For the outdoor users (Figure 45b), the active set consists of an MBS and several closest FAPs. The exact number of the FAPs included in the active set depends on the offered traffic level for the capacity based FCS. In the case of the proposed FCS and the conventional FCS, the number of FAPs in the active set is further influenced by  $\alpha$  and by hysteresis respectively. The average size of the active set is presented in Figure 45c. Note that based on standalone size of the active set can be concluded neither lower nor higher active set size is profitable. This parameter just show typical amount of cells involved in the active set communication, which can be further used, for example, in optimization of cooperative communication.

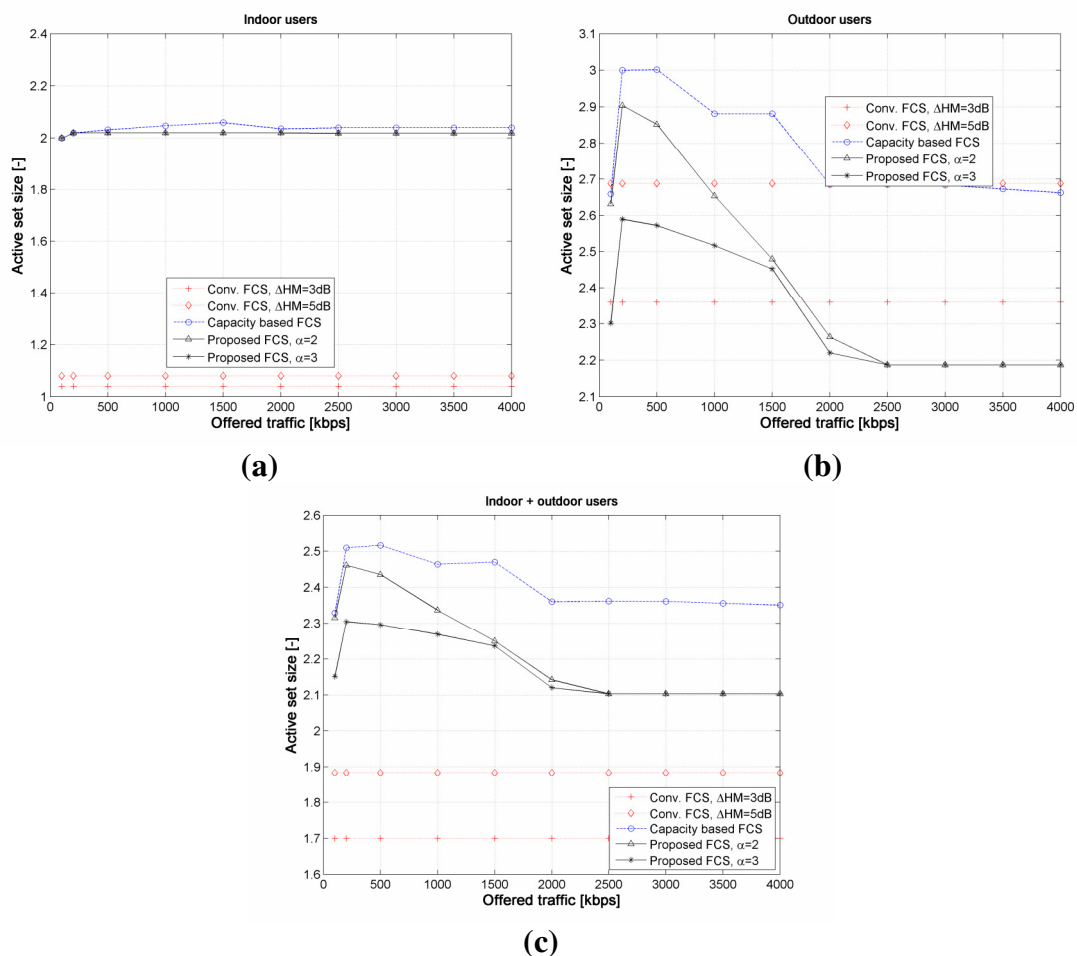


**Figure 45. Average amount cells included in active set for: (a) only indoor users; (b) only outdoor users; (c) all users.**

Last set of figures (Figure 46a - c) presents the impact of individual FCS algorithms on the ratio of the time, when the user's requirements on capacity are not fulfilled. Comparing the indoor (Figure 46a) and outdoor (Figure 46b) UEs, the satisfaction of the outdoor UEs is lower comparing to the indoor UEs. The reason is that the indoor UEs are usually not limited by the radio capacity. The bottleneck is typically located on the FAP backhaul, which is of a higher capacity comparing to the radio capacity of an MBS.

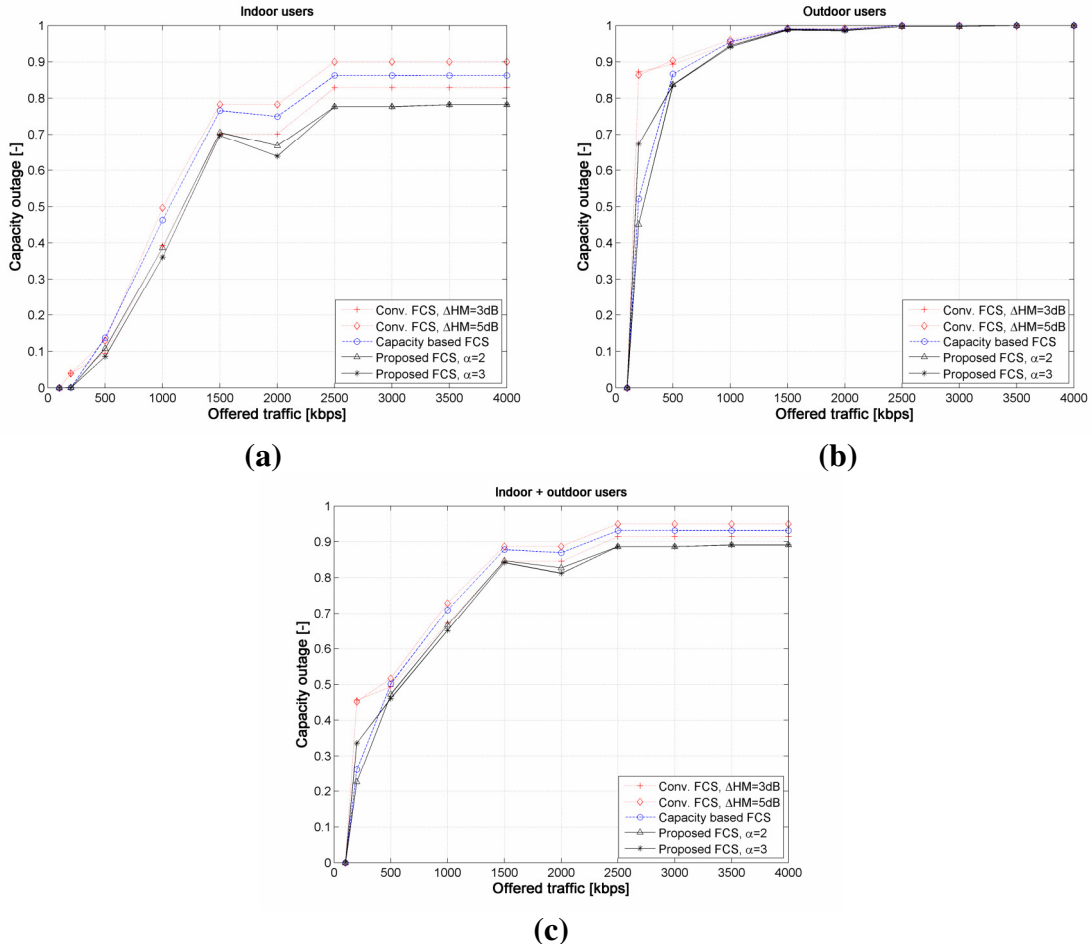


**Figure 46. Average ratio of time spent in the state when UEs requested capacity is not fully provided for: (a) only indoor users; (b) only outdoor users; (c) all users.**

The profit achieved by the proposal rises with offered traffic load and it is almost independent on the value of  $\alpha$  for the indoor users. The improvement is up to 13%, 7%, and 12% when compared to the conventional FCS with 3dB hysteresis, the conventional FCS with 5dB hysteresis, and the capacity based FCS respectively. For the outdoor UEs, the maximum profit (50%) is reached for 100 kbps of the offered traffic if comparing the proposal with the conventional FCS. The performance of the capacity based and the proposed FCS is roughly the same for the outdoor users. Nevertheless, the

proposed algorithm is outperformed by none of both competitive algorithms for all UEs (indoor and outdoor) and for all offered traffic levels. The efficiency of the proposal comparing to both competitive schemes consists in more efficient selection of the cells included in the active sets of individual UEs.

Besides the capacity constrain for the backhaul of the FAPs, also a delay outage should be tackled. By the delay outage is understood the situation when a UE's requirements on the delay are not met. Our proposal suppresses the outage delay to the minimum achievable level. This minimum is given by occurrence of the situations when none of the neighboring cell is able to provide sufficient delay. However, this problem is not related to FCS active set management. The delay outage of the competitive FCS schemes depends on the quality of the backhaul of the FAPs. During our simulations, the delay outage for both competitive FCS schemes was roughly in range of 1 - 2.5 % above the outage of our proposed scheme, which reaches the delay outage under 1% even for heavy traffic load. Note that the delay outage introduced by our scheme is only due to the overloading of the system by high amount of offered traffic by the UEs.

#### **6.2.4 CONTROL INFORMATION FOR THE PROPOSED ACTIVE SET MANAGEMENT**

To enable FCS in networks with FAPs, exchange of control information among the FAPs and the MBSs must be defined. Information on the backhaul quality and the FAP's radio quality must be reported to the serving cell. However, the quality of the radio channel is periodically reported for common handover purposes. Therefore, no additional overhead is introduced by the proposed algorithm in term of information on the radio channel quality.

Each FAP is aware of its approximate backhaul quality as it needs this information to schedule users' data over the backhaul. Moreover, estimation based on the latest experienced backhaul quality can be considered. Nevertheless, the information on the backhaul quality must be delivered to the serving cell, which is supposed to take control over the handover decision. Thus, each potential candidate for inclusion in an active set should report the available capacity and the packet delay to the serving cell. The reporting of the backhaul quality can be included in the control information for the coordination of the MBSs and the FAPs.

The information on the backhaul delay can be provided in form of the range of the delays related to the experienced service class. It means, the delay does not need to be reported as an exact number but only as an index representing appropriate range of the delays. Therefore, its size is only of several bits. For example, 4 bits enable to distinguish 16 classes, which is sufficient number, higher than amount of classes used by IP protocol or in LTE-A. The information on the capacity should be expressed as an absolute amount of available resources. The number of bits required for this information depends on accuracy of reporting information. Sufficient amount is 16 bits as it enables to distinguish  $2^{16}$  levels of the available capacity (for example, it is the resolution of 4 kbps for 16 Mbps backhaul).

Transmission of the information on the backhaul quality can be either triggered by a handover request or periodical. The drawback of the handover triggered reporting is an additional delaying of handover (in tens of ms) due to delivering information on the backhaul status to the serving cell. However, its overhead is negligible since only few additional bits are transmitted per a handover. On the other hand, the periodic reporting does not delay handover but it increases signaling overhead. The maximal amount of the overhead generated during the periodical reporting can be determined as follows. The bit rate necessary for the reporting can be expressed as:

$$BR_{rep} = \frac{S_{ri}}{T_{rep}} \quad (39)$$

where  $S_{ri}$  is the size of the reported information and  $T_{rep}$  is the interval between two reports. The maximum size of a report is 16+4 bits as stated earlier. The minimum reporting period is supposed to be equal to the frame duration, which is 10 ms in LTE-A. Then the maximum reporting overhead is 2 000 bps. This amount of the overhead is still negligible comparing to the expected backhaul capacity in Mbps.

Like in the conventional FCS or in the capacity based FCS, information on status of the radio resources (muted or not) must be forwarded by the serving cell to all cells in the active set. This information is carried in the FCS command message (see Table 9). Note that the information on occupied resources is delivered to the cells in the active set even in the conventional FCS. Therefore, the only difference in the overhead is in delivery of the information on muting. The information on muting for each cell in active set is represented by one bit (just on or off is indicated). Considering average size of the

active set around two cells (see Figure 45), the overhead due to our proposal is up to 0.2 kbps (2 cells reported once per 10 ms frame). Even if this message introduces additional overhead, the overhead is increased only negligibly related to the conventional FCS (difference of tens of bps). Contrary, the overhead is even slightly lower (again only tens of bps) than in the case of the capacity based FCS since the active set size of our proposal is lower (see Figure 45).

### 6.3 CONCLUSIONS

In this chapter, first, we investigate the performance of FCS and hard handover if the small cells, connected to the network via either limited or unlimited backhaul, are considered. The results show slight increase in the amount of mobility events (AS updates) if FCS is used. On the other hand, FCS fully eliminates the interruption due to the user mobility. Therefore, FCS is profitable for real-time services such as voice calls. In term of the throughput, FCS introduces significant gain for all UEs for the unlimited backhaul capacity, i.e., for the pico/microcells. This confirms observations presented by other researchers for the scenarios with macrocells only as the only difference between the macro and the pico/micro cells consists in the cell radius. On the other hand, the throughput is improved by FCS only for the outdoor UEs offering low throughput up to 2 Mbps if the backhaul capacity is limited (that is, for femtocells). Therefore, if the small cells are deployed, the conventional FCS can even decrease performance in term of the throughput if the backhaul capacity is not considered in the active set management. Hence, algorithms for mobility support should be aware of the available capacity of the small cell backhaul to maximize the throughput of users.

Based on the observation of the FCS's performance, the algorithm related to FCS active set management considering backhaul limitations introduced by deployment of FAPs in networks is designed. The proposed algorithm is based on comparison of the amount of MBS's radio resources consumed if a cell is included to the UE's active set or not. The simulation results show notable increase in throughput for indoor as well as outdoor users. Simultaneously, the amount of generated overhead is significantly reduced by the proposal. Moreover, the proposed algorithm reduces the time, when users are not fully satisfied with experienced capacity and delay.

As the simulations show, the most efficient active set always contains an MBS. For indoor users, the closest FAP deployed in the same house should be included as

well. The amount of FAPs included in the active set together with MBS for outdoor users depends on mutual distance between the UE and neighboring FAPs. Further, the number of FAPs slightly varies with offered traffic level. In average, roughly 1.3 FAPs and 1.5 FAPs are included in active set of outdoor UE for low/high traffic level and for medium traffic (100kbps - 1500 kbps).

## 7 TEMPORARY ACCESS TO CLOSED FAP

This section addresses the problem of a dynamic management of a CSG list of a closed FAP (denoted as CSG FAP). The goal is to ensure simple and easy management of “adding” or “removing” new UEs, so called "Visiting UEs", to or from the CSG list. The reference scenario is depicted in Figure 47. Users included on the CSG list of a CSG FAP are denoted as CSG UEs.

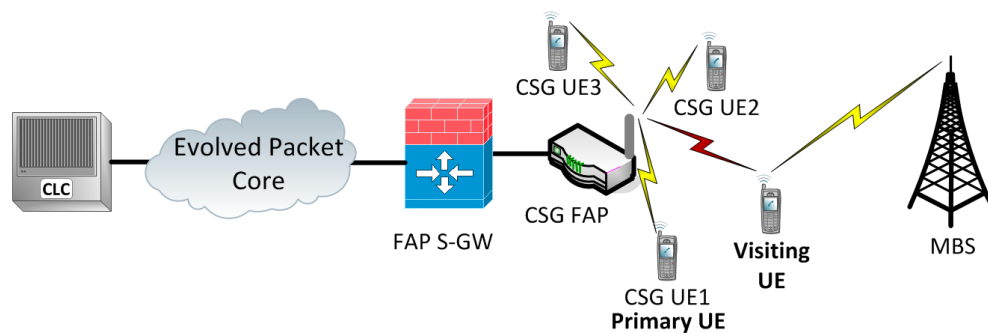


**Figure 47. Reference scenario for management of visiting users.**

Each UE is aware of all CSG FAPs that this UE can access. These CSG FAPs are included in each UE's CSG whitelist. The whitelist is a combination of Allowed CSG list and Operator CSG list. The former one is under control of both the operator and the user, while the latter one is under exclusive control of the operator (for more information, see [38]). Both lists should be stored in the UE's USIM (Universal Subscriber Identity Module). Each UE can access all CSG FAPs included on at least one of the lists. Therefore, if the CSG FAP in the UE's range is listed in the whitelist, the conventional procedures for connection control defined in [58] are performed. In this paper, we focus on the scenario when the CSG FAP is not included in the UE's whitelist but the UE still would like to access this FAP. In this case, the UE must obtain permission from a subscriber of the CSG FAP. By the CSG FAP subscriber is understood a user with the CSG FAP in its whitelist and with permission to allow/deny



access of the V-UEs. In the simplest way, the user who is the operator's signed subscriber (denoted as Primary UE in this chapter) should be the user in charge of the CSG list management. Besides the Primary UE, a list of potential users with permission to control the CSG list of admitted UEs should be defined in case the Primary UE is out of the CSG FAP range or if the Primary UE is willing to grant such rights to other members of the CSG list (e.g., other members of the family or selected employees).

If a V-UE moves close to a FAP and the V-UE is able to receive and recognize an identity of this cell, it also receives information about CSG status. This means, the V-UE is able to determine whether this FAP utilizes closed or open access. This is indicated by a CSG indication flag set to "true" broadcasted by each FAP together with other information (see [36]). If the UE would like to perform handover to this cell, it should conduct a measurement of the signal level received from this CSG FAP. Handover can be performed even if no measurements are reported to the network. However, this introduces a risk of the UE's disconnection or QoS degradation if the CSG FAP signal is interfering heavily to the UE connected to another cell. Therefore, even if the measurement is optional, it is recommended to perform the measurement before the handover initiation. The current 3GPP standards imply exclusion of CSG FAP from signal measurement and reporting if no CSG FAP is in the UE's whitelist (see [10], [36]). Therefore, a modification enabling the UE to measure and to report signal to the network even if no CSG FAP is included in its whitelist is necessary. For the inclusion of such a CSG FAP in measurement and reporting, we introduce a new flag *MeasCSGFlag*. The *MeasCSGFlag* is kept in the USIM of the UE along with the whitelist. This flag can be set either manually by the V-UE, if it is willing to enter a CSG FAP or automatically by the network if a strong interferer for a long time is noted by the V-UE and the network expects handover to this FAP.

## **7.1 CONTROL PROCEDURE ENABLING ACCESS OF V-UES**

In this section, the general framework of the management message flow is outlined. Furthermore, two approaches, in-band and out-of-band, are described in more detail.

### **7.1.1 GENERAL FRAMEWORK**

The general overview of the proposed CSG management is depicted in Figure 48. If a V-UE detects a CSG FAP, it can try to enter this FAP. In the conventional way, the

V-UE's attempt to enter the CSG FAP without permission would be rejected as both the FAP and the network consider this request as unjustified. Therefore, the request from the V-UE must contain a new flag, "Not Allowed" ("NA"). This flag indicates that the V-UE is aware of the fact that it cannot access this CSG FAP, and that the V-UE applies for negotiation of access to the CSG FAP.

After that, the FAP, in cooperation with the network, finds an appropriate user who has the right to accept or deny the V-UE request (i.e., the Primary UE or its representative is found). The selection of the Primary UE is done only among CSG FAP users with permission to grant the access. Among those UEs, the one with the highest priority for CSG list management out of all CSG UEs in FAP's range is chosen. This selected UE (shown as Primary UE in Figure 48), is asked if the V-UE can be admitted to the CSG FAP. The Primary UE then either approves or rejects this request. If the access of the V-UE is accepted, the Primary UE must provide an input for authentication purposes and a Class of V-UE. The authentication input is understood as a definition of access password for verification of the V-UE. The Class of V-UE stands for set of limitations for the V-UE (e.g., bandwidth limit, overall amount of transferred data, restriction of some applications or services, duration of the access, etc.). Note that observance and enforcement of Class of the V-UE is in charge of the FAP.

The restrictions set by the Primary UE are then negotiated with the V-UE. Also, the V-UE is asked to verify its identity by password. The handover to the CSG FAP can be initiated only if the password entered by the V-UE is identical to the one provided by the Primary UE and if the V-UE accepts all restrictions and conditions set in the Class of V-UE.

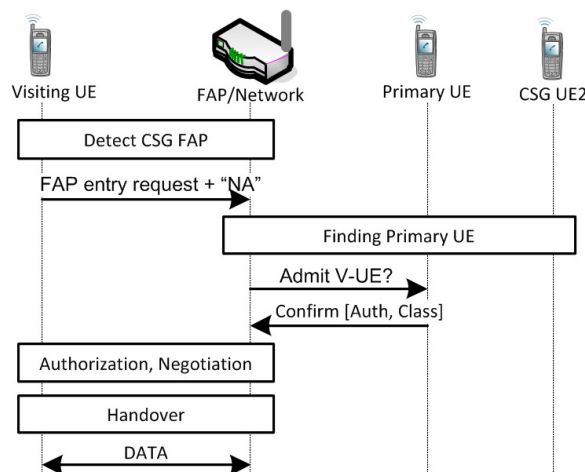


**Figure 48. General outline of the procedure for V-UE entering the CSG FAP.**

This new scheme can introduce potential problem related to malicious attacks when a UE could continuously try to enter a CSG FAP. This can be easily avoided by definition of a minimum interval between two consecutive requests to enter the CSG FAP issued by the same V-UE. Beside, also a blacklist of UEs with restricted access the CSG FAP should be established. This blacklist should be under control of the CSG FAP and the Primary UE.

Two options of management of the V-UE access are proposed in the following subsections: In-Band (IB) and Out-Of-Band (OOB). The first one assumes signaling for handling the V-UE entry within a conventional band used by the UE for all types of communications (including data) with the network. The second one requires other radio technology, such as Bluetooth, for the signaling.

### **7.1.2 IN-BAND APPROACH**

The flow of control messages for admission of the V-UE to the CSG FAP with utilization of IB is depicted in Figure 49. Both signaling over radio and backhaul are illustrated. If the V-UE is able to detect the CSG FAP, it sends a request for access to this FAP. The request is transmitted to the serving MBS since communication with the FAP is not yet established. If the "NA" access is indicated by the V-UE, the MBS forwards the request to the CSG FAP via backhaul. The FAP then transmits the *V-UE Request* message to the Primary UE. This message contains only identification of the V-UE to minimize redundant signaling overhead. Note that structure and detailed content of all new required control messages is presented in the next section.

The Primary UE can either grant or deny the request using a *V-UE Response* message. This message contains the ACK or NACK indication (grant or deny). If ACK is present, then the Primary UE can define additional requirements or limiting conditions for using the CSG FAP (Class of V-UE). Moreover, a password for verification of the V-UE must be included in this message. This message is further forwarded to the V-UE through the FAP, the FAP backhaul, and the serving MBS. For security reasons, the password is not forwarded by the FAP. This means, the password is delivered only from the Primary UE to the CSG FAP and then it is removed from the message.

After reception of the *V-UE Response*, the V-UE enters either the password with acknowledgment or rejection of the Class of V-UE set by the Primary UE. This

feedback is delivered to the CSG FAP via the serving MBS in *V-UE Info* message. Note that the *V-UE Response* and *V-UE Info* messages can be exchanged more than once if the agreement on Class of V-UE is not agreed in the first round. The CSG FAP then compares both passwords. If both passwords are identical, the FAP confirms admission of the V-UE to the Primary UE and to the network by means of a *V-UE Confirm* message. Based on this message, the network includes the V-UE on the list of UEs with access to this CSG FAP and handover can be initiated. To avoid a security risk, the conventional authorization and security procedures are performed during handover. It means, even if an attacker obtain permission from the Primary UE, it has to pass network authentication and authorization procedure before it can communicate with the network.

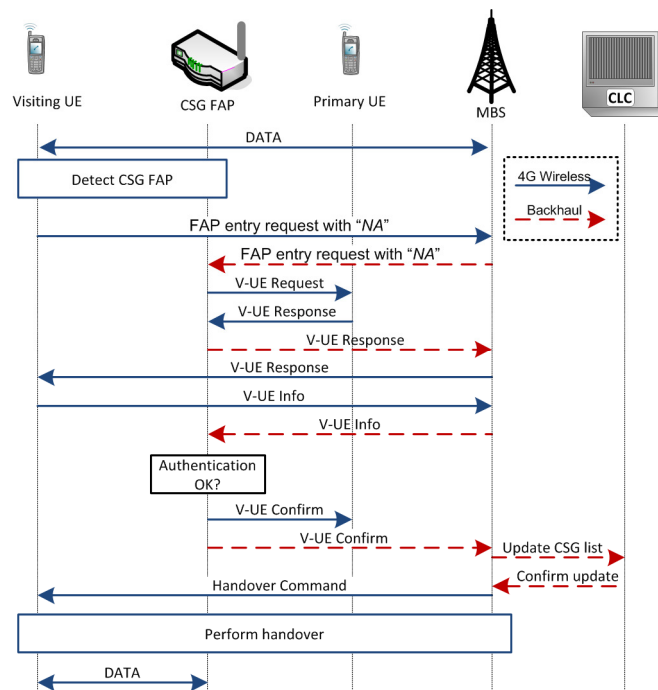


**Figure 49. Flow of control messages for V-UE access using IB approach.**

Since the temporary agreement on enabling the V-UE access to the CSG FAP does not imply any commitments to allow access in the future, no update of the whitelist in the V-UE is performed. After an expiration of the granted access, all new records in the CLC must be deleted. Therefore, a timer must be run to ensure deletion of such records. Update of the whitelist in USIM of the V-UE is necessary only if the Primary UE indicates unlimited access grant for the V-UE (note that this is not indicated in Figure 49 since we focus mainly on temporary access).

### 7.1.3 OUT-OF-BAND APPROACH

Another option for managing V-UE access is to use OOB communication since nearly all mobile devices available at the market are equipped with a short-range communication technology such as Bluetooth. If the V-UE comes to the vicinity of the CSG FAP and if the Primary UE is in the range of OOB communication technology, the V-UE can initiate the procedure via OOB by transmission of *V-UE Request* (see Figure 50). This message is sent via OOB directly to the Primary UE with the same content as in the case of IB communication. The Primary UE can either accept or reject the V-UE by a *V-UE Response*. In the case of accepting the V-UE request, a password and additional limitations can be set by the Primary UE in the same way as for the IB method. The confirmation of those requirements is sent by the V-UE together with the password in *V-UE Info*. Again, the *V-UE Response* and *V-UE Info* messages can be exchanged until an agreement on Class of V-UE is reached. If the OOB is used, the Primary UE is responsible for verification of the V-UE authenticity. Like in Bluetooth pairing, the password from the Primary UE to the V-UE is not transmitted via radio. The Primary UE delivers the password to the visiting user personally (the primary user says it or writes it down to the visiting user). Once the V-UE agrees to the conditions defined by the Primary UE and both entered passwords match, the final acknowledgment is sent to the V-UE in *V-UE Confirm*. At the same time, the Primary UE informs the CSG FAP of the temporary inclusion of the V-UE to the list of UEs with enabled access (*V-UE Confirm*) and of Class of V-UE (*V-UE Response*). The CSG FAP forwards *V-UE Confirm* to the CLC via backhaul. Handover can be initiated by the serving MBS after the reception of CLC update confirmation. Note that all conventional authorization and security procedures are performed during handover to avoid security risks as explained before for the IB approach.

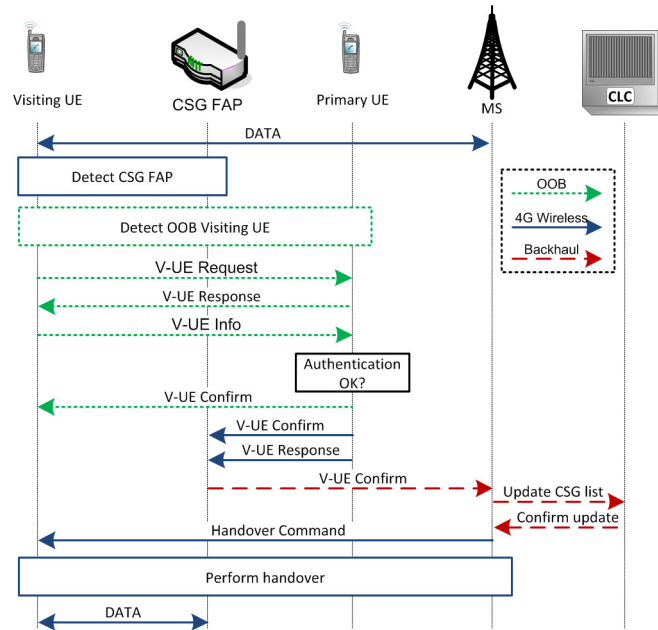


Figure 50. Flow of control messages for V-UE access using OOB approach.

## 7.2 MANAGEMENT MESSAGES FOR VISITOR ACCESS

In this section, a content of new management messages and comparison of IB and OOB are presented.

For both approaches of handling V-UE access, four new messages must be designed: *V-UE Request*, *V-UE Response*, *V-UE Info*, and *V-UE Confirm*. Each message starts with a message ID to distinguish its purpose. The second part of all messages is an identification of the V-UE by 64-bits IMSI (International Mobile Subscriber Identity).

The *V-UE Request* message contains both IDs (message and V-UE). Optionally, also a name of the V-UE assigned by the user can be included. This field is not indicated in Table 15 as it just increase overhead and it is not necessary for successful V-UE entry. The content of the *V-UE Request* message is presented in Table 15.

Table 15. Structure of V-UE Request message

Message field	Size	Description
Message ID	TBD	Identification of the message
ID of V-UE	64 bits	Identification of the V-UE by IMSI

The second message, *V-UE Response*, is presented in Table 16. This message contains identification of the message and identification of the V-UE like the *V-UE Request*. Further, ACK/NACK of the access is indicated. If access is granted, a

password must be included for IB communication. For OOB, the password is told to V-UE by Primary UE and it is carried neither in OOB nor in 4G channels for data communication. The length of the password field depends on the encrypting algorithm and the password length. The password can be followed by optional conditions, restrictions, or duration of the V-UE access defined in the Class of V-UE. The length of this field depends on the amount of restrictions and conditions set by the Primary UE.

**Table 16. Structure of V-UE Response message**

Message field	Size	Description
Message ID	TBD	Identification of the message
ID of V-UE	64 bits	Identification of the V-UE by IMSI
ACK/NACK	1 bit	ACK ... access of the V-UE enabled NACK ... access of the V-UE disabled
Password	Variable	Password for verification of the V-UE
Class of V-UE	Variable	Defines restriction to the V-UE and duration of granted access

The next message, *V-UE Info*, is presented in Table 17. This message is a feedback from the V-UE to the *V-UE Response*. Beside the IDs of the message and the V-UE, the additional field, ACK/NACK, is mandatory. It indicates whether the V-UE accepts the condition for the FAP's access defined by the Primary UE. If the conditions are accepted, the field with the password is included just after the ACK/NACK field.

**Table 17. Structure of V-UE Info message**

Message field	Size	Description
Message ID	TBD	Identification of the message
ID of V-UE	64 bits	Identification of the V-UE by IMSI
ACK/NACK	1 bit	ACK ... acceptance of Class of UE NACK ... rejection of Class of UE
Password	Variable	Password for verification of V-UE's

The last message, *V-UE Confirm*, is presented in Table 18. This message ends the process of granting the V-UE access to the CSG FAP. In addition to the message ID and the ID of the V-UE, 9 bits with the FAP's ID is included. We suppose to use the same indicator as the Physical Cell ID (PCI). The PCI distinguishes up to 504 cells [58], thus 9 bits are required for the FAP identification. This ID is included just for CLC purposes (CLC always contains pairs - ID of the CSG FAP and related ID of the admitted V-UE).

Finally, information on the duration of the access to the CSG FAP is presented in the message. This information must be delivered to the network to ensure deletion of the record from the CSG list in CLC after an expiration of the access grant.

**Table 18. Structure of V-UE Confirm message**

Message field	Size	Description
Message ID	TBD	Identification of the message
ID of V-UE	64 bits	Identification of the V-UE by IMSI
CSG FAP ID	9 bits	Identification of the FAP, the same number as the FAP's Physical Cell ID can be used.
Access grant duration	TBD	Information on duration of enabled access to the CSG FAP. If this field equals zero, unlimited access is indicated.

Comparing IB and OOB, the latter one imposes a lower amount of signaling overhead on radio interface and backhaul links than IB (five messages are transferred via IB radio and backhaul instead of thirteen). Contrary, OOB requires enabled OOB communication technology on both UEs (V-UE and Primary UE). Therefore, the OOB could negatively influence the battery lifetime of both involved devices due to the need of other additional radio communication technology. It means there is a trade-off between battery life-time and signaling overhead. Nevertheless, the OOB is used only for a very short time before entering CSG FAP (up to few minutes). As well, only negligible overhead is generated by this procedure (up to few kilobits). Hence, appropriate way can be arbitrary selected according to users and/or operators preferences.

### **7.3 IMPACT OF THE TEMPORARY V-UE ACCESS ON THE V-UE'S PERFORMANCE**

The proposed management of the temporary V-UE access allows to change the access mode for a V-UE. It means, a closed FAP becomes temporary the open FAP for the V-UE. Therefore, change in performance of the V-UE corresponds to the difference between the open and closed accesses. This problem has already been investigated, for example, in [1] and results demonstrate a gain in throughput due to the open access if the UE is close to the FAP. Therefore, we show only illustrative impact of the



temporary V-UE access on its SINR (Signal to Interference plus Noise Ratio) measured by the V-UE.

For evaluation, we consider model with an MBS and a FAP deployed in mutual distance denoted  $d_{MBS-FAP}$ . The MBS and FAP transmit with 46 and 15 dBm respectively. Signal from the MBS is propagated according to the Okumura-Hata model while signal inside the building follows ITU-R P.1238 model as recommended by Small Cell Forum for residential buildings in small to medium city [43]. The building is of a rectangular shape with a size of 10 x 10 m. Carrier frequency of 2 GHz and noise with density of -174 dBm/Hz are also considered for signal propagation. As the FAP is placed in the middle of a building, wall attenuation of 10 dB is taken into account for communication between the V-UE and the outdoor MBS.

Cumulative density function (cdf) of SINR experienced by the V-UE if the access to the closed FAP is disabled or enabled is depicted in Figure 51. The SINR is derived for 121 normally distributed positions of the V-UE inside the building and for 500 values of  $d_{MBS-FAP}$  distance. The  $d_{MBS-FAP}$  is also normally distributed in the range from 0 to 500 m. If the V-UE cannot access the closed FAP and stays connected to the MBS, it suffers from heavy interference incurred by the FAP. In this case the observed SINR varies only between -30 dBm and 12 dBm. Consequently, the V-UE is not able to receive signal from the MBS with sufficient quality most of the time. However, if the V-UE is temporarily admitted to the FAP, its SINR improves dramatically. To be more specific, SINR measured by the V-UE is in a range of -10 dBm and 30 dBm.

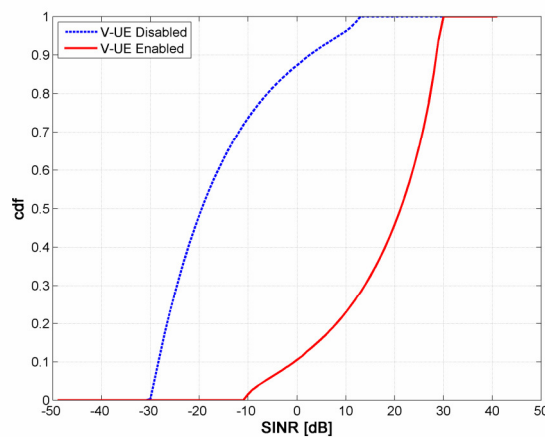


**Figure 51. SINR experienced by V-UE if temporary access is not enabled (dashed blue line) and if the V-UE is enabled to access this FAP (solid red line).**

As could be expected, higher  $d_{MBS-FAP}$  distance reduces signal quality observed by the V-UE from the MBS as shown in Figure 52. This figure depicts average SINR measured by the V-UE at 121 normally distributed positions within the building. According to the results presented in Figure 52, the temporary access of the V-UE should be applied especially in the case when the signal from the MBS is weak comparing to the signal of the FAP. On the other hand, if the FAP is close to MBS (distance up to 60 m), it is better for the V-UE to stay connected to the MBS. This is in compliance with fact that the deployment of the FAP is advantageous mainly for location with weak signal quality from the MBS.

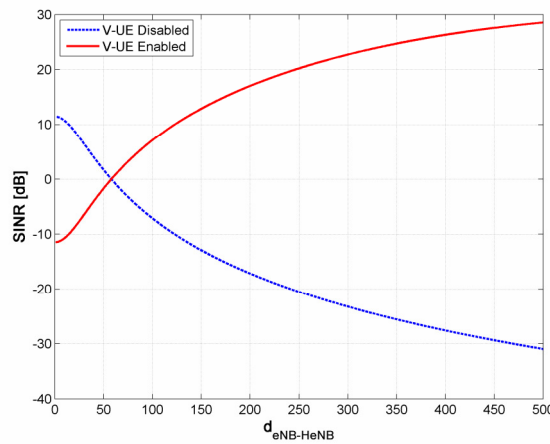


**Figure 52. SINR experienced by V-UE over distance between MBS and FAP if temporary access is not enabled (dashed blue line) and if the V-UE is enabled to access this FAP (solid red line).**

## 7.4 CONCLUSIONS

This chapter introduces new procedure to enable temporary access of a visiting user to the CSG FAPs. Contrary to the existing solutions, the new one is convenient for frequent update and easy management of the CSG list. For this purpose, we have defined chart flow of control messages as well as their content for IB and OOB way of the V-UE access management. Signaling overhead introduced by the new procedure is only few kilobits per access and can be neglected. Since both approaches still exploit full conventional authorization and security procedures before the V-UE is admitted to the CSG FAP, increased security risk is introduced by non of both ways of management.

## 8 CONCLUSIONS AND FUTURE WORK

This thesis is focused on management of problems related to the mobility of users in mobile networks with small cells. Three major topics are addressed: hard handover, fast cell selection, and temporary access to closed femtocells.

In the area of hard handovers, two algorithms for elimination of redundant handovers are proposed. Both proposed schemes differ in its requirements on modifications of current standards. While the first scheme, adaptive techniques, exploits only conventionally observed and monitored parameters, the second one, ETG, requires estimation of user's throughput. The second scheme significantly outperforms the first one in both user's throughput and efficiency in elimination of redundant handovers. However, it is at the cost of higher computational complexity and additional signaling overhead. Nevertheless, both proposed schemes show higher performance comparing to the conventional and competitive proposals. Performance of adaptive techniques could be improved, in the future, by sensing capabilities of the femtocells. It means, the maximum level of signal should be determined exactly according to the measurement of the signal level directly by the femtocells. Future enhancement of ETG can be achieved by advanced estimation of the signal evolution or interference. Moreover, more precise estimation of time spend in the cell by each user based on personnel characteristics and behavior of each user could further enhance performance of ETG.

Further, the performance of FCS and hard handover if the small cells are deployed in the networks is investigated. Analogically to the macrocells, FCS introduces significant gain in throughput for all UEs if small cell backhaul is of unlimited capacity, i.e., for the pico/microcells. However, the throughput is improved by FCS only for the outdoor UEs offering low throughput if the femtocell backhaul capacity is limited. Otherwise, the throughput is even degraded by FCS. Hence, the algorithm related to

FCS active set management considering backhaul limitations introduced by deployment of FAPs in networks is designed. The proposed algorithm is based on comparison of the amount of MBS's radio resources consumed if a cell is included to the UE's active set or not. The simulation results show significant gain in throughput for indoor as well as outdoor users. Moreover, the proposed algorithm reduces signaling overhead related to the active set management and the time when users are not fully satisfied with experienced capacity and delay. The proposed algorithm can be further extended for FAP's downlink power control to reduce interference from cells that cannot fulfill UE's requirements.

Last part tackles the problem of temporary access of visiting UEs to the closed FAPs. The proposed solution is convenient for frequent update and easy management of the CSG list. To enable new management procedure, several new control messages are proposed. Moreover, the chart flow of control messages for IB and OOB way of the V-UE access management are designed as well. OOB approach requires enabled additional communication technology (e.g. Bluetooth) on both involved devices. However, it reduces signaling overhead in communication band.

Beside further incremental enhancement of individual algorithms and techniques to improve their performance, the mobility management can adopt prediction approaches considering a periodicity in users' behavior. It means, to exploit the fact that users usually follows similar patterns in daily movement and daily traffic.

Also a problem of merging mobile communications with other technologies such as cloud computing should be considered in future research. In this case, user's movement could significantly influence computation or transmission of large amount of data between the cloud and the user. In this case, management of routing of user's data and data processing should be aware of the user's requirements on computational and storage capacities of remote clouds. To that end, distribution of a centralized cloud closer to the users (e.g. to small cells) can significantly improve user's experienced QoS.

## SUMMARY OF RESEARCH CONTRIBUTIONS

The habilitation thesis is focused on the support of user's mobility in networks with small cells. The contributions of the thesis into the area of handovers are following:

### *Chapter 5*

- Proposal and evaluation of the adaptive techniques for minimizing negative impact of handover on the user's throughput and improving efficiency in elimination of redundant handovers.
  - Related results are includes in following papers:
    1. **Z. Becvar** - P. Mach, "Adaptive Hysteresis Margin for Handover in Femtocell Networks," *International Conference on Wireless and Mobile Communications (ICWMC 2010)*, Valencia, Spain, 2010.
    2. **Z. Becvar** - P. Mach, "Adaptive Techniques for Elimination of Redundant Handovers in Femtocells," *International Conference on Networks (ICN 2011)*, St. Maarten, Netherlands, 2011.
    3. **Z. Becvar** - P. Mach - M. Vondra, "Handover Procedure in Femtocells," In *Femtocell Communications and Technologies*. IGI Global, 2012, pp. 157-179, edited by R.A. Saeed, B.S. Chaudhari, R.A. Mokhtar.
  
- Proposal and evaluation of the algorithm for handover decision exploiting estimation of user's gain in throughput for minimizing negative impact of handover on the user's throughput and improving efficiency in elimination of redundant handovers
  - Related results are includes in following papers:
    4. **Z. Becvar** - P. Mach, "On Enhancement of Handover Decision in Femtocells," *4th IFIP Wireless Days*, Niagara Falls, Canada, 2011.
    5. **Z. Becvar** - P. Mach, "Estimation of Throughput Gain for Handover Decision in Femtocells," submitted to journal *Mobile Information Systems* in May 2012.

### **Chapter 6**

- Evaluation of the performance of the FCS in networks with small cells for various types of users.
  - Related results are includes in following papers:
    6. **Z. Becvar** - P. Mach, "On Enhancement of Handover Decision in Femtocells," submitted to *5th IFIP Wireless Days*, Dublin, Ireland, 2012.
- Proposal on active set management considering amount of MBS's resources consumption if femtocells are deployed and included in active sets.
  - Related results are includes in following papers:
    7. **Z. Becvar** - P. Roux - P. Mach, "Fast Cell Selection with Efficient Active Set Management in OFDMA Networks with Femtocells," accepted for publication in *EURASIP Journal on Wireless Communications and Networking*, 2012.

### **Chapter 7**

- Design of the control procedure for temporary admission of visiting users to closed femtocells to improve users signal quality.
  - Related results are includes in following papers:
    8. **Z. Becvar** - P. Mach, " Management Procedure for Temporary Access of Visiting Users to Closed Femtocells," submitted to journal *KSII Transactions on Internet and Information Systems* in September 2012.

As this thesis have been completed in frame of FP7 FREEDOM project, all results are also included in deliverables *D4.1 – "Advanced procedures for handover in femtocells"* and *D4.2 – "Design and evaluation of effective procedures for MAC layer"* of the project. Both documents are available at [www.ict-freedom.eu](http://www.ict-freedom.eu).

---

**REFERENCES**

- [1] G. de la Roche, A. Valcarce, D. Lopez-Perez, J. Zhang " Access control mechanisms for femtocells," *IEEE Communication Magazine*, vol.48, no. 1, pp. 33-39, January 2010.
- [2] Small Cells Forum, "Femtocells – Natural Solution of Offload," June 2010.
- [3] D. Lopez-Perez, A. Valcarce, A. Ladanyi, G. de la Roche, and J. Zhang, "Intracell Handover for Interference and Handover Mitigation in OFDMA Two-Tier Macrocell-Femtocell Networks," *EURASIP Journal on Wireless Communications and Networking*, 2010, 15 pages, 2010.
- [4] P. Xia, V. Chandrasekhar, and J. G. Andrews, "Open vs. Closed Access Femtocells in the Uplink," *IEEE Transactions on Wireless Communications*, Vol. 9, No. 12, 3798 - 3809, .2010.
- [5] Small Cell Forum whitepaper, " Small cells – what’s the big idea? Femtocells are expanding beyond the home," February 2012.
- [6] V. Chandrasekhar, J. Andrews, A. Gatherer, "Femtocell Networks: A Survey," *IEEE Communication Magazine*, vol.46, no. 9, June 2008.
- [7] S. Moghaddam, V. Tabataba, and A. Falahati, "New handoff initiation algorithm (optimum combination of hysteresis and threshold based methods)," *IEEE VTC 2000-Fall*, September 2000.
- [8] D. Rose, T. Jansen, T. Kurner, "Modeling of Femto Cells - Simulation of Interference and Handovers in LTE Networks," *IEEE VTC 2011-Spring*, 2011.
- [9] T. Jansen, I. Balan, J. Turk, I. Moerman, and T. Kurner, "Handover parameter optimization in LTE self-organizing networks," *IEEE VTC 2010-Fall*, September 2010.
- [10] 3GPP Technical Specification TS 36.133 v 10.6.0, "Technical Specification Group Radio Access Network; Evolved Universal Terrestrial Radio Access (E-UTRA); Requirements for support of radio resource management (Release 10)," March 2012
- [11] M. Zonoozi, P. Dassanayake, and M. Faulkner, "Optimum hysteresis level, signal averaging time and handover delay," In *IEEE VTC 1997*, pp. 310 – 313, 1997.
- [12] K.I. Itoh, S. Watanabe, J.S. Shih, and T. Sato, "Performance of handoff algorithm based on distance and RSSI measurements," *IEEE Transactions on Vehicular Technology*, Vol. 51, No. 6, 1460 – 1468, 2002.
- [13] S. Lal and D. K. Panwar, "Coverage Analysis of Handoff Algorithm with Adaptive Hysteresis Margin," In *ICIT 2007*, pp. 133 – 138, 2007.
- [14] J.M. Moon and D.H. Cho, "Efficient Handoff Algorithm for Inbound Mobility in Hierarchical Macro/Femto Cell Networks," *IEEE Communications Letters*, Vol. 13, No. 10, 755- 757, 2009.
- [15] J.M. Moon and D.H. Cho, "Novel Handoff Decision Algorithm in Hierarchical Macro/Femto-Cell Networks," In *IEEE WCNC 2010*, pp. 1- 6, 2010.

- 
- [16] H. Zhang, X. Wen, B. Wang, W. Zheng, and Y. Sun, "A Novel Handover Mechanism between Femtocell and Macrocell for LTE based Networks," In ICCSN2010, 2010.
- [17] L. Barolli, "A speed-aware handover system for wireless cellular networks based on fuzzy logic," *Mobile Information Systems*, Vol. 4, No. 1, pp. 1-12, 2008.
- [18] G. Mino, L. Barolli, F. Xhafa, A. Durresi and A. Koyama, "Implementation and performance evaluation of two fuzzy-based handover systems for wireless cellular networks," *Mobile Information Systems*, Vol. 5, No. 4, pp. 339-361, 2009.
- [19] H. Claussen, F. Pivit, and L.T.W.Ho, "Self-Optimization of Femtocell Coverage to Minimize the Increase in Core Network Mobility Signalling," *Bell Labs Technical Journal*, Vol. 14, No. 2, pp. 155–184, 2009.
- [20] H.S. Jo, Ch. Mun, J. Moon, and J.G. Yook, "Self-Optimized Coverage Coordination in Femtocell Networks," *IEEE Transactions on Wireless Communications*, Vol. 9, No. 10, pp. 2977-2982, 2010.
- [21] S. Y. Yun and D. H. Cho, "Traffic Density based Power Control Scheme for Femto AP," In *IEEE PIMRC 2010*, pp. 1378-1383, 2010.
- [22] Y. Choi and S. Choi, "Service Charge and Energy-Aware Vertical Handoff in Integrated IEEE 802.16e/802.11 Networks," In *IEEE INFOCOM 2007*, 2007.
- [23] P. Fülöp, S. Imre, S. Szabó and T. Szálka, "Accurate mobility modeling and location prediction based on pattern analysis of handover series in mobile networks," *Mobile Information Systems*, Vol. 5, No. 3, pp. 255-289, 2009.
- [24] P. Bellavista, M. Cinque, D. Cotroneo, and L. Foschini, " Self-Adaptive Handoff Management for Mobile Streaming Continuity," *IEEE Transactions on Networks and Service Management*, Vol. 6, No. 2, 2009.
- [25] J. Martinez-Bauset, J.M. Gimenez-Guzman and V. Pla, "Optimal Admission Control in Multimedia Mobile Networks with Handover Prediction," *IEEE Wireless Communications*, Vol. 15, No.5, 2008.
- [26] 3GPP TR 25.433 v10.4.0, "Technical Specification Group Radio Access Network; UTRAN Iub interface Node B Application Part (NBAP) signalling, Release 10," September 2011.
- [27] 3GPP TR 25.848 v4.0.0, "Technical Specification Group Radio Access Network; Physical layer aspects of UTRA High Speed Downlink Packet Access, Technical report," Release 4, March 2001.
- [28] S.-W. Kim, Y.-H. Lee, "Adaptive MIMO Mode and Fast Cell Selection with Interference Avoidance in Multi-cell Environments," In *Fifth International Conference on Wireless and Mobile Communications ICWMC '09*, Cannes, La Bocca, 23-29 August 2009.
- [29] H.-H. Choi, J.B. Lim, H. Hwang, K. Jang, "Optimal Handover Decision Algorithm for Throughput Enhancement in Cooperative Cellular Networks," In *IEEE VTC 2010-Fall*, Ottawa, 6-9 September 2010.
- [30] H.-H. Choi, "An Optimal Handover Decision for Throughput Enhancement," *IEEE Commun. Lett.* Vol. 14, No. 9, pp. 851-853, 2010.
-



- 
- [31] NTT DOCOMO, "Investigation on Coordinated Multipoint Transmission Schemes in LTE-Advanced Downlink," In 3GPP TSG RAN WG1 Meeting #55bis , R1-060298, Ljubljana, 12-16 January 2009.
- [32] M. Feng, X. She, L. Chen, Y. Kishiyama, "Enhanced Dynamic Cell Selection with Muting Scheme for DL CoMP in LTE-A," In IEEE VTC 2010-Spring, Taipei, 16-19 May 2010.
- [33] K.-W. Lee, J.-Y. Ko, Y.-H. Lee, "Fast Cell Site Selection with Interference Avoidance in Packet Based OFDM Cellular Systems," In IEEE Globecom 2006, San Francisco, 27 November - 1 December 2006.
- [34] A. Das, B. Krishna, F. Khan, S. Ashwin, H.-J. Su, "Network controlled cell selection for the high speed downlink packet access in UMTS," in IEEE WCNC 2004, 21-25 March 2004.
- [35] H. Fu, D. Kim, "Scheduling performance in downlink WCDMA networks with AMC and fast cell selection," *IEEE Trans. Wireless Commun.*, Vol. 7, No. 7, pp. 2580-2591, 2008.
- [36] 3GPP TS 36.304 v10.5.0, "3rd Generation Partnership Project; Technical Specification Group Radio Access Network; Evolved Universal Terrestrial Radio Access (E-UTRA); User Equipment (UE) procedures in idle mode (Release 10)," Mar. 2012.
- [37] 3GPP TS 36.133, v10.6.0, "3rd Generation Partnership Project; Technical Specification Group Radio Access Network; Evolved Universal Terrestrial Radio Access (E-UTRA); Requirements for support of radio resource management (Release 10)," Mar. 2012.
- [38] G. Horn, "3GPP Femtocells: Architecture and Protocols," Qualcomm, Sept. 2010.
- [39] ITU-R Document 5D/TEMP/89r1, "Draft new Report ITU-R M.[IMT.TECH], Requirements related to technical system performance for IMT-Advanced radio interface(s)," 2008.
- [40] R. Srinivasan, et. al, "IEEE 802.16m Evaluation Methodology Document (EMD)," Description of Evaluation of IEEE 802.16m System Performance, Rev. IEEE 802.16m-08/004r2, July 2008.
- [41] T. Camp, J. Boleng, V. Davies, "A Survey of Mobility Models for Ad Hoc Network Research," *Wireless Communications & Mobile Computing*, Vol. 2, No. 5, 2002.
- [42] ETSI UMTS 30.03, "Selection Procedures for the Choice of Radio Transmission Technologies of the UMTS," ETSI Technical Report, 1998.
- [43] Small Cell Forum, "Interference management in OFDMA femtocells," March 2010.
- [44] G. Vivier, A. Agustin, J. Vidal, O. Muñoz, S.Barbarossa, L. Pescosolido, et al., "Scenario, requirements and first business model analysis," Deliverable D2.1 of ICT-248891 STP FREEDOM project, June 2010.
- [45] C. Yu, W. Xiangming, L. Xinqi, and Z. Wei1, "Research on the modulation and coding scheme in LTE TDD wireless network," In ICIMA 2009, pp. 468 - 471, 2009.
-

- 
- [46] 3GPP TS 36.211 v 9.0.0, "3rd Generation Partnership Project; Technical Specification Group Radio Access Network; Evolved Universal Terrestrial Radio Access (E-UTRA); Physical Channels and Modulation," Dec. 2009.
- [47] Z. Becvar, J. Zelenka, "Implementation of Handover Delay Timer into WiMAX," Proc. of 6th Conference on Telecommunications (ConfTele 2007), Peniche, Portugal, May 2007.
- [48] N. P. Singh and B. Singh, "Performance of Soft Handover Algorithm in Varied Propagation Environments," World Academy of Science, Engineering and Technology, vol. 45, 2008.
- [49] ITU-R P.1238-6 Recommendation, "Propagation data and prediction methods for the planning of indoor radiocommunication systems and radio local area networks in the frequency range 900 MHz to 100 GHz," 2009.
- [50] Z. Becvar, P. Mach, "On Enhancement of Handover Decision in Femtocells," In IFIP Wireless Days 2011, Niagara Falls, Canada, 2011.
- [51] K. Kobayashi and T. Katayama "Analysis and Evaluation of Packet Delay Variance in the Internet," IEICE Transactions on Communications, Vol. E-85B, No. 1, pp. 35 - 42 , 2002.
- [52] H. Hariyanto, R. Wulansari, T. A. Nugraha, H. Ahmadi, A.K. Widiawan, J. Stéphan, Y. Corre, A. Cordonnier, R. Charbonnier, "Trial report," Deliverable D6.2.1 of ICT-248891 STP FREEDOM project, February 2012.
- [53] W. Daamen and S.P. Hoogendoorn, "Free Speed Distributions for Pedestrian Traffic," presented at Transportation Research Board, 85th Annual Meeting, 2006.
- [54] S. Sesia, I. Toufik, and M. Baker, LTE—the UMTS long term evolution: From Theory to Practice. West Sussex: Wiley, 2009.
- [55] H. Claussen, L.T.W. Ho, and L.G. Samuel, "Self-optimization of Coverage for Femtocell Deployment," IEEE Wireless Telecommunication Symposium WTS 2008, pp. 278-285, April 2008.
- [56] ITU-R M.2135 Recommendation, "Guidelines for evaluation of radio interface technologies for IMT-Advanced," 2008.
- [57] 3GPP TS36.331, v10.5.0, "3rd Generation Partnership Project; Technical Specification Group Radio Access Network; Evolved Universal Terrestrial Radio Access (E-UTRA); Radio Resource Control (RRC); Protocol specification (Release 10)," Mar. 2012.
- [58] 3GPP TS 36.300, v10.7.0, "3rd Generation Partnership Project; Technical Specification Group Radio Access Network; Evolved Universal Terrestrial Radio Access (E-UTRA) and Evolved Universal Terrestrial Radio Access Network (E-UTRAN); Overall description; Stage 2 (Release 10)," Mar. 2012.
-

## APPENDIX

### VARIATION OF TIME IN FEMTOCELL

The determination of limits for error in estimation of  $t_c$  is as follows. The distance covered by  $j$ -th user in the femtocell is  $d_{f,j} = d_{f,avg} \pm \Delta_{d,j}$ ; where  $d_{f,avg}$  corresponds to average distance covered by all users in the FAP's area and  $\Delta_{d,j}$  represents distance deviation of  $j$ -th user's. Further, the speed of  $j$ -th user is  $v_j = v_{j,avg} \pm \Delta_{v,j}$ ; where  $v_{j,avg}$  is the average speed of pedestrians and  $\Delta_{v,j}$  stands for the speed variation. Since only pedestrians are considered and since the mean speed of users is normally distributed along  $1.34ms^{-1}$  with  $\Delta_{v,j,max} = \pm 0.37ms^{-1}$ , i.e.,  $v_j = 1.34 \pm 0.37ms^{-1}$  according to [53].

In compliance with above mentioned, average  $t_c$  is defined as:  $t_{c,j,avg} = d_{f,avg} / v_{j,avg}$ . In relation to environment in femtocell, the lower and upper limit for  $t_c$  can be defined. The simplest case of infrastructure deployment is represented by a single direct street as depicted in Figure 53.

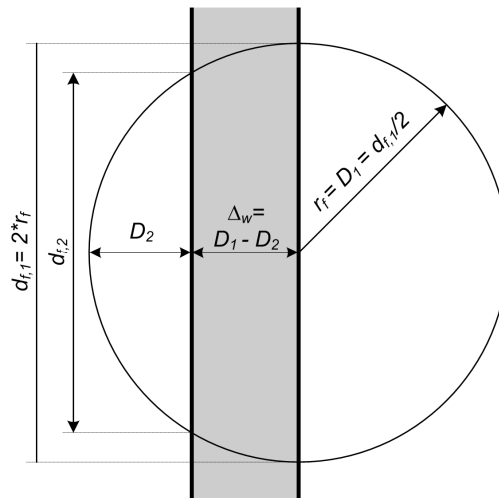


**Figure 53. Notation for determination of  $t_c$  limits.**

The real  $t_c$  of individual user moving along direct street as depicted in Figure 53 is limited from lower boundary to:

$$t_{c,min} = (d_{f,avg} - \Delta_{d,j}) / (v_{j,avg} + \Delta_{v,j,max}) = (d_{f,avg} - \Delta_{d,j}) / 1.71 \quad (40)$$

The  $t_{c,min}$  depends on the position of a street in relation to the FAP radius. The street is of a width  $\Delta_w$  and its borders are in distances  $D_2$  and  $D_1$  from the cell edge.

Assuming the direct movement of users along the street, then  $t_{c,min}$  is related to  $D_2$ . The distance  $d_{f,2}$  covered by a user in the femtocell along the path distanced  $D_2$  from the cell edge, is equal to  $d_{f,2} = 2\sqrt{r_f^2 - (r_f - D_2)^2}$ . Therefore the  $t_{c,min}$  as a function of  $D_2$  is:

$$t_{c,min} = d_{f,2} / (v_{j,avg} + \Delta_{v,j,max}) = 2\sqrt{r_f^2 - (r_f - D_2)^2} / 1.71 \quad (41)$$

The upper bound for  $t_c$  is derived analogically to (40) assuming  $d_{f,1} = 2r_f / 0.97$  (see Figure 53):

$$t_{c,max} = (d_{f,avg} + \Delta_{d,j}) / (v_{j,avg} - \Delta_{v,j,max}) = (d_{f,avg} + \Delta_{d,j}) / 0.97 = 2r_f / 0.97 \quad (42)$$

Dependence of  $t_{c,min}$  and  $t_{c,max}$  over  $D_2$  is shown in Figure 54. This figure is depicted for condition  $D_1 = r_f$ , which corresponds to the maximum  $d_{f,1}$  ( $d_{f,1} = 2r_f$ ) and thus to the worst case scenario. As Figure 54 shows, the variation of  $t_c$  is up to roughly 2.1 multiple of the cell radius. This maximum variation occurs if the area of user's movement (a street or a sidewalk) covers at least a half of the cell radius ( $\Delta_w = r_f$ ). However, the variation of  $t_c$  is still significantly lower than in the case of the MBS since  $t_{c,max}^{macro} = 2.1 \times r_B$ ;  $t_{c,max}^{femto} = 2.1 \times r_f$  and  $r_B \gg r_f$ . Thus we can declare  $t_{c,max}^{macro} \gg t_{c,max}^{femto}$ .

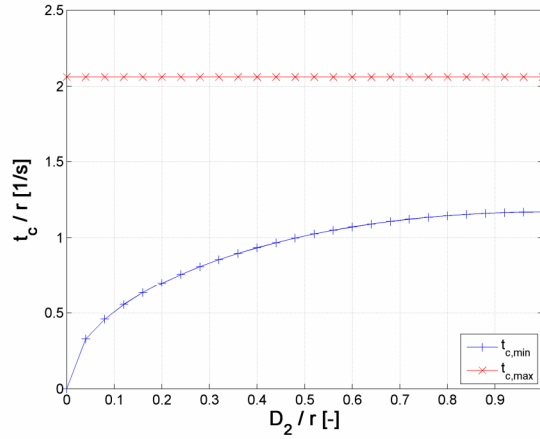


**Figure 54. Deviation of  $t_{c,min}$  and  $t_{c,max}$  over relative distance of users' path from the FAP's position.**

In more complex situation, the users are not limited to the direct movement. Their movement is influenced by other factors such as a deployment of streets in the cell, position of points of interests, users' behavior, etc. All these factors can be represented by function  $\xi$ . Further, the time in cell is affected by a probability  $TC$  that the user will

---

stay longer in the cell, e.g., due to turn away from a direct movement or due to stop. Therefore,  $TC$  is related to the  $\xi$ . Neither  $\xi$  nor  $TC$  can be easily determined. However, both are clearly proportional to the cell radius as larger cell can cover more complex infrastructure lay-out (e.g., more street crosses, more points of interests, etc.). Therefore, the probability  $TC$  is significantly higher for larger cells:

$$TC_{r_B} = f(\xi); \xi = f(r_B) \gg TC_{r_f} = f(\xi); \xi = f(r_f) \quad (43)$$

Above mentioned shows that the dispersion of minimum and maximum time in cell is significantly lower for cells with low radius.